©Copyright 2024

Hao Zhou

An *In vitro* Model to Study the Monocyte-Endothelial Interaction in Pediatric Cardiopulmonary Bypass

Hao Zhou

A dissertation
submitted in partial fulfilment of
the requirements for the degree of

Doctor of Philosophy

University of Washington
2024

Reading Committee:
Marta Scatena, Chair
Cecilia Giachelli
Ying Zheng

Program Authorized to Offer Degree:
Department of Bioengineering

University of Washington

Abstract

An *In vitro* Model to Study the Monocyte-Endothelial Interaction in Pediatric Cardiopulmonary Bypass

Hao Zhou

Chair of the Supervisory Committee:
Marta Scatena
Department of Bioengineering

Cardiopulmonary bypass (CPB) is a technique used in open-heart surgeries to create a bloodless field in the heart and maintain circulation in pediatric patients with congenital heart diseases (CHDs). Due to unoptimized settings in pediatric CPB, perioperative and postoperative complications often occur. However, there is no effective treatment to counteract them. Therefore, a CPB-specific mechanism needs to be determined for the development of targeted therapy. Shear stress in the bypass tubing was identified as a major factor that induces mechanical trauma and inflammatory response of the blood components. Previous study recognized monocytes as the blood cell population that responded the most to the CPB shear. However, the inflammatory response of CPB also involves endothelium that actively mediates the monocyte insult. In this dissertation, I further investigated the endothelial response to CPB-activated monocytes and cytokines derived from CPB-activated monocytes. Monocyte adhesion and transmigration assays were developed as a part of the *in vitro* CPB mode. Monocytes activated by CPB shear are more

likely to adhere to and transmigrate through the monolayer of human neonatal dermal microvascular endothelial cells (HNDMVECs). Treatment of CPB-activated monocytes disrupted the VE-cadherin and cytoskeleton arrangement of confluent endothelium. The monocyte-endothelial cell interaction is accompanied by increasing IL-8 level in the co-culture media. The correlation between IL-8 and monocyte adhesion is studied by loss and gain of function experiments. Inhibiting IL-8 signaling on endothelial cells with reparixin resulted in significant decrease of monocyte adhesion. Treating HNDMVECs with IL-8 induced the adhesion of naïve monocytes. Results of qPCR showed IL-8 treatment selectively upregulated intercellular adhesion molecule 1 (ICAM-1) and vascular cell adhesion molecule 1 (VCAM-1) expression in the HNDMVECs, which mediated the monocyte adhesion. Inhibiting the IL-8 expression in HNDMVECs resulted in reduced monocyte adhesion, suggesting that IL-8 produced by endothelial cells played an important role during cellular interactions. To investigate the cytokines derived from CPB-activated monocytes and the effect of anti-inflammatory drugs including dexamethasone and FK506, the conditioned media from CPB-activated monocytes with or without drug treatment were collected and assayed. ELISA showed CPB shear caused increasing production of IL-8 and tumor necrosis factor α (TNF-α) from the monocytes. Both cytokines expression and production can be reduced by dexamethasone and FK506 with the FK506 being more effective. Luminex multiplex assay showed that dexamethasone and FK506 alter the cytokine release profile of sheared monocytes in different ways. I further studied the effect of conditioned media on endothelial cells. Conditioned media derived from sheared monocytes disrupted the VE-cadherin and cytoskeleton arrangement in confluent HNDMVECs. Live and dead assays showed that treating HNDMVECs with shear conditioned media led to lower viability. Finally, the shear conditioned media treatment resulted in increasing naïve

monocyte adhesion mediated by upregulated adhesion molecules including E-selectin and ICAM-1. The study in this dissertation provided insight into the mechanisms that led to CPB-induced inflammatory response of monocytes and endothelial cells. Therapies that target the IL-8 and TNF-α pathways may be developed to treat CPB-related complications.

Table of Contents

List of Figures

Acknowledgement

I want to thank my committee members for their guidance in helping me set the course of this project and develop as a scientist. Especially, I want to thank my advisors, Dr. Marta Scatena and Dr. Cecilia Giachelli for providing me with valuable comments and support throughout my PhD program. Thanks to folks from Seattle Children's, Dr. Vishal Nigam, Dr Lan N Tu, and Lance Hsieh for conceptualizing the *in vitro* CPB model and giving feedback to the outcomes of this project. Thanks to every member of Scatena lab and Giachelli lab for building such an inclusive, supportive, and vibrant lab energy. I would not be able to make it to this PhD without this beautiful lab environment. Lastly, I want to thank my funding resources, the Bioengineering Cardiovascular Training Program. Thanks to the steering committee of the program and the two managers whose names are both Katie for organizing the program to prepare me for life after PhD.

Dedication

Due to a lot of reasons, I was not able to go back and see my family for 7 years. I want to dedicate this dissertation to my family for providing me moral and financial support from the other side of the globe. I also started a new family here. I want to do a special shout out to UW for giving me the opportunity to meet my wife. To my wife, thank you for always being around to give me the support and love that I need. I could not make it this far without you. I love you sincerely.

Chapter 1. INTRODUCTION

1.1 BACKGROUND

1.1.1 Overview of CPB

CPB is a technique to create a bloodless space in the heart while allowing for circulation outside of the patient's body (1). It not only maintains circulatory functions to prevent ischemic damage during surgeries on cardiac tissue or great vessels, but also provides respiratory support with temperature management (2). A typical CPB circuit consists of pumps, oxygenator, heat exchanger, tubing, and reservoir (Figure 1.1).

i. Pumps

Roller pumps are commonly used in CPB of shorter term to propel the blood in a circuit. It includes two rollers placed on a rotating arm, which pressurize a section of the tubing to generate forward flow (3). The force exerted on the tubing not only generates tubing debris with longer bypass time but also compresses the blood components and leads to hemolysis (3). For longer procedures with CPB, centrifugal pumps are used (4). A centrifugal pump consists of stacked cones wrapped by a housing. When the cones rotate, the inlets at the center of the cones generate negative pressure to suck the blood into the housing. A pressure gradient is established across the radius of the housing and the blood flows out through a side opening of the housing. The two pumps have their own advantages. For example, while the roller pump is a cheaper

option and restricts the backflow of blood, a centrifugal pump is often portable, induces less trauma to the blood, and produces less air embolism.

ii. Oxygenator

Membrane oxygenators are used in CPB to perform the function of lungs. They consist of polypropylene fibers with hydrophobic micropores filled with oxygen rich gas. Venous blood passes from the outside of the fibers, encounters the gas flow, and completes oxygenation through gas diffusion (5). In most designs of oxygenators, a heat exchanger is incorporated to cool and rewarm the blood for hypothermic or deep hypothermic CPB. Regulating the temperature of the blood also prevents the generation of emboli due to change in solubility of gas.

iii. Tubing

The tubing in the CPB provides physical support for the blood flow. Adult CPB tubing usually is sized at 1/2 inch in diameter (6). It is commonly made of polyvinyl chloride (PVC) materials which is durable and does not cause excessive hemolysis. The plasticizers in PVC such as di(2-ethylhexyl) phthalate, which enhances the flexibility of the tubing, can leach into the circulation and are potentially toxic to the patients (7). However, PVC is still a state-of-the-art material due to its chemical stability, and low cost.

iv. Reservoir

The reservoir provides a space for blood collection. An open reservoir is capable of removing air bubbles as well as foam in the venous drain and suctioned blood (1). A Closed reservoir offers limited volume for blood but minimizes the blood contact area with artificial materials (1). A closed system is less likely to trigger inflammatory response and keeps the sterility of the venous drain (1).

v. Arterial line filter

Arterial line filter is used to reduce the transmission of emboli from the venous circulation and oxygenator. It works by reducing the velocity of the blood flow so that buoyancy dominates the movement of the bubbles, which increases the tendency of the bubbles to rise instead of passing (8).

vi. Ultrafiltrators

Ultrafiltrators condense blood by removing water through a semipermeable membrane. In an ultrafiltrator, the blood flows through the membrane under a hydrostatic pressure gradient and water is removed from the CPB circuit (9). Excess water in the circuit can be caused by the crystalloid in the cardioplegia, solutions used in the surgery or a pre-surgical condition of the patient. The addition of ultrafiltrators in a CPB circuit provides benefits to patients with volume-overload or insufficient renal functions and reduces the onset of edema buildup (10).

vi. Cardioplegia

Cardioplegia provides myocardial protection while the cross-clamping at the aorta induces ischemia in the heart during intracardiac repair. Cardioplegia creates electrical quiescence and thus, electromechanical arrest in the heart, which reduces oxygen demand in the myocardial tissue (11). Cardioplegia was first used in CPB in the early 1950s, when Dr. Melrose used high levels of potassium citrate to induce cardiac arrest (12). Solutions of other ions such as calcium, sodium and magnesium, as well as substances such as lidocaine, bicarb, and glucose are all used as components of cardioplegia due to their cardioprotective properties (11).

1.1.2 Conduct of CPB

A schematic illustration of CPB is shown in Figure 1.1. To perform a CPB, the circuit is started at the right heart side, where the venous return blood is drained into a reservoir through venous cannulas. The flow to the reservoir is accomplished by gravity, where the reservoir is placed lower than the patient. The blood in the reservoir is then driven by a blood pump and propelled to the oxygenator. In the oxygenator, the venous blood is oxygenated and ready to be used. The oxygenated blood stream splits in the returning line. The first line goes back to the patients through the aortic cannula, which is usually located at the distal ascending aorta. Another line is mixed with cardioplegia and goes back to the patients through a cannula that is closer to the ascending aorta. This cardioplegic line is controlled by a separate pump with its own temperature and pressure management.

1.1.3 Temperature Management in CPB

It is still debatable whether a hypothermic state should be applied to patients during CPB. A moderate hypothermia state is achieved by cooling the patients to a temperature of 25-34°C. Deep hypothermia requires an even lower temperature at 18-19°C. The main purpose of inducing hypothermia is to reduce the oxygen demand and thus protect the organs. While the use of cardioplegia can reduce oxygen consumption by 90%, hypothermia inflicts an additional 5% to 20% reduction in oxygen consumption (13). Warm cardioplegia, however, has its benefits by fulfilling the energy demands of the heart, lowering risk of reperfusion injury, and shortening the time for rewarming (14,15).

1.1.4 Complications Associated With CPB

i. Arrhythmia

Atrial fibrillation (AF) occurs in 40-50% of the CPB patients. This arrhythmia may lead to hypotension, tachycardia, heart failure, and stroke (16,17). The cause of CPB-induced AF is multifactorial. The upregulations of inflammatory mediators such as IL-2, C3a, and white blood cells after CPB are found in patients who developed AF (16). The onset of AF is also dependent on the age of the patients, where 69 is the age median of patients developed AF (17). In another study, mild hypothermia at 34°C showed protective effects from AF as opposed to moderate hypothermia at 28°C (18).

ii. Pulmonary Dysfunction

Pulmonary dysfunction is commonly observed after CPB patients. 20% of patients will require mechanical ventilation after cardiac surgery with CPB for at least 48 hours due to pulmonary edema (19). Postoperative biopsy showed that lung permeability was compromised with infiltration of neutrophils and erythrocytes (20). This further causes the necrosis of pneumocytes and pulmonary endothelial cells, buildup of alveolar protein, and loss of lung compliance (20). In rare cases, patients develop acute respiratory distress syndrome (ARDS), which is associated with a high mortality rate from 15% to 70% (21).

iii. Renal Dysfunction

Renal dysfunction affects up to 30% of the CPB patients and 1% of them will require dialysis (22). These patients are characterized with decrease in creatinine clearance, increase in albumin-to-creatinine ratio, and increase in N-acetyl glycosaminidase activity (23). CPB-induced renal injury is associated with high mortality rate, longer intensive care unit (ICU) stay, and higher risk of infections (24). Studies have shown that the levels of C-reactive protein and IL-6 in the patients suffered from severe renal dysfunction (25). Hypoperfusion during CPB is also

believed to play a role in renal injury since kidneys are sensitive to changes in cardiac output and perfusion rate (26).

iv. Cerebral Injury

The damage in the brain is usually caused by CPB-induced cerebral emboli as well as reperfusion injury (27,28). Although the damage can be augmented by oxygenator and arterial line filter, cerebral injury still occurs and is associated with life-threatening outcomes (29). One study showed that in 76 CPB patients experiencing cerebral damage, 13 patients developed persistent neurological focal deficits, 18 patients developed stupor or coma, 18 patients developed temporary focal deficits, and 27 developed seizures (29). 29% of these patients passed away due to cerebral complications (29).

v. Systemic Inflammatory Response Syndrome (SIRS)

Many of the organ dysfunction after CPB can be attributed to the systemic inflammatory response. CPB may specifically activate the systemic inflammatory response through two mechanisms including contact activation and ischemia-reperfusion injury (30,31).

Contact activation is caused by the exposure of blood components to the artificial surface of the CPB circuit, which starts with factor XII converting the prekallikrein to kallikrein, and eventually leads to thrombin formation (31). In an alternative pathway, the complement system is also activated during the contact since the CPB circuit does not inhibit the cofactor C3 activation like the endothelium does (31). This promotes the formation of anaphylatoxins C3a and C5a which further mediates chemotaxis, inflammatory response, and the secretion of reactive oxygen species (32). C3a and C5a levels in the patients may be indicative of cardiac, pulmonary, renal, and hemostatic dysfunction after CPB (32). Strategy such as using heparin-coated tubing showed

efficacy in reducing the complement activation and may enhance the postoperative outcomes (33). Alternatively, anti-C5a antibody is promising in reducing the myocardial and cerebral injuries in the CPB patients (34).

Ischemia-reperfusion injury occurs when the aorta is clamped off during CPB. As a result, organs such as the brain, heart, lungs, and kidneys don't receive enough blood supply and are rendered hypoxia. When the clamps come off, the restored blood circulation can cause insult to the ischemic organs with increasing free radicals, inflammatory cytokines and changes in endothelial nitric oxide synthase (eNOS) and induced nitric oxide synthase (iNOS) (35-38). No effective treatment against ischemia-reperfusion injury has been developed clinically. Statins have been studied to counter the ischemia-reperfusion injury by enhancing endothelial function, decreasing oxidative stress in vivo but the dose is 10-fold of the clinical dose (39).

1.1.5 Endothelial Cell and Leukocyte Interaction During Inflammation

The inflammatory response to CPB follows a common cascade at cellular level where both endothelial cells and leukocytes are actively involved. Following exposure to CPB circuit, endothelial cells express P-selectin which promotes the adhesion of leukocytes in an initial rolling process (40). Following that, leukocytes bind firmly to the endothelial cells through the bonding between the integrins on the leukocytes and adhesion molecules on the endothelial cells, such as lymphocyte function-associated 1- intercellular adhesion molecule 1 (LFA1-ICAM-1), Integrin α4β1-vascular adhesion molecule 1 (VLA4-VCAM-1) (41,42). The adhered leukocytes migrate through the tight junctions between endothelial cells and infiltrate into perivascular tissue, which can further cause disruption of vascular barrier function, intravascular volume

depletion, and edema buildup. A schematic of endothelial cell and leukocyte interaction is shown in Figure 1.2.

1.1.6 Pediatric CPB and Challenges

CPB is used in the correction surgeries to fix congenital heart defects (CHDs) in pediatric patients. While less invasive techniques such as catheterized procedures are developed and implemented, open-heart surgery is still the most effective way to correct CHDs with features that are difficult to classify. Since its first use in a surgery to close an atrial septal defect (ASD) in 1953, CPB has been an important part of the surgical procedures to repair CHDs (43). However, due to lack of optimization in the pediatric CPB setup, patients frequently develop perioperative and post-CPB complications. Systemic inflammation which impacts the cardiopulmonary, renal, and cerebral systems is commonly observed in response to the activation of cells exposed to the CPB environment (44). Several factors that need to be optimized in pediatric CPB include prime volume, temperature management and bypass flow rate.

Pediatric patients are prone to CPB complications due to the disparity between the size of the equipment and the patients with the bypass volume being 2 to 3 times of the patients' own blood volume (45). The bypass volume includes the solutions, such as crystalloid, colloids, or blood products to prime the circuit. The specific prime volume is determined by the size of the tubing, venous reservoir, and oxygenator and can vary from 244 to 268 cc (46). Disproportionately high prime volume in pediatric patients can lead to hemodilution, which will increase the onset of tissue edema and complement and stress hormone release (47). While hemodilution can be resolved by transfusion of red blood cells, the postoperative mortality is correlated to the transfusion according to several studies (48,49). One potential solution to this

dilemma is to minimize the CPB circuit. This not only reduces the contact surface of the blood, but also decreases the demand for prime volume. In a design of an oxygenator with integrated arterial line filter, the hollow fiber of the oxygenator is surrounded by layers of the filter (50). Subsiding the arterial line filter by incorporating it into the oxygenator can reduce the prime volume by 20% (50). Other efforts have been made to minimize the tubing, which accounts for 75% of the prime volume. For example, thinner tubing of 1/8 inch, 3/16 inch, and 1/4 in diameter was used, which reduced the prime volume by approximately 60% (51). However, in these cases, a majority of the patients will still require transfusion to reverse the hemodilution and maintain hematocrit (52-54).

The temperature at which CPB is conducted can impact the outcome of the pediatric CPB. Although it is still debatable whether hypothermia should be performed with pediatric CPB, hypothermia is generally recognized as the best approach to prevent neurological sequelae. A hypothermia is defined as mild ranging from 30-34°C, moderate ranging from 25-30°C, and deep ranging from 15-22°C. The optimal temperature for pediatric CPB is not determined and the actual systemic temperature can vary depending on the disease and age group. For example, normothermic conditions are shown to be as safe as hypothermic conditions in patients with simple CHD (55). While normothermic conditions can induce less organ dysfunction both in adults and pediatric patients, hypothermia conditions are advocated by the pediatric centers since low temperature reduces the metabolic rates and oxygen demand (56). Theoretically, this provides a protective effect to the organs, especially the brain with high demand for glucose supply. Other advantages of hypothermia include allowing for a lower pump flow rate, therefore inducing less blood trauma, and improving the visibility of the surgical field (57). On the other side of the spectrum, hypothermic conditions can be detrimental to patients by inhibiting

enzymatic activities such as the coagulation pathway, promoting oxidative stress, which will provoke the onset of organ dysfunction (58). Additionally, it increases the permeability of the membrane and can cause capillary leak (59). However, these adverse effects can be reversed by rewarming.

The current bypass flow rate for pediatric patients is extrapolated from the adult setting. Using high flow rate is common in pediatric patients since their metabolic rate is nearly two times that of adults. In CPB, High flow rate is generally considered beneficial since it prevents the increase in lactate level, which is associated with postoperative mortality (60). Additionally, some evidence has shown that using higher flow can reduce the incidence of acute kidney injury in pediatric patients (61). Although the CPB flow rate is customized with the body area of the patients, the optimal flow rate in pediatric patients is unknown because of their variable anatomic structure of the heart. For example, patients with left-to-right shunts will have low physiological flow rate due to the reduction in the systemic flow (62).

1.1.7 Shear Stress in Pediatric CPB

CPB can expose blood components to a high-shear-stress environment. Shear stress is defined as the dragging force generated by flowing liquids to its boundary. In a CPB circuit, shear stress is generated when the blood flows through the tubing made of artificial material and being squeezed by the roller pump head (63,64). This creates a shear-stress environment that is different from the native blood vessel with endothelial lining. Additionally, high flow rate in pediatric CPB can translate to high velocity gradient in CPB tubing with constant cross-sectional area. This further increases the shear stress since it is proportional to the velocity gradient. As a result, blood components in the circuit can experience an average shear stress up to 2.1 Pa, which

is twice as much as the physiological shear stress in a blood vessel (65). Study has shown that this level of shear stress can induce apoptotic and necroptotic death of the leukocytes in a duration of 2 hours, which is a typical time span for CPB (65). The leukocytes activated by CPB shear can release proinflammatory cytokine and damage-associated molecular patterns to cause systemic inflammatory response and organ damage. Moreover, high shear stress can also rupture the red blood cells, causing the release of free hemoglobin (fHb), and lead to hemolysis (66). Normally, fHb can be scavenged by haptoglobin made by the liver. In pediatric patients, the level of fHb almost always exceeds the scavenging capability of haptoglobin (66,67). This leads to elevating fHb level in the blood, which further causes systemic dystonia, clotting disorders and increased mortality rate (66).

1.2 SIGNIFICANCE

CHD is the most common type of birth defect that affects nearly 1% of births in the US annually (68). Around 25% of the infants with severe CHD will need open-heart surgery within one year from birth (69). To reduce the ischemic damage during cardiac surgeries, the infants are usually placed on CPB (70). This extracorporeal circuit provides physical support and creates a bloodless field in the heart to facilitate surgical interventions. However, exposure to CPB can result in systemic inflammation and multiorgan dysfunction due to the mechanical insults to the blood components. This translates to a high mortality or severe complication rates of 10.7% and 29.2%, respectively in pediatric patients (71).

Shear stress has been recognized as a major factor that contributes to blood trauma and inflammatory response in pediatric CPB (64,72-75). A recent study focused on investigating the CPB-induced trauma to leukocytes, in which THP-1 cells were sheared in an *in vitro* CPB circuit (65). The CPB shear upregulated proinflammatory cytokine levels, especially TNF-α and IL-8 in THP-1 cells through calcium-dependent signaling pathways and gave rise to a subpopulation of THP-1 cells undergoing TNF-α-mediated necroptosis (65). The inflammatory response of CPB also involves the endothelium playing an active part. Leukocyte insult on the endothelium, including adhesion and transmigration, was observed in CPB patients with organ dysfunction but the molecular mechanism is unclear (76). Knowing the role of CPB shear in mediating the crosstalk between blood cells and endothelium may reveal the targetable pathway to counteract CPB-induced inflammations.

1.3 INNOVATION

The overarching aim of this study is to elucidate the mechanisms that lead to complications and mortality following CPB in pediatric patients. The status quo treatment utilizing corticosteroids and non-pharmacological interventions have had limited success in addressing the complications associated with CPB since none of the approaches are targeted to specific pathways (77-79). Hereby, we identified CPB shear as a key element that initiates the inflammatory cascade, including the interplay between monocytes and endothelium and pro-inflammatory cytokines derived from shear-activated blood cells. This is accomplished by using a novel *in vitro* CPB model to decouple the effect of shear stress from other factors such as temperature and surgical trauma. In all, the results of this study will help discover targetable CPB-specific pathways to reduce the systemic inflammatory response in pediatric patients. The findings from the study will shift the paradigm for clinical treatment and improve the prognosis of CPB-related complications in pediatric patients.

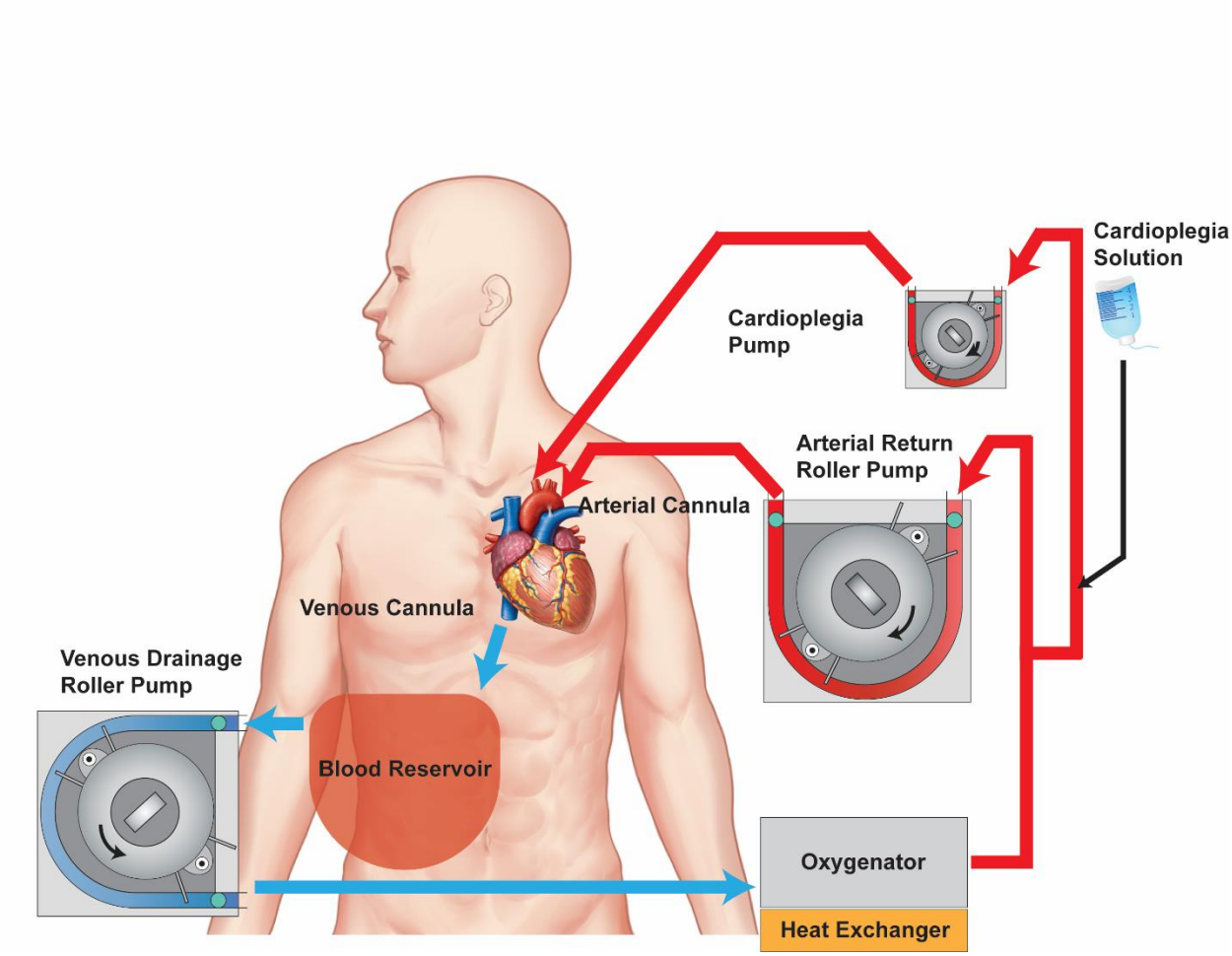

Figure 1.1. Schematic of CPB. The venous return blood is drained into a reservoir through venous cannula (blue line and arrows). The blood in the reservoir is then driven by the venous drainage pump, propelled to the oxygenator. In the oxygenator, the venous blood is oxygenated and ready to be used. The oxygenated blood stream (red line and arrows) splits in the returning line. The first line goes back to the patients through the aortic cannula, which is usually located at the distal ascending aorta. Another line is mixed with cardioplegia and goes back to the patients through a cannula that is closer to the ascending aorta.

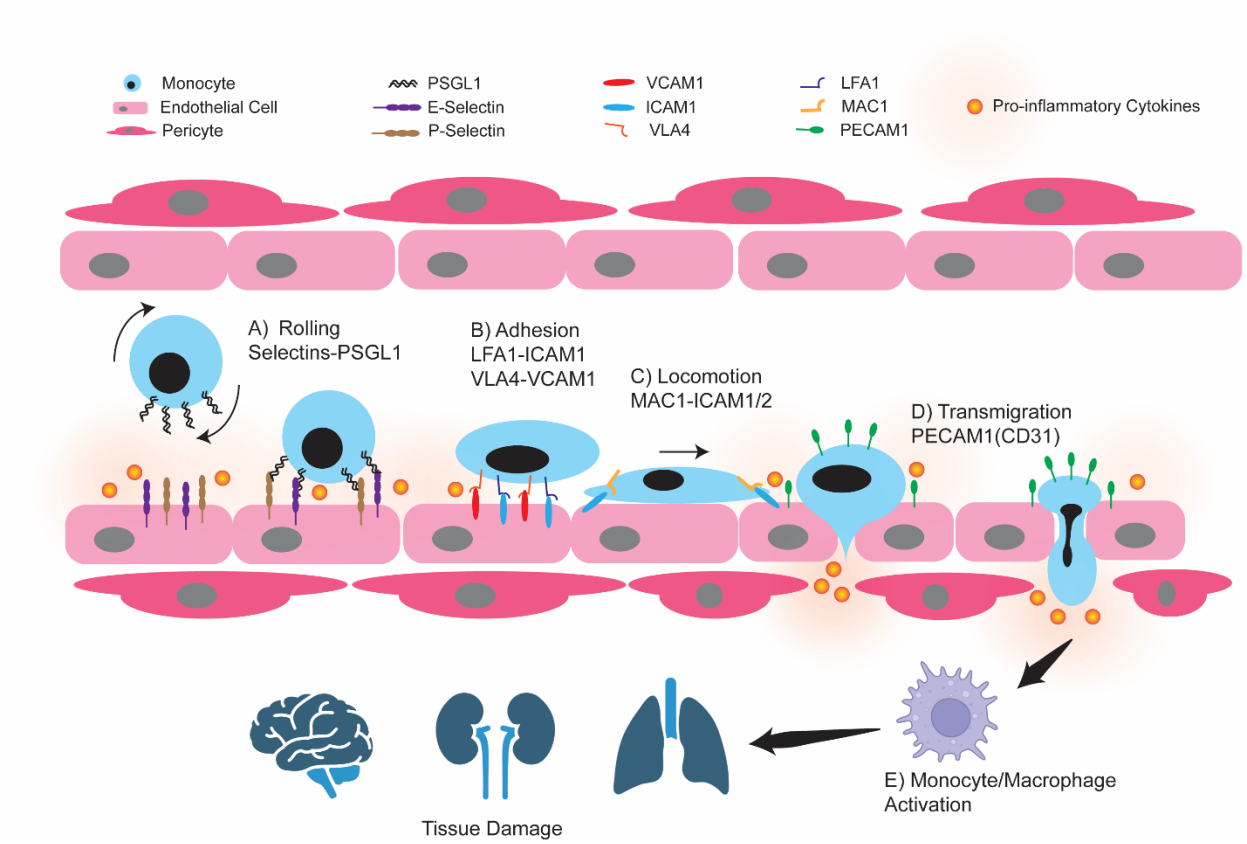

Figure 1.2. Schematic of endothelial cell and leukocyte interaction. A) Rolling process is promoted by the selectin-PSGL1 interaction. B) Adhesion of leukocytes is mediated by the bonding between integrins and adhesion molecules. C) Leukocyte migration is mediated by macrophage-1 antigen (MAC1) and intercellular adhesion molecule. D) Leukocyte transmigration through the endothelium. E) Activated monocyte/macrophage infiltrate and damage organs.

Chapter 2. RESEARCH GOALS

The objective of this study is to investigate the mechanism of inflammatory response induced by CPB shear through monocyte and endothelial cell interaction and endothelial response to CPB-derived cytokines. Previous studies proposed different mechanisms to regulate the inflammatory response of leukocytes and endothelial cells. For example, high levels of inflammatory cytokines, such as TNF-α, IL-8, and IL-6, in the serum of neonatal patients were found to be linked to days in the intensive care unit and inotropic support (80-89). Additionally, shedding of endothelial glycocalyx into the patients' plasma in response to increased damage associated molecular patterns released by necroptotic leukocytes resulted in the damage to the endothelial monolayer (90). Other studies interrogating blood or plasma during and after CPB found circulating soluble factors such as P-selectin, E-selectin, von Willebrand factor, and angiopoietin-2 in the plasma contributed to the endothelium hyperpermeability, which facilitated the infiltration of leukocytes (91-95). However, since these studies were obtained with clinical samples from patients undergoing cardiac surgery, the results cannot decouple the effects of CPB shear and surgical intervention.

Given this background, I propose using an *in vitro* model to study the mechanisms that may drive the inflammatory response after CPB procedure in pediatric patients. In this *in vitro* model, blood cells will only be affected by shear stress exerted by the pump head and plastic tubing. This model will help us discover CPB-specific mechanisms that lead to the inflammatory response. The overall hypothesis is that CPB shear regulates the interaction between monocytes and endothelial cells by altering the adhesion and transmigration of the monocytes, and cytokine release profile of the monocytes and monocyte-endothelial cell co-culture. To test this hypothesis, I propose the following specific aims:

Specific Aim 1. Determine the inflammatory cytokines that regulate the CPB-specific inflammatory response.

Hypothesis: *THP-1 monocyte-like cells activated by CPB shear 1) lead to increasing adhesion to and transmigration through endothelial monolayer, 2) affect the barrier function of the endothelial monolayer, and 3) change the cytokine release profile of monocyte-endothelial co-culture.*

To study the sole effect of CPB shear, an *in vitro* CPB model was developed, which consists of PVC tubing, a peristaltic roller pump and a temperature-controllable water bath. THP-1 cells, a neonatal human monocyte-like cell line, were sheared in the *in vitro* CPB circuit and collected for downstream analysis. Previous studies have demonstrated that CPB shear specifically upregulates the expression and secretion of IL-8 and TNF-α in THP-1 cells using this *in vitro* CPB setup (65). The inflammatory response after CPB, however, involves the interaction between monocytes and vascular endothelial cells. With the driver of the monocyte-endothelium crosstalk remaining unclear, I propose this study to elucidate the role of specific cytokines in mediating the monocyte-endothelium interaction after monocyte exposure to CPB shear. In this aim, a monocyte adhesion assay and transmigration assay were developed to assess the interaction between monocytes and endothelium. The barrier function of the endothelium treated with sheared monocytes was characterized by examining the VE-cadherin and intercellular gap formation. Lastly, the monocyte and endothelial cell co-culture media was collected and the levels of IL-1β, IL-6, IL-8 and TNF-α were measured using ELISA.

Specific Aim 2. Determine the CPB-induced mechanism of inflammatory response.

Hypothesis: *The inflammatory response of monocytes and endothelial cells induced by CPB sheared monocytes is mediated by the IL-8 signaling pathway.*

In Aim 1, I demonstrated that IL-8 was significantly upregulated in the co-culture media in the sheared monocyte-treated group, along with increasing monocyte adhesion and transmigration, disruption of endothelial adherens junction, and reorganization of endothelial cytoskeleton. These results suggest that IL-8 was pivotal in mediating the crosstalk between monocytes and the endothelial cells. IL-8 is well-known to regulate neutrophil functions by promoting chemotaxis, causing release of lysosomal enzymes, increasing intracellular calcium, and priming of the oxidative burst (96-100). Much less is known on the functions of IL-8 in monocytes and endothelium interaction. Based on my findings in Aim 1, I speculate that CPB sheared-monocyte treatment specifically upregulates the production of IL-8 in one or both of the co-culture cell types, and this may affect the endothelial cells through either paracrine or autocrine processes. In this aim, I investigated the mechanism of inflammatory response induced by CPB shear through blocking, promoting, and silencing the IL-8 signaling pathway.

Specific Aim 3: Investigating the effect of anti-inflammatory drugs on the soluble factor composition of media conditioned by sheared monocytes.

Hypothesis: *CPB shear upregulates the release of inflammatory cytokines by the monocytes, and the cytokine composition of sheared monocytes can be modified by dexamethasone and FK506*

Soluble factors released by sheared blood cells during CPB play important roles in mediating the inflammatory response. In this aim, the shear conditioned media, which contains the soluble factors derived from CPB shear, was studied. I first determined the cytokine release profile of monocytes affected by CPB shear. ELISA and Luminex multiplex assay were used to

measure the levels of soluble factors including cytokines, chemokines and growth factors in the sheared conditioned media. In addition, corticosteroid has shown high potency attenuating inflammatory response but not that induced by CPB. The failure of corticosteroid may be due to its ineffectiveness in modifying the cytokine released by sheared monocytes. Therefore, I probed the soluble factors release profile of sheared monocytes in response to a commonly used corticosteroid, dexamethasone using ELISA and Luminex multiplex assay. FK506, a calcineurin inhibitor with known effect in reducing shear-stress-induced inflammatory cytokines in monocytes, was used as a positive control.

Specific Aim 4. Investigating the effect of shear conditioned media on endothelial cells

Hypothesis: *The inflammatory response of endothelial cells can 1) be induced by conditioned media derived from sheared monocytes, and 2) be attenuated by conditioned media derived from monocytes sheared with dexamethasone or FK506.*

The endothelial dysfunction in CPB can be triggered by the exposure to the inflammatory cytokines released by shear activated blood cells. In this aim, the response of endothelial cells to CPB-induced soluble factors were characterized. Endothelial cells were treated with conditioned media from sheared monocytes, monocytes sheared with dexamethasone, and monocytes sheared with FK506. The response of endothelial cells was investigated using immunofluorescent staining, rhodamine phalloidin staining, live and dead assays, qPCR, and monocyte adhesion assay.

Chapter 3. CHARACTERIZING THE INTERACTION BETWEEN SHEARED MONOCYTES AND VASCULAR ENDOTHELIAL CELLS USING THE *IN VITRO* CPB MODEL

3.1 ABSTRACT

The use of CPB is associated with sterile systemic inflammation that leads to morbidity and mortality. Pediatric patients with CHD are particularly vulnerable to CPB exposure due to unoptimized settings. Previous work has demonstrated that the shear stresses existing during CPB are sufficient to stimulate non-adherent monocytes, which can initiate the inflammatory cascade. The interactions between shear-stimulated monocytes and vascular endothelial cells, however, have not been investigated. In this chapter, I tested the hypothesis that supraphysiological shear stress experienced by monocytes during CPB affects the integrity and function of the endothelial monolayer. I used an *in vitro* CPB model to study the interaction between THP-1 monocyte-like cells and HNDMVECs. THP-1 cells were sheared in PVC tubing at 2.1 Pa, twice of physiological shear stress, for 2 hours. Adhesion assay, transmigration assay, immunofluorescent staining and ELISA were used to assess the interactions between THP-1 cells and HNDMVECs during co-culture. I found that sheared THP-1 cells adhered to and transmigrated through the HNDMVEC monolayer more readily than static THP-1 controls. Treatment of Sheared THP-1 cells lead to disruption of the VE-cadherin and reorganization of cytoskeletal F-actin in HNDMVECs. In the sheared THP-1 and HNDMVEC co-culture medium,

IL-8 level was upregulated compared to static THP-1 and HNDMVEC medium. These results showed that the *in vitro* model recapitulated the monocyte and endothelial cell interaction during CPB and may reveal novel mechanisms of CPB-related complications.

3.2 INTRODUCTION

CPB is used in the surgical repair of CHDs to maintain the blood circulation in an extracorporeal circuit in which blood is propelled by mechanical pumps and flows in plastic tubing. This technique renders the heart bloodless to facilitate open-heart surgery, while minimizing the ischemic damage to the organs. However, CPB patients experience significant postoperative inflammation, especially within the pediatric population, with a complication rate of 29.2% [1]. These complications can lead to systemic inflammation and multiorgan dysfunction, which translates to longer intensive care unit stay and a mortality rate of 10.7% in the pediatric patients. The survivors of cardiac surgeries involving CPB also suffer from long-term complications such as the decreased cardiac systolic and diastolic function (101,102). This can eventually develop into Low Cardiac Output Syndrome in 46% of the neonates, which is associated with a dramatic decrease of quality of life (103). Long CPB duration can also induce cardiac fibrosis, which can negatively impact the cardiac function in the long term (104, 105). Additionally, CPB is correlated to impaired cognitive development in pediatric patients. Specifically, 30% of patients suffered weakened motor skills and executive function (106). Abnormal alterations of brain structure were observed in young patients after CPB (107). Given that CPB can cause a high incidence of severe complications, the understanding of the pathogenic mechanism of CPB is however very limited. Efforts have been made to suppress the inflammatory response through corticosteroid administration, coating the CPB tubing, and filtrating the blood postoperatively, no significant improvement has been reported (77-79). At

present, finding a CPB-specific pathway that leads to the inflammatory response in pediatric patients is the key to reducing the complication and motility rate.

Different mechanisms to regulate the inflammatory response in CPB have been proposed in previous studies. For example, neonatal patients with longer intensive care unit stay and inotropic support are found to have elevated levels of inflammatory cytokines in serum, such as TNF-α, IL-8, and IL-6 (80-89). Shedding of endothelial glycocalyx into the patients' plasma in response to increased damage associated molecular patterns (DAMPs) released by necroptotic leukocytes is indicative of the damage in the endothelium (90). Other studies found increasing circulating soluble factors such as P-selectin, E-selectin, von Willebrand factor, and angiopoietin-2 in the plasma of CPB patients contributed to the endothelium hyperpermeability, which facilitated the infiltration of leukocytes (91-95). However, since these studies were obtained with clinical samples from patients undergoing cardiac surgery, the results are likely to be caused by multiple factors induced by the surgical procedure, including surgical trauma, temperature management, and cardioplegia infusion. It remains challenging to find targeted pathways that prevent the inflammatory response specific to CPB.

In a recent study, CPB-induced shear stress has been identified as a major cause of inflammatory response of leukocytes. The study designed an *in vitro* CPB model to distinguish the non-CPB factors such as surgical trauma, blood transfusion, drug administration, and the specific condition of the patient from CPB-specific inflammatory changes (65). Using this model, the study demonstrated that CPB shear stress specifically upregulated the expression of IL-8 and TNF-α in monocytes, as well as giving rise to a subpopulation of monocytes undergoing TNF-α-mediated necroptosis (65). The inflammatory response of CPB also involves the interaction between leukocytes and endothelial cells with the endothelium adjusting the vascular barrier

function to allow adhesion and infiltration of the leukocytes. While the membrane integrity and permeability can be affected through different molecular and cellular mechanisms, finding the CPB-specific mechanism can help advance the understanding of leukocyte and endothelial cell interplay and strategize targetable therapies to counteract the inflammatory response of CPB. Hereby, I expanded this *in vitro* CPB model with cell adhesion assays, transmigration assays, immunofluorescent staining to characterize the interaction between leukocyte activated by CPB shear and endothelial cells.

3.3 MATERIALS AND METHODS

3.3.1 Cell Lines and Culture Methods

HNDMVECs (Cat # CC-2516) were purchased from Lonza (Walkersville, MD) and cultured in endothelial cell growth medium MV2 (PromoCell, Heidelberg, Germany, Cat # C-22121) with 100U/mL penicillin-streptomycin (Gibco, Waltham, MA, Cat # 15140122). The medium was changed every other day, and the cells were harvested by trypsinization. A HEK293T cell line was purchased from American Type Culture Collection (ATCC) (Manassas, VA, Cat # CRL-3216) and cultured in Dulbecco's Modified Eagle Medium (DMEM) (Gibco, Waltham, MA, Cat # 11995065) with 10% fetal bovine serum (FBS) (Atlanta Biologicals, Flowery Branch, GA, Cat # S11150) and 100U/mL penicillin-streptomycin. The medium was changed every other day, and the cells were harvested by trypsinization. The human acute leukemia monocytic cell line THP-1 (Cat # TIB-202) was purchased from ATCC and cultured in Roswell Park Memorial Institute (RPMI) 1640 medium (ATCC Modification) (Gibco, Waltham, MA, Cat # A1049101) with 10% FBS. The medium was changed every other day. Human peripheral blood mononuclear cells (hPBMCs) were purchased from Lonza (Walkersville, MD,

Cat # CC-2702) and maintained in RPMI 1640 medium (Gibco, Waltham, MA, Cat # 11875093) with 10% FBS.

3.3.2 GFP Positive THP-1 Cell Production

A THP-1 cell line that expresses GFP (G-THP-1) was produced by lentiviral transduction. Vectors carrying the plasmids of pSL3 (vesicular stomatitis virus G envelope), pSL4 (HIV-1 gag/pol packing genes), pSL5 (rev gene required for HIV-1 envelope protein expression) were a gift from Dr. Murry (University of Washington, Seattle, WA). The plasmid vector pCDH-EF1-MCS-T2A-copGFP was purchased from System Biosciences (Palo Alto, CA, Cat # CD526A-1). The lentiviral vector was packaged in HEK293T cells as previously described. Briefly, $3x10^6$ of HEK293T cells were plated in 10-cm dishes in DMEM with 10% FBS and 100U/mL penicillin-streptomycin until reaching 60% confluency. Prior to transfection, the culture media was changed. A total of 20µg plasmid DNA including 7.5µg of pCDH-EF1-MCS-T2A-copGFP, 2.5µg of pSL3, 6.7µg of pSL4, and 3.3µg of pSL5, and 24µL of lipofectamine 2000 ((Thermofisher, Waltham, MA, Cat # 11668019)) dissolved in 1600µL Opti-MEM I Reduced Serum Medium (Thermofisher, Waltham, MA, Cat # 31985062) were used for the transfection of one dish. The media was replaced after incubating for 6 hours at 37°C with 5% CO_2. The viral supernatant was collected at 48 hours from the media and filtered by a 0.45-µm filter. The viral supernatant was applied to the THP-1 cells at a multiplicity of infection (MOI) of 6 while being centrifuged at 800xg for 30 minutes. The transduced THP-1 cells (G-THP-1) were maintained in RPMI 1640 medium to proliferate and sorted for GFP expression using a BD Aria III cell sorter at the UW Laboratory Medicine and Pathology Flow Cytometry Core. A transduction efficiency of 92% was obtained (Figure 3.1).

3.3.3 Monocyte Adhesion Assay

HNDMVECs were seeded on 24-well plates at 5000 cells/cm^2 and cultured 7 days to form a confluent monolayer. Monocytes or hPBMCs were sheared as previously described. Briefly, G-THP-1 cells or hPBMCs at a density of 2 million cells/mL were sheared in a 10 foot-long Masterflex Tygon E-3603 L/S13 pump tubing (Cole-Parmer, Vernon Hills, IL, Cat # MMK-06509-13), using a Masterflex miniflex pump model 115/230 VAC 07525-20 (Cole-Parmer, Vernon Hills, IL, Cat # MK-07525-20) at 10 mL/min for 2 hours. The long side tubing was submerged in a water bath with temperature control at 37°C (CPB circuit arrangement shown in Figure 3.2). At the end of shear, the G-THP-1 cells or hPBMCs were collected, spun down and resuspended in fresh media. As a control, G-THP-1 cells or hPBMCs were incubated in a PVC flask at a density of 2 million cells/mL, 37°C with 5% CO_2 for 2 hours. G-THP-1 cells or hPBMCs, sheared or statically incubated, were then added to a monolayer of HNDMVECs ($1x10^6$ cells per well), followed by incubation for 1 hour. The co-cultures were gently rinsed twice with sterile phosphate-buffered saline (PBS) to remove nonadherent G-THP-1 cells or hPBMCs (Schematic of experiment shown in Figure 3.3) The adhered G-THP-1 were visualized using a Nikon Eclipse TE200 microscope (Tokyo, Japan) and a Photometric CoolSNAP MYO camera (Tucson, AZ) with a GFP filter. The adhered hPBMCs were visualized with the same microscope and camera with brightfield imaging. The experiments were run in triplicates. The number of adherent G-THP-1 cells or hPBMCs were counted in five randomly selected visible fields and quantified using ImageJ (108).

3.3.4 Monocyte Transmigration Assay

HNDMVECs were seeded in the upper chamber of a transwell tissue culture insert (6.5 mm diameter, 8 μm pore size polycarbonate membrane; Corning, NY, Cat # 3422) at 5000

cells/cm^2 and cultured 7 days to form a confluent monolayer. Sheared or statically incubated G-THP-1 cells were then added to the upper chamber ($2x10^5$ cells/well) with the lower chamber filled with RPMI 1640 media. After 24 hours of incubation, the upper chamber was removed and the THP-1 cells in the lower chamber were visualized using a Nikon Eclipse TE200 microscope and a Photometric CoolSNAP MYO camera and quantified with ImageJ (108). The migrated G-THP-1 cells in the lower chamber were quantified to determine the capability of tranendothelial migration (Schematic of experiment shown in Figure 3.4). The experiment was run in triplicates.

3.3.5 Immunofluorescent Staining

HNDMVECs were seeded on 8-chamber slides (354118, Corning, NY) at 5000 cells/cm^2 and cultured 7 days to form a confluent monolayer. The sheared or statically incubated G-THP-1 cells were then added to a monolayer of HNDMVECs ($1x10^6$ cells per well), followed by incubation for 6 hours at 37°C with 5% CO_2. The cell co-cultures were washed twice with sterile PBS, fixed with formalin. To stain the co-culture, the fixed cells were permeabilized with 0.1% Triton-X-100 for 10 minutes, blocked with 1% BSA and human BD Fc block (BD Bioscience, Franklin Lakes, NJ, Cat # 564219) for 1 hour, followed by incubation with 1:200 vascular endothelial cadherin (VE-cadherin) monoclonal antibody (16B1), Biotin (Thermofisher, Waltham, MA, Cat # 13-1449-82) for 1 hour, 1:500 streptavidin, Alexa Fluor 594 Conjugate (Thermofisher, Waltham, MA, Cat # S11227) for 45 minutes. Nuclei were stained with DAPI. The slides were then washed, mounted, and imaged using a Leica DMI6000 microscope with Leica SP8X confocal. VE-cadherin staining was quantified by fluorescent intensity using ImageJ (108).

3.3.6 Rhodamine-Phalloidin Labeling

HNDMVECs were seeded on 8-chamber slides at 5000 cells/cm^2 and cultured 7 days to form a confluent monolayer. The sheared or statically incubated G-THP-1 cells were then added to a monolayer of HNDMVECs ($1x10^6$ cells per well), respectively, followed by incubation for 6 hours at 37°C with 5% CO_2. The cell co-cultures were washed twice with sterile PBS, fixed with formalin, permeabilized with 0.1% Triton-X-100, and blocked with 1% BSA. The cells were then incubated with Rhodamine Phalloidin (ThermoFisher, Waltham, MA, Cat # R415) for 20 minutes at room temperature, stained with DAPI, washed, mounted, and imaged using a Leica DMI6000 microscope with Leica SP8X confocal. Intercellular gap area was quantified using ImageJ on the slides stained by the Rhodamine Phalloidin (108).

3.3.7 Enzyme-linked Immunosorbent Assays (ELISA)

The media supernatants of the HNDMVECs and THP-1 cells were collected at 0.5, 1, 3, and 6 hours of the co-culture. The levels of IL-1β, IL-6, IL-8 and TNF-α were measured using ELISA kits from Invitrogen (Catalog# BMS224-2, 88-7066-88, 88-8086-88, BMS223-4). Plates were read at 450 nm, normalized to standard solutions. Experiments were run in both biological and technical triplicates.

3.3.8 Statistical Analysis

All experiments were run in triplicates. All quantitative data were expressed as mean ± standard deviation within groups. Pairwise comparisons between groups were conducted using ANOVA test and Tukey's post-hoc test. Statistical significance is denoted by '*'. P values less than 0.05 are indicated by single star symbol and P values less than 0.01 are indicated by double star symbol.

3.4 RESULTS

3.4.1 CPB shear promotes mononuclear cell adhesion to and transmigration through endothelial monolayer.

The inflammatory response in CPB includes monocyte. Upon and after exposure to the CPB circuit, activated monocytes adhere to the vascular wall and migrate through the intercellular tight junctions, damaging different organs (76). To characterize this interaction between the CPB-activated monocytes and endothelial cells, a cell adhesion assay was developed. THP-1 cells were sheared in an *in vitro* CPB circuit (65), co-cultured with confluent HNDMVECs for 1 hour, and attached THP-1 cells were quantified. As shown in Figure 3.5A (More images shown in Figure 3.6), THP-1 cells activated by CPB shear are two-fold more likely to adhere to the HNDMVEC monolayers compared to static THP-1 cells. A similar trend was observed in PBMCs, where significantly more sheared mononuclear cells were quantified adhering to the endothelial cells compared to the static mononuclear cells (Figure 3.7A). Moreover, we found more sheared THP-1 cells transmigrated through the HNDMVEC monolayer grown on the transwell membrane and reached the bottom of the transwells compared to the static THP-1 cells (Figure 3.5D, more images shown in Figure 3.6). These results indicate that mononuclear cells are more adherent after exposure to CPB shear and more likely to transmigrate through a monolayer of endothelial cells.

3.4.2 Treating confluent HNDMVECs with sheared THP-1 cells resulted in disrupted intercellular junction and increasing gap formation.

The increasing transmigration of the sheared mononuclear cells indicates that the barrier function of the endothelial cells is compromised to allow for mononuclear cell infiltration. I

examined the intercellular adherens junction and cytoskeleton by staining the VE cadherin and F-actin filaments using immunofluorescent staining and rhodamine phalloidin staining, respectively. When HNDMVECs were co-cultured with sheared THP-1 cells, a loss of VE-cadherin junction signal was observed (Figure 3.8A). When HNDMVECs were co-cultured with static THP-1 cells, robust VE-cadherin junction was maintained (Figure 3.8B). These results suggested that THP-1 cells activated by the CPB shear are capable of disrupting the intercellular junction of the HNDMVECs.

Similarly, in the co-culture of sheared THP-1 cells and HNDMVECs, clustering of THP-1 cells was observed at the intercellular area of endothelial cells (Figure 3.10A). Quantification of intercellular gap formation showed an increasing gap area and a compromised cytoskeleton of the endothelial cells. In the co-culture of static THP-1 cells and HNDMVECs, fewer to no gap areas and adherent THP-1 cells were observed (Figure 3.10B). These results suggested that HNDMVECs reorganize the cytoskeleton for the infiltration of CPB-activated THP-1 cells.

3.4.3 Co-culture of sheared THP-1 cells and HNDMVECs results in increased IL-8 levels in the media

To analyze the inflammatory cytokine composition during the co-culture of THP-1 cells and HNDMVECs, we collected the co-culture media at 0.5, 1, 3, and 6 hours. The levels of IL-1β, IL-6, IL-8 and TNF-α in the co-culture media were measured using ELISA since these four cytokines point to unfavorable clinical outcomes in CPB patients. At every time point, the level of IL-8 in the sheared group was significantly higher than that in the static group (Figure 3.12A). The IL-8 concentration in the sheared group continued to increase over the period of 6 hours while the IL-8 concentration in the static group plateaued after 3 hours (Figure 3.12A). IL-6

levels in the sheared group increased at 3 and 6 hours but the concentration was extremely low (Figure 3.12B). We did not detect significant release of IL-1β and TNF-α in co-culture (Figure 3.13C, TNF-α data not shown). These results suggest that treating the HNDMVECs with sheared THP-1 cells specifically upregulated the IL-8 levels in the co-culture media.

3.5 DISCUSSION

This study is the first to show that monocytes activated by shear stress in a CPB-like condition adhere to and migrate through a confluent and unstimulated endothelial monolayer. I used an *in vitro* CPB model to investigate the interaction between shear-activated monocytes and HNDMVECs. My results showed that an average CPB shear stress of 2.1 Pa or 21 dyne/cm^2 promoted the adhesion and transmigration of monocytes to and through the endothelial monolayer. This occurred along with the disruption of VE-cadherin and the reorganization of cytoskeleton in the HNDMVECs. When probing cytokine composition, we found that IL-8 was significantly upregulated in the co-culture media, suggesting a key role of IL-8 in mediating the monocyte-endothelial interaction.

In this *in vitro* CPB model, the adhesion and transmigration of leukocytes through endothelial monolayer is recapitulated and characterized. The process of leukocyte rolling and binding to endothelial cells and transmigration through the endothelial monolayer is a fundamental cascade of inflammatory response to blood trauma. Previous study demonstrated that when using this *in vitro* CPB to recapitulate a prolonged CPB procedure, increasing expression of IL-8 and TNF-α were detected in monocytes sheared in the CPB circuit for 2 hours (65). With this expanded *in vitro* CPB model, we further found that sheared monocytes are more likely to adhere and transmigrate without additional stimulation. These results suggest that CPB

shear stress is sufficient to induce monocyte adhesion and transmigration. Importantly, in this study, monocyte adhesion and transmigration were independent of the material that the monocytes were cultured in since control cells incubated statically in PVC containers showed similar adhesion characteristic to cells statically cultured on tissue culture plastic (data not shown). Moreover, monocyte adhesion to endothelial cells have been reported, but with endothelial stimuli, commonly TNF-α (109,110). For example, Baratchi et al described activation of monocytes through calcium influx dependent pathway in response to elevated shear stress, which promoted their adhesion to TNF-α stimulated human umbilical endothelial cells (HUVECs) (110). My ELISA data showed no significant TNF-α release after the sheared monocytes were resuspended in fresh media, which suggests that TNF-α is not playing a role in the monocyte-endothelial interaction described in this study. A potential explanation is that shear stimulus leads to transient upregulation of TNF-α expression. When the shear conditioned media was removed along with the shear stress, the monocytes stopped producing TNF-α. These results indicate that different mechanisms regulate the monocyte-endothelial interaction in our model.

THP-1 cell line was used in this study as the monocyte model. THP-1 cell line has been commonly used to study the response of monocytes to mechanical stimuli due to its robust mechanosensing ability (111,112). For example, Fahy et al. studied the effect of shear and dynamic compression on THP-1 cells encapsulated in agarose gel (113). The difference between the immortalized THP-1 cell line and primary monocytes still exists. One notable difference is that the THP-1 cells lack CD14, which is a glycosylphosphatidylinositol-anchored monocyte differentiation antigen localized on cell surface. In primary monocytes, CD14 is highly expressed, which resulted in their superior ability to secrete pro-inflammatory cytokines such as IL-8 in response to LPS (114). In order to address this difference, I tested the *in vitro* model using

PBMCs, which consists of 10-20% of primary monocytes. We found that shearing PBMCs in the CPB circuit also promoted their ability to adhere to the endothelial monolayer. This suggests that the effect of CPB shear is ubiquitous across monocytes, whether from immortalized cell lines or primary sources.

Besides monocytes, other cellular components can react to shear stress during CPB. Increasing level of neutrophil extracellular traps (NETs) was detected in patients after CPB, indicating the activation of sterile inflammatory response with thrombosis in neutrophils (115). Limiting the neutrophil activity with leukocyte inhibition module resulted in lower neutrophil count in peripheral blood as well as higher cardiac indices in vivo (116). In an *in vitro* system, shear stress could override the signaling of soluble factors and modulate the activation of neutrophils (117). CPB is also correlated to decreases of T cells and lymphocytes in patients (118,119). However, monocytes are reported to contribute the most to the CPB-induced inflammatory response at transcriptional level compared to other cell populations in the blood (65). Therefore, the CPB model in this study is representative of the primary driver in CPB-related inflammatory response.

In conclusion, I used the *in vitro* CPB model to recapitulate inflammatory response of monocytes and endothelial cells. The ability of sheared monocytes to adhere to and transmigrate through the endothelial monolayer is significantly increased compared to monocytes statically cultured in a PVC container. The infiltration of the sheared monocytes is likely caused by the disruption of adherens junction in the endothelial cells and the increase in intercellular gap as indicated by the VE-cadherin immunofluorescent staining and F-actin cytoskeleton staining. The monocyte-endothelial interaction is also accompanied by a change in the cytokine profile with the IL-8 being upregulated in the sheared monocyte-treated group at all time points. In the next

chapter, the correlation between IL-8 and monocyte-endothelial interaction will be further addressed.

\

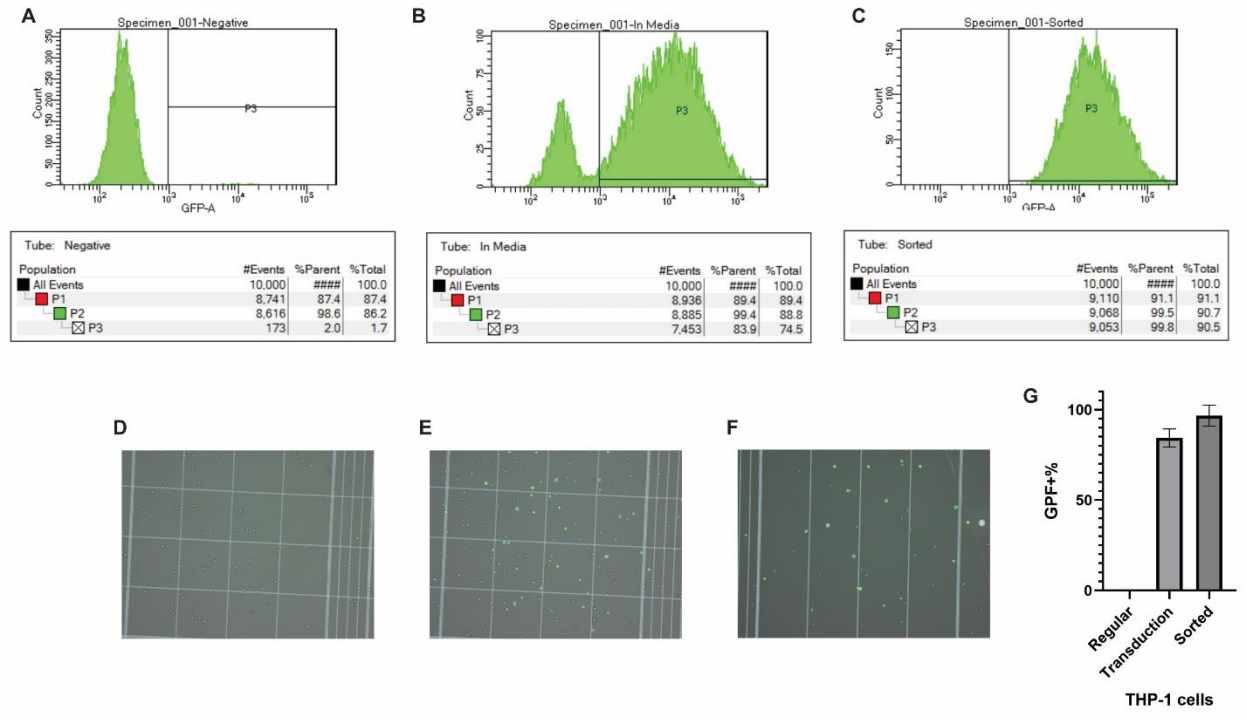

Figure 3.1. GFP population of THP-1 cells measured by flow cytometry in A) regular THP-1 cells, B) transduced THP-1 cells, and C) sorted THP-1 cells. Images of D) regular THP-1 cells, E) transduced THP-1 cells, and F) sorted THP-1 cells. Channels of bright field and GFP were merged. E) Quantified GFP population in the THP-1 cells.

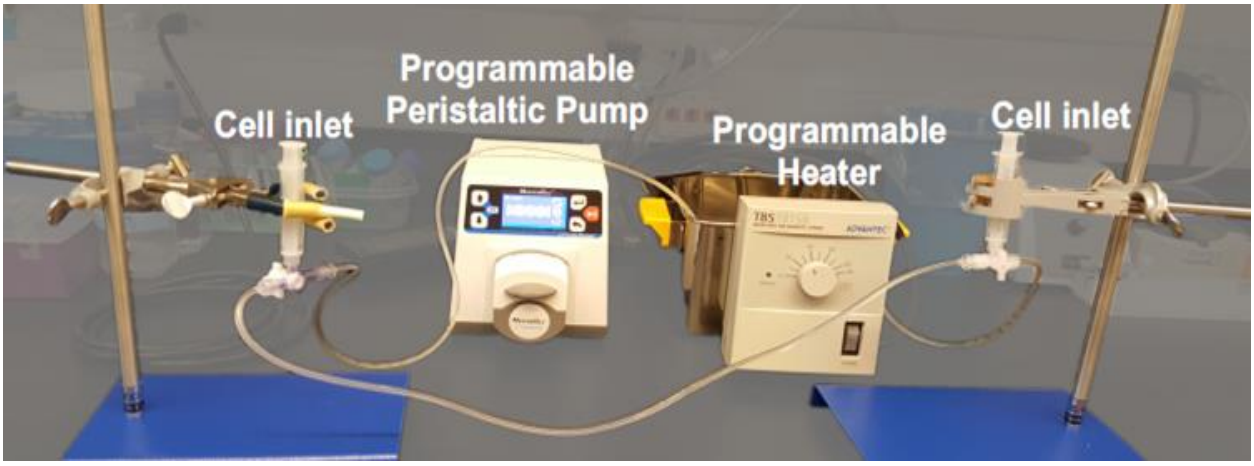

Figure 3.2. Arrangement of *in vitro* CPB circuit. The circuit consists of PVC tubing, cell inlets, a peristaltic pump, and a programmable heater. Cells are loaded in the inlet, propelled by the peristaltic pump. The heater is used to maintain the temperature of the cell suspension.

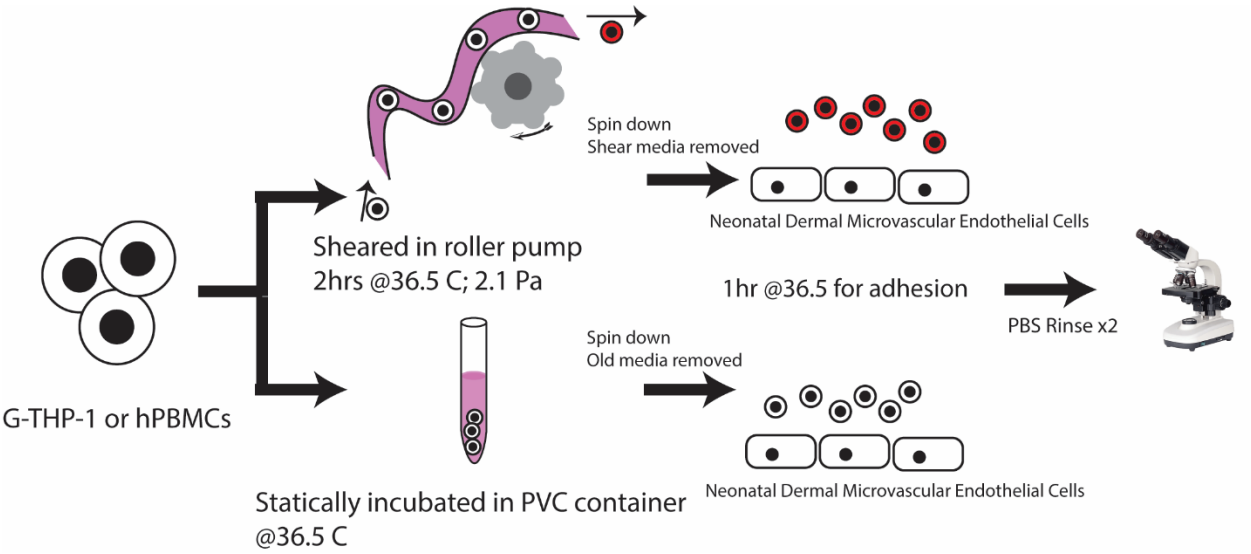

Figure 3.3. Schematic of adhesion assay

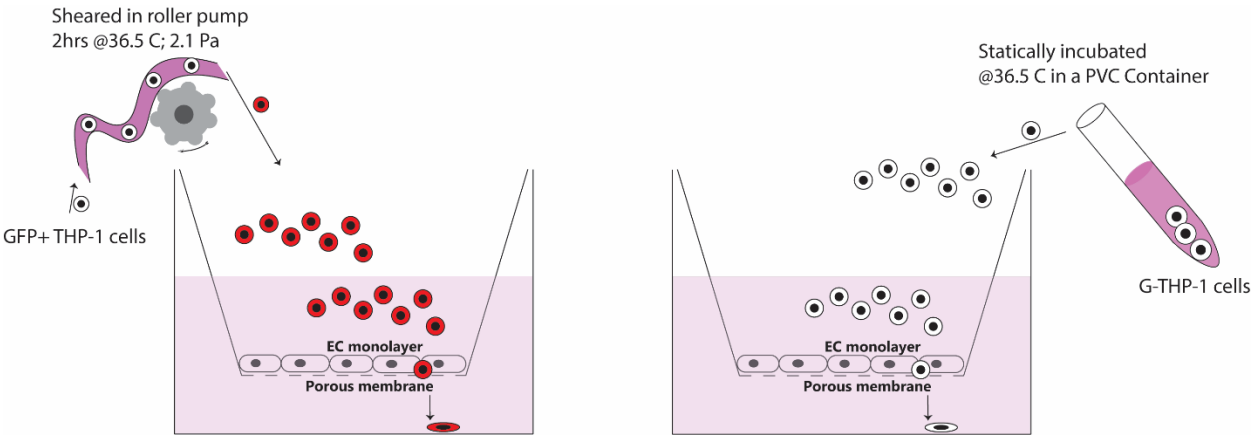

Figure 3.4. Schematic of transmigration assay

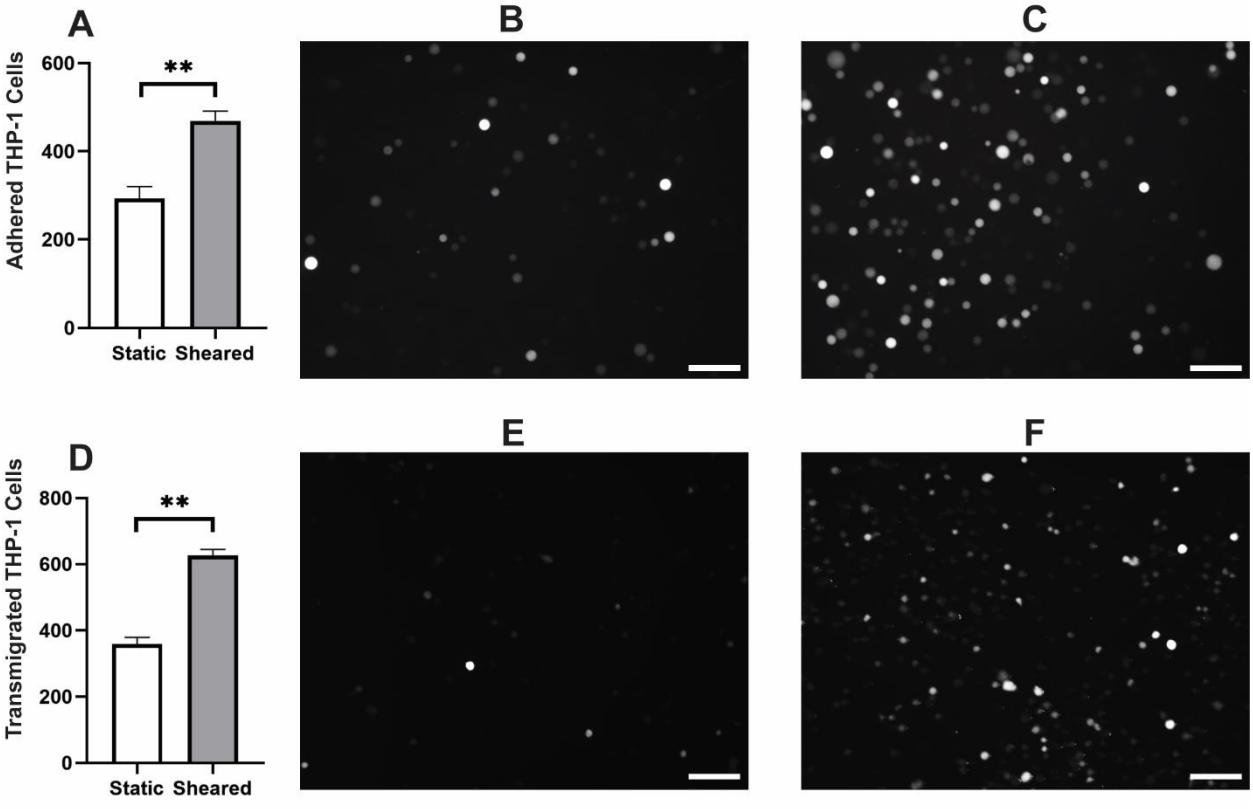

Figure 3.5. Figure 1. A) Quantitative analysis of adhered G-THP-1 cells on the endothelial cell monolayer. B) Adhesion of G-THP-1 cells incubated statically in a PVC flask. C) Adhesion of G-THP-1 cells sheared in a CPB circuit. D) Quantitative analysis of transmigrated THP-1 cells through endothelial cell monolayer. E) Transmigrated G-THP-1 cells incubated statically in a PVC flask. F) Transmigration of G-THP-1 cells sheared in a CPB circuit. Scale bar = 100 μm. Additional images see Figure 3.6. Statistical significance is denoted by '*'. P values less than 0.05 are indicated by one star symbol and P values less than 0.01 are indicated by double star symbol.

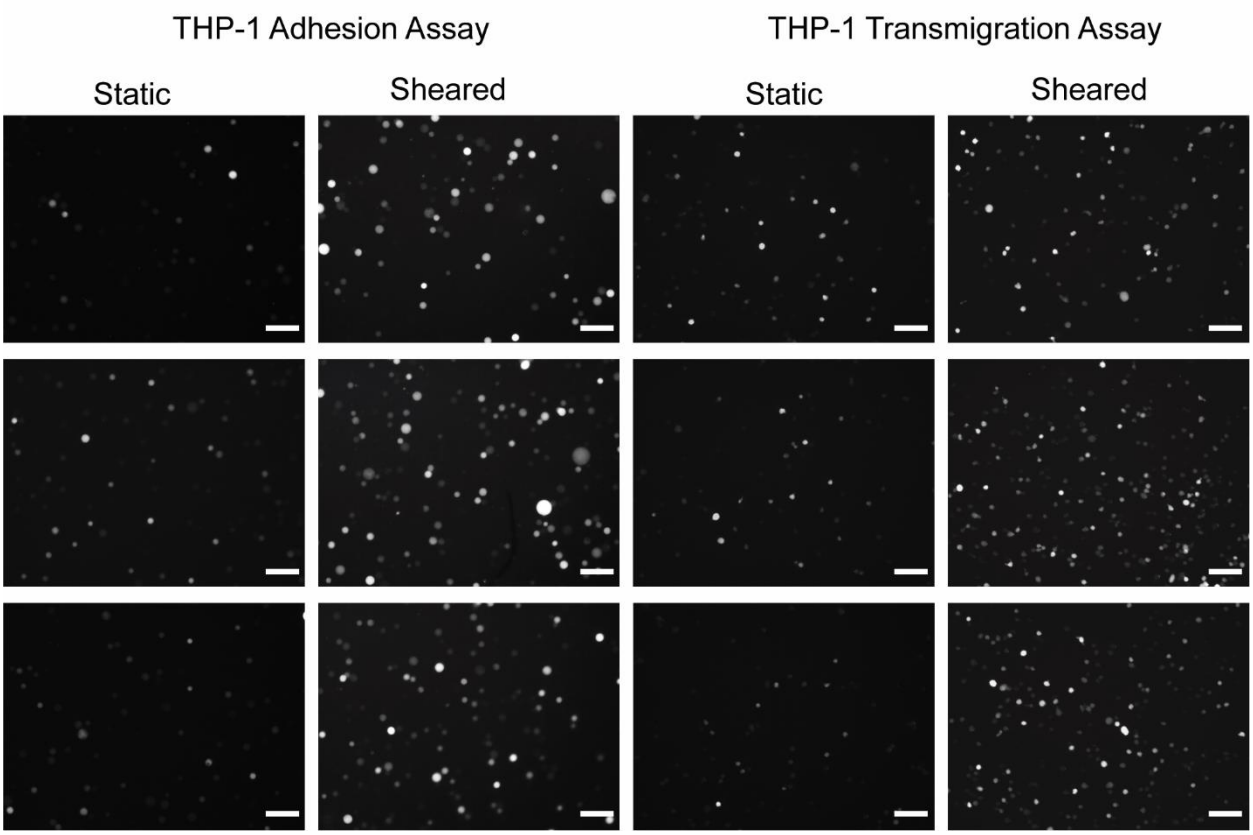

Figure 3.6. Additional images of adhered and transmigrated THP-1 cells were used for quantitative analysis. Scale bar = 100 μm.

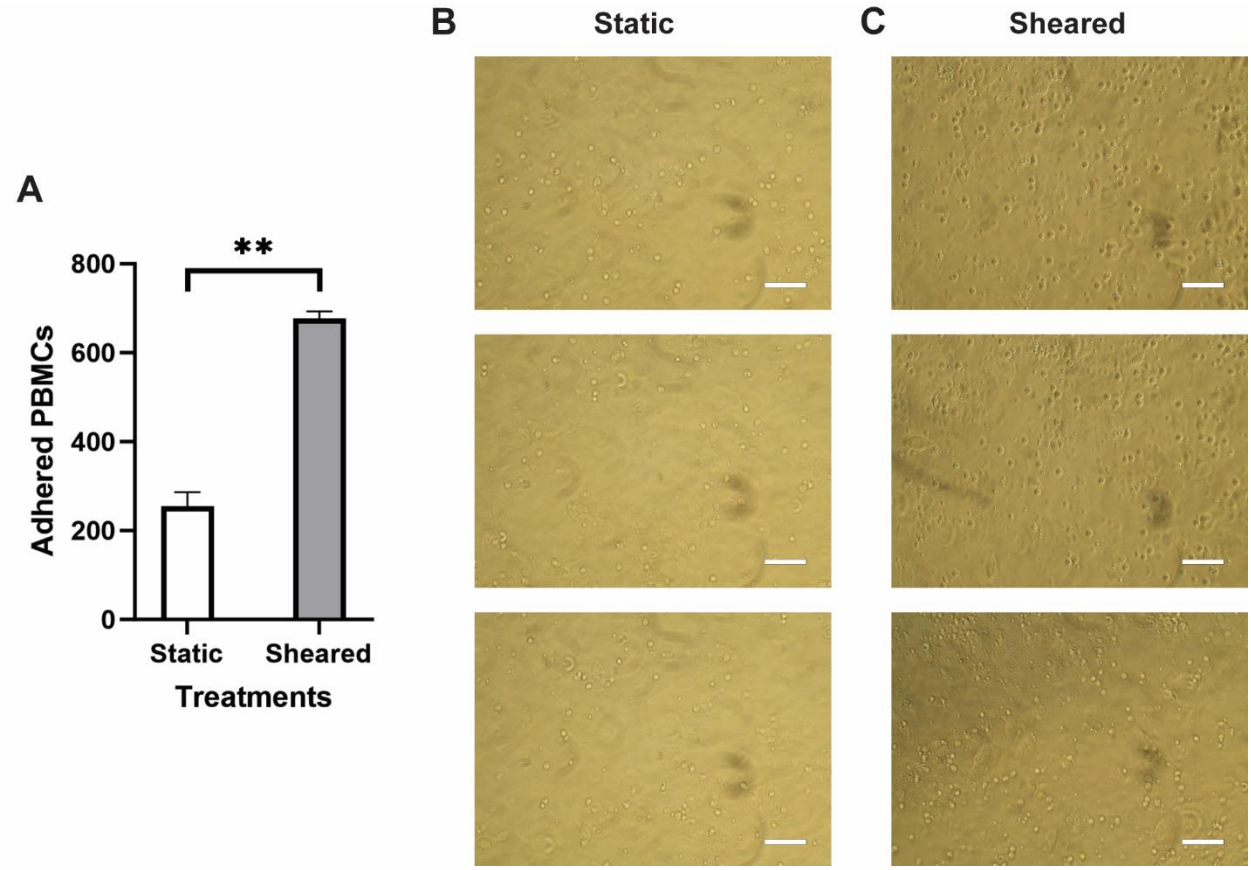

Figure 3.7. A) Quantitative analysis of adhered PBMCs on the endothelial cell monolayer. B) Adhesion of PBMCs incubated statically in a PVC flask. C) Adhesion of PBMCs sheared in a CPB circuit. Scale bar = 100 μm. Statistical significance is denoted by '*'. P values less than 0.05 are indicated by single symbol and P values less than 0.01 are indicated by double symbols.

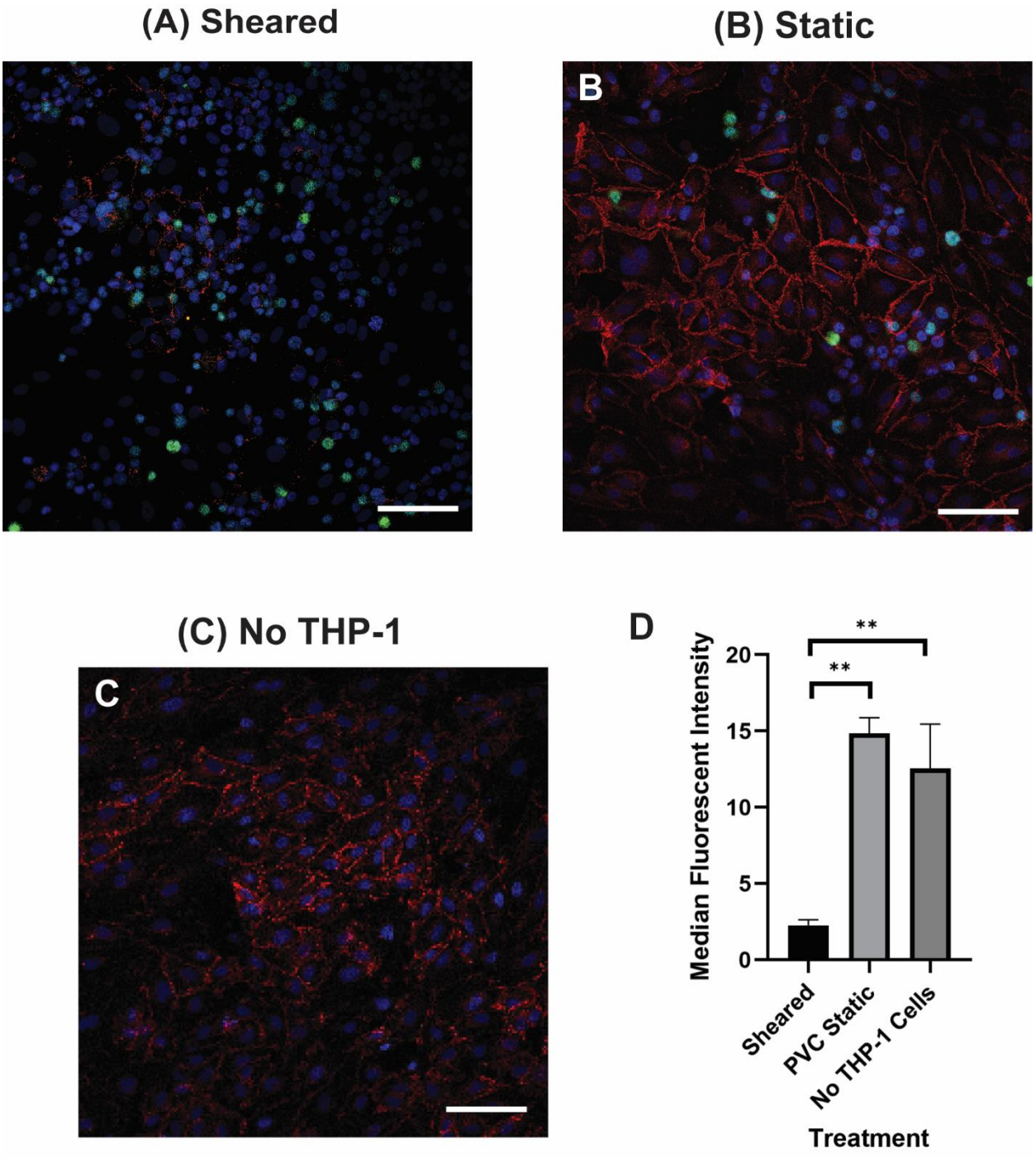

Figure 3.8. VE-cadherin of HNDMVECs co-cultured with A) sheared THP-1 cells, B) THP-1 cells statically incubated in PVC flask, and C) No THP-1 treatment, visualized by immunofluorescent staining. Additional images see Figure 3.9. Red = VE-Cadherin, Green = THP-1 Cells, Blue = DAPI. Scale bar = 100 μm. D) Quantification of VE cadherin staining.

Statistical significance is denoted by '*'. P values less than 0.05 are indicated by one star symbol and P values less than 0.01 are indicated by double star symbol.

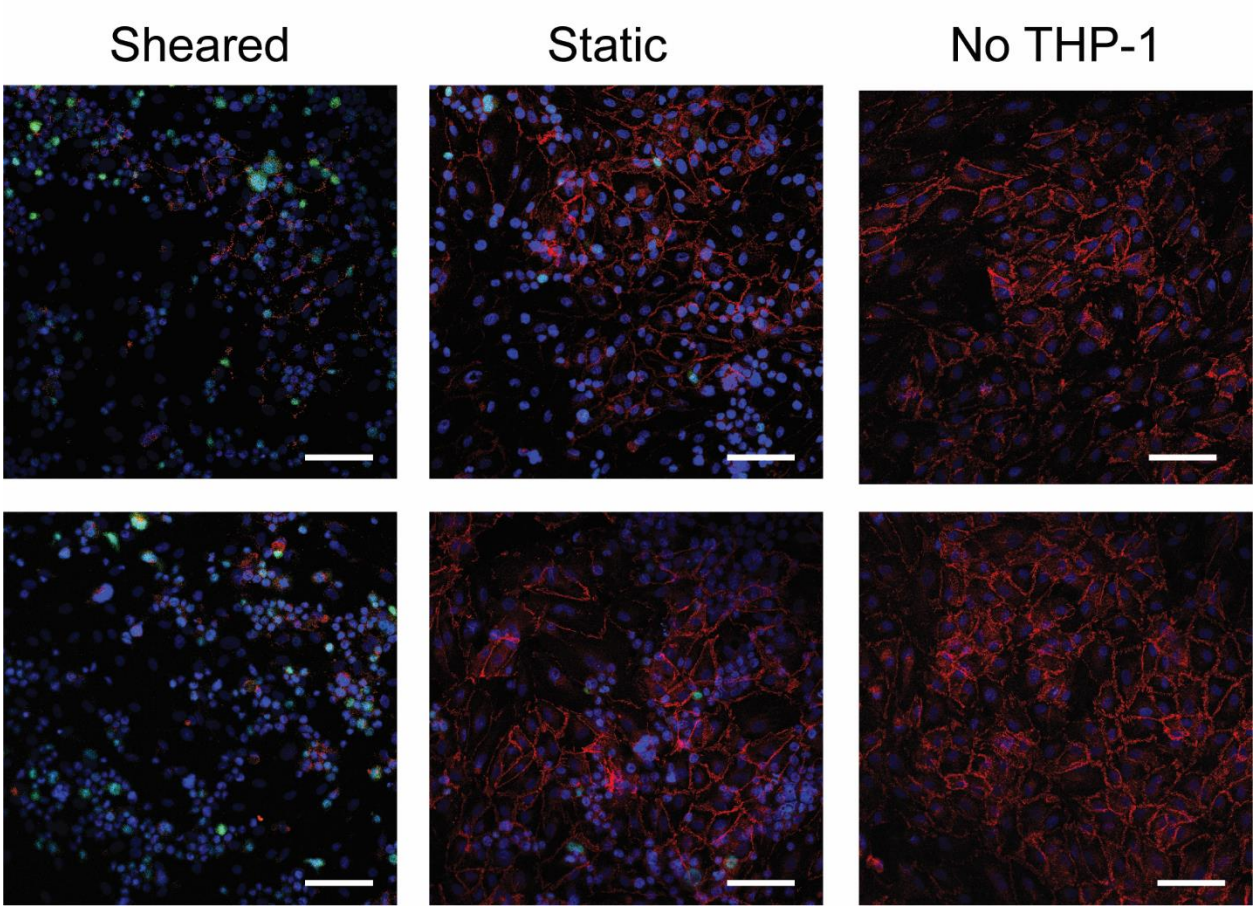

Figure 3.9. Additional images of VE-cadherin staining. Scale bar = 100 μm.

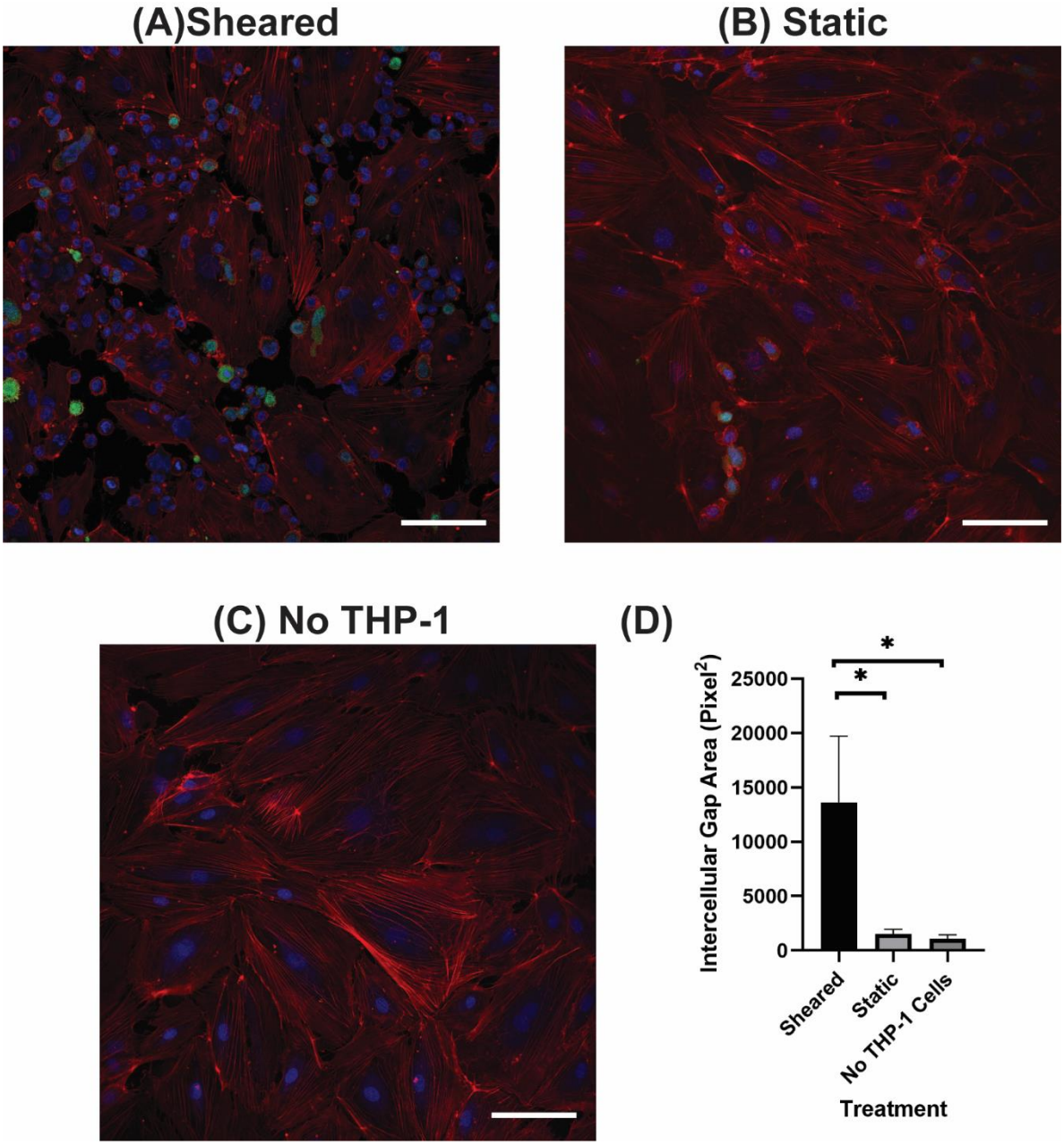

Figure 3.10. F-actin of HNDMVECs co-cultured with A) sheared THP-1 cells, B) THP-1 cells statically incubated in PVC flask, and C) No THP-1 treatment, stained by rhodamine phalloidin. Additional images see Figure 3.11. Red = F-actin, Green = THP-1 Cells, Blue = DAPI. Scale bar = 100 μm. D) Quantification of intercellular gap areas of endothelial cells. Statistical

significance is denoted by ‘*’. P values less than 0.05 are indicated by one star symbol and P values less than 0.01 are indicated by double star symbol.

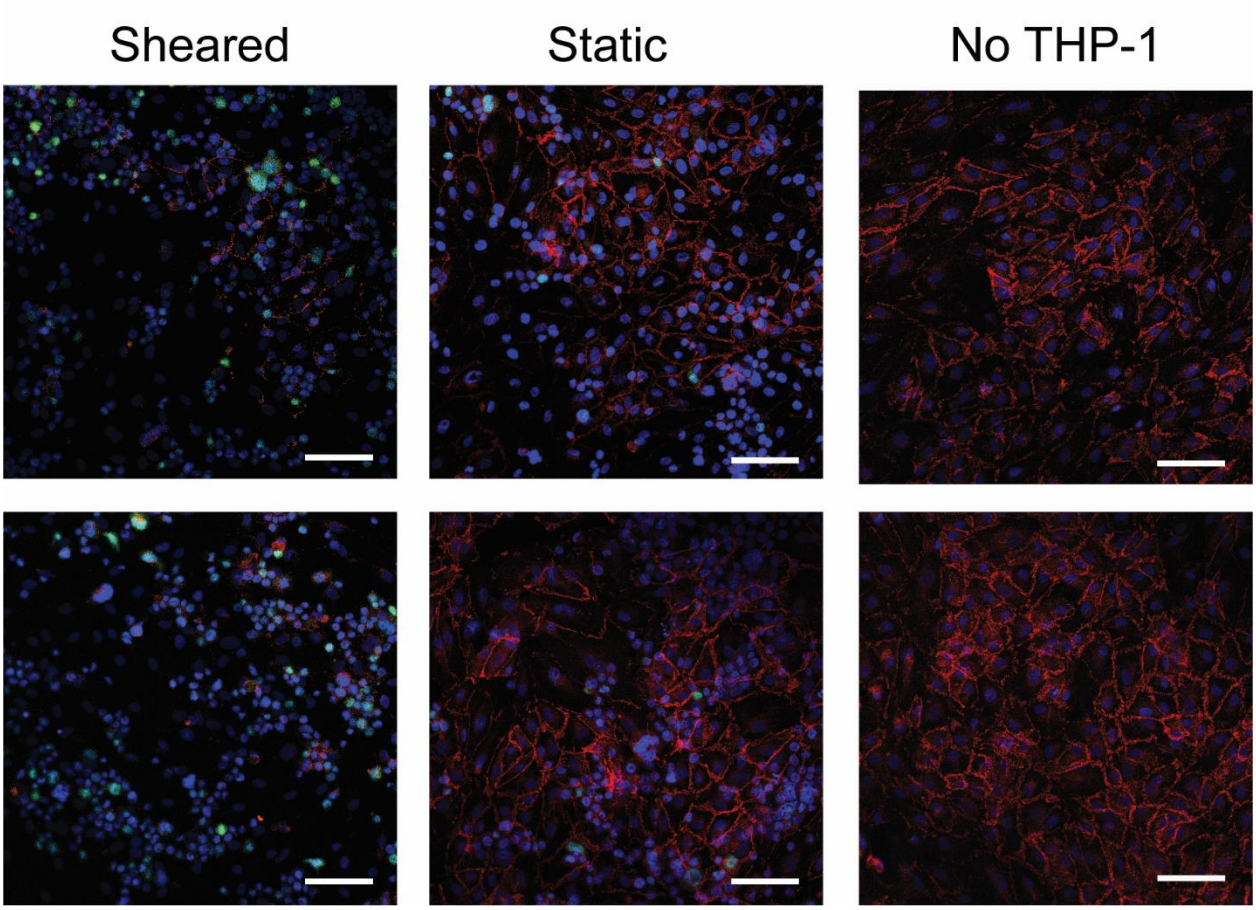

Figure 3.11. Additional images of F-actin staining. Scale bar = 100 μm.

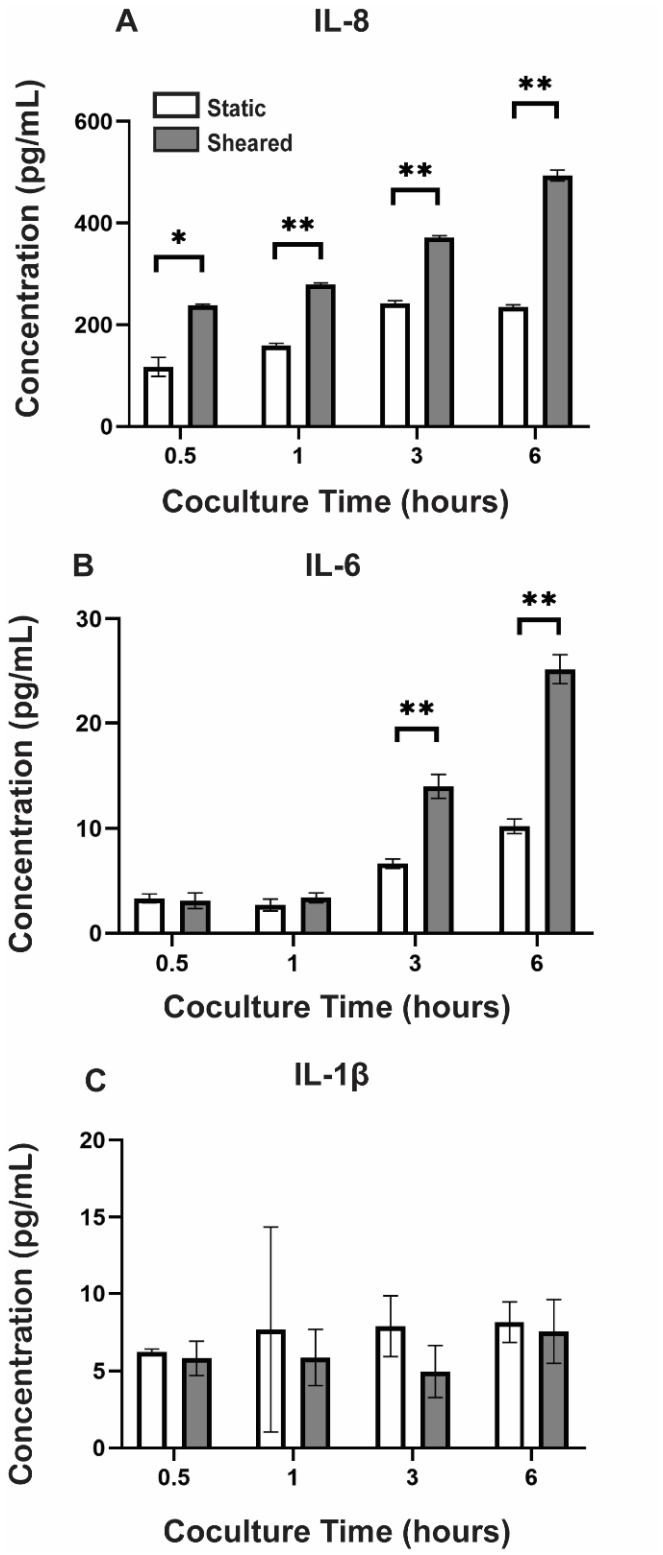

Figure 3.12. Cytokine levels of A) IL-8, B) IL-6, and C) IL-1β in the co-culture media of sheared or static THP-1 cells and HNDMVECs measured at 0.5, 1, 3, and 6 hours. Statistical

significance is denoted by '*'. P values less than 0.05 are indicated by one star symbol and P values less than 0.01 are indicated by double star symbol.

Chapter 4. INVESTIGATING THE ROLE OF IL-8 IN MEDIATING THE INTERACTION BETWEEN SHEARED MONOCYTES AND ENDOTHELIAL CELLS

4.1 ABSTRACT

Previous study has shown that the monocyte-endothelial interaction is accompanied with increased IL-8 level in the co-culture media. In this chapter, the role of IL-8 in mediating the monocyte-endothelial interaction will be tested through loss of function study, with IL-8 receptor on endothelial cells blocked by reparixin, and gain of function study, with addition of IL-8 amplifying the signaling pathway. These studies showed that the adhesion of sheared THP-1 cells positively related to the IL-8 signaling. Silencing the IL-8 expression in the endothelial cells resulted in the reduction of monocyte adhesion, suggesting that endothelial-derived IL-8 contributes to the adhesion. Endothelial cells treated with IL-8 showed upregulated adhesion molecules, which may explain the mechanism of monocyte adhesion.

4.2 INTRODUCTION

In Chapter 3, I showed that CPB shear enhanced monocyte adhesion to and transmigration through endothelial monolayer. These events occurred concomitant with the disruption of VE-cadherin and increasing intercellular gap in the endothelial cells. Interestingly, these intercellular events were also accompanied by the increase of IL-8 levels in the monocyte-endothelial cell co-culture. In this chapter, I tested the hypothesis that the adhesion of sheared monocytes to endothelial cells was mediated by the IL-8 signaling pathway.

IL-8 is a chemoattractant produced by monocytes, macrophages, and endothelial cells. Its primary function is to regulate the recruitment of neutrophils, basophils, and T-cells during an inflammatory response (120). The receptors for IL-8 are the G protein-coupled serpentine receptors CXCR1 and CXCR2, which present on a wide range of cell types, including endothelial cells, monocytes, neutrophils, fibroblasts, with CXCR1 having more specific affinity to the IL-8 than CXCR2 (121). In CPB patients, high level of perioperative plasma IL-8 level is associated with longer inotropic support, longer mechanical ventilation, and higher incidence of acute kidney injuries (122-126). Based on this information and my data in Chapter 3, I hypothesize that the onset of CPB-induced inflammatory response at the cellular level is mediated by the IL-8 signaling pathway. In this study, I tested this hypothesis using the *in vitro* CPB model. By characterizing the monocyte-endothelial cell interaction with loss and gain of function experiments, I identified IL-8/CXCR signaling pathway as a regulator of leukocyte adhesion to the endothelial cell monolayer.

4.3 MATERIALS AND METHODS

4.3.1 Cell Lines and Culture Methods

HNDMVECs (Cat # CC-2516) were purchased from Lonza (Walkersville, MD) and cultured in endothelial cell growth medium MV2 (PromoCell, Heidelberg, Germany, Cat # C-22121) with 100U/mL penicillin-streptomycin (Gibco, Waltham, MA, Cat # 15140122). The medium was changed every other day, and the cells were harvested by trypsinization. The human acute leukemia monocytic cell line THP-1 (Cat # TIB-202) was purchased from ATCC and cultured in RPMI 1640 medium (ATCC Modification) (Gibco, Waltham, MA, Cat # A1049101) with 10% FBS. The medium was changed every other day. G-THP-1 cells were generated

through lentiviral transduction as mentioned in the previous chapter and cultured in RPMI 1640 medium (ATCC Modification) (Gibco, Waltham, MA) with 10% FBS. Media was changed every other day.

4.3.2 Loss of Function Cell Adhesion Assay with Reparixin

HNDMVECs were seeded on 24-well plates at 5000 cells/cm^2 and cultured 7 days to form a confluent monolayer. Monocytes were sheared as previously described. Briefly, G-THP-1 cells at a density of 2 million cells/mL were sheared in a 10 foot-long Masterflex Tygon E-3603 L/S13 pump tubing (Cole-Parmer, Vernon Hills, IL, Cat # MK-06509-13), using a Masterflex miniflex pump model 115/230 VAC 07525-20 (Cole-Parmer, Vernon Hills, IL, Cat # MK-07525-20) at 10 mL/min for 2 hours. The long side tubing was submerged in a water bath with temperature control at 37°C. At the end of shear, the G-THP-1 cells were collected, spun down and resuspended in fresh media. As a control, G-THP-1 cells were incubated in a PVC flask at a density of 2 million cells/mL, 37°C with 5% CO_2 for 2 hours. For the pretreatment group, HNDMVECs were incubated with 5 nM of reparixin (Sigma-Aldrich, St. Louis, MO, Cat # SML2655-5MG) for 30 minutes. The pretreatment was then removed and the HNDMVECs were washed with sterile PBS. After that, G-THP-1 cells, sheared or statically incubated, were added to a monolayer of HNDMVECs ($1x10^6$ cells per well), followed by incubation for 1 hour. The co-cultures were gently rinsed twice with sterile PBS to remove nonadherent G-THP-1 cells. The adhered G-THP-1 were visualized using a Nikon Eclipse TE200 microscope (Tokyo, Japan) and a Photometric CoolSNAP MYO camera (Tucson, AZ) with a GFP filter. A schematic of the experiment is shown in Figure 4.1. The experiments were run in triplicates. The number of adherent G-THP-1 cells were counted in five randomly selected visible fields and quantified using ImageJ (108).

4.3.3 Gain of Function Cell Adhesion Assay with IL-8

HNDMVECs were seeded on 24-well plates at 5000 cells/cm^2 and cultured 7 days to form a confluent monolayer. Monocytes were sheared as previously described. Briefly, G-THP-1 cells at a density of 2 million cells/mL were sheared in a 10 foot-long Masterflex Tygon E-3603 L/S13 pump tubing (Cole-Parmer,Vernon Hills, IL, Cat # MK-06509-13), using a Masterflex miniflex pump model 115/230 VAC 07525-20 (Cole-Parmer, Vernon Hills, IL, Cat # MK-07525-20) at 10 mL/min for 2 hours. The long side tubing was submerged in a water bath with temperature control at 37°C. At the end of shear, the G-THP-1 cells were collected, spun down and resuspended in fresh media. As a control, G-THP-1 cells were incubated in a PVC flask at a density of 2 million cells/mL, 37°C with 5% CO_2 for 2 hours. For the pretreatment group, HNDMVECs were incubated with 50 or 200 ng/mL of human recombinant IL-8 (R&D Systems, Minneapolis, MN, Cat # 208-IL-010/CF) for 1 hour. The pretreatment was then removed and the HNDMVECs were washed with sterile PBS. After that, G-THP-1 cells, sheared or statically incubated, were added to a monolayer of HNDMVECs ($1x10^6$ cells per well), followed by incubation for 1 hour. The co-cultures were gently rinsed twice with sterile PBS to remove non-adherent G-THP-1 cells. The adhered G-THP-1 were visualized using a Nikon Eclipse TE200 microscope (Tokyo, Japan) and a Photometric CoolSNAP MYO camera (Tucson, AZ) with a GFP filter. A schematic of the experiment is shown in Figure 4.2. The experiments were run in triplicates. The number of adherent G-THP-1 cells were counted in five randomly selected visible fields and quantified using ImageJ (108).

4.3.4 siRNA Transfection to Silence IL-8 Expression in HNDMVECs

HNDMVECs were seeded on 6-well plates at 5000 cells/cm^2 and cultured 7 days to form a confluent monolayer. Lipofectamine RNAiMAX Transfection Reagent (Thermofisher,

Thermofisher, Waltham, MA, Cat # 13778150) was used to prepare liposomes with the IL-8 siRNA (Thermofisher, Waltham, MA, s7327, Cat # 4390824) or scramble RNA (Thermofisher, Waltham, MA, Cat # 4404021) according to the manufacturer's instructions. Both the transfection reagent and siRNAs were diluted with fixed volumes of OptiMEM I Reduced Serum Medium (Thermofisher, Waltham, MA, Cat # 31985062) and then mixed. HNDMVECs were incubated with the siRNA-lipid complex for 2 days at 37°C. To demonstrate IL-8 expression was silenced, HNDMVECs were treated with 10 ng/mL TNF-α (R&D Systems, Minneapolis, MN, Cat # 210-TA) for 1 hour. Then, the IL-8 expression in the HNDMVECs were measured by quantitative real-time PCR. Briefly, total RNA was isolated using the RNeasy Mini Kit (Qiagen, Hilden, Germany, Cat # 74104) and RNase-Free DNAse Set (Qiagen, Hilden, Germany, Cat # 79254). A Total RNA of 150 ng was used for cDNA synthesis using the Omniscript RT Kit (Qiagen, Hilden, Germany, Cat # 205113). Quantitative real-time PCR was performed on a QuantStudio 6 Pro real-time PCR system (Thermofisher, Waltham, MA, Cat # A43180) and Taqman Universal PCR Master Mix (Thermofisher, Waltham, MA, Cat # 4304437) according to the manufacturer instructions. Both biological and technical triplicates were run. Taqman primer of IL-8 (Hs00174103_m1, Cat # 4331182) was purchased from Thermofisher.

4.3.5 Adhesion Assay with IL-8-silenced HNDMVECs

HNDMVECs were seeded on 24-well plates at 5000 cells/cm^2 and cultured 7 days to form a confluent monolayer. Monocytes were sheared as previously described. Briefly, G-THP-1 cells at a density of 2 million cells/mL were sheared in a 10 foot-long Masterflex Tygon E-3603 L/S13 pump tubing (Cole-Parmer, Vernon Hills, IL, Cat # MK-06509-13), using a Masterflex miniflex pump model 115/230 VAC 07525-20 (Cole-Parmer, Vernon Hills, IL, Cat # MK-07525-20) at 10 mL/min for 2 hours. The long side tubing was submerged in a water bath with

temperature control at 37°C. At the end of shear, the G-THP-1 cells were collected, spun down and resuspended in fresh media. 2 days before the assay was performed, HNDMVECs were transfected with IL-8 siRNA. Then the transfection reagent was removed and the HNDMVECs were washed with sterile PBS before the assay was conducted. After that, sheared G-THP-1 cells were added to a monolayer of HNDMVECs ($1x10^6$ cells per well), followed by incubation for 1 hour. The co-cultures were gently rinsed twice with sterile PBS to remove non-adherent G-THP-1 cells. The adhered G-THP-1 were visualized using a Nikon Eclipse TE200 microscope (Tokyo, Japan) and a Photometric CoolSNAP MYO camera (Tucson, AZ) with a GFP filter. A schematic of the experiment is shown in Figure 4.3. The experiments were run in triplicates. The number of adherent G-THP-1 cells were counted in five randomly selected visible fields and quantified using ImageJ (108).

4.3.6 Effect of IL-8 on HNDMVECs

i. Transendothelial Electrical Resistance (TEER) Test

IL-8 has been shown to increase the membrane permeability and barrier function of the endothelium. This response of the cells can be assessed by TEER. In this experiment, HNDMVECs were seeded in the upper chamber of a transwell tissue culture insert (6.5 mm diameter, 8 μm pore size polycarbonate membrane; Corning, NY, Cat # 3422) at 5000 cells/cm^2 and cultured 7 days to form a confluent monolayer. Before TEER test, HNDMVECs were incubated with 50 or 200 ng/mL of human recombinant IL-8 (R&D Systems, Minneapolis, MN, Cat # 208-IL-010/CF). The TEER was measured by placing a chopstick-like pair of electrodes in the culture media, with one in the upper chamber and one in the bottom chamber. The electrode will apply a low frequency current across the cells on the membrane of the transwell and the

resistivity will be measured by an electrometer. During the measurement, the well plate was placed on a heat pack to maintain the temperature, which can affect the resistivity measurement. The measurements were taken before the IL-8 treatment and 0.5, 1, 2, 4, and 8 hours after the treatment.

ii. Adhesion Molecule Expression Quantified by Quantitative Real-time PCR

HNDMVECs were treated with 200 ng/mL human recombinant IL-8 (R&D Systems, Minneapolis, MN, Cat # 208-IL-010/CF) for 1 hour, and total RNA was extracted using the RNeasy Mini Kit (Qiagen, Hilden, Germany, Cat # 74104) and RNase-Free DNAse Set (Qiagen, Hilden, Germany, Cat # 79254). A total RNA of 150 ng was used for producing cDNA with the Omniscript RT Kit (Qiagen, Hilden, Germany, Cat # 205113). Quantitative real-time PCR was performed with Taqman Universal PCR Master Mix (Thermofisher, Waltham, MA, Cat # 4304437) on a QuantStudio 6 Pro real-time PCR system (Thermofisher, Waltham, MA, Cat # A43180) according to the manufacturer instructions. Both biological and technical triplicates were run. Taqman primers of selectin E (Hs00174057_m1, Cat # 4331182), intercellular adhesion molecule 1 (ICAM-1) (Hs00164932_m1, Cat # 4331182) and vascular cell adhesion molecule 1 (VCAM-1) (Hs01003372_m1, Cat # 4331182) were purchased from Thermofisher.

4.3.7 Statistical Analysis

All experiments were run in triplicates. All quantitative data were expressed as mean ± standard deviation within groups. Pairwise comparisons between groups were conducted using ANOVA test and Tukey's post-hoc test. Statistical significance is denoted by '*'. P values less than 0.05 are indicated by single star symbol and P values less than 0.01 are indicated by double star symbol.

4.4 RESULTS

4.4.1 Reparixin, a CXCR2 antagonist, inhibits the adhesion of sheared THP-1 cells while IL-8 promotes the adhesion of untreated THP-1 cells

My data in the previous chapter suggested that the adhesion of THP-1 cells on the endothelial cell is positively correlated to the IL-8 levels in the co-culture. To investigate the role of IL-8 in mediating the interaction between THP-1 cells and the endothelial cells, I pretreated the HNDMVECs with Reparixin to inhibit the activation of IL-8 receptors on the endothelial cells, and then co-cultured with sheared THP-1 cells (CXCR2 staining of HNDMVECs see Figure 4.4). Reparixin treatment reduced adhesion of sheared THP-1, and the count of adhered monocytes is comparable to static control (Figure 4.5C). In the vehicle group where DMSO was used, the adhesion of the sheared THP-1 cells was not affected. When I promoted the IL-8 signaling by pre-treating HNDMVECs with 50 and 200 ng/mL IL-8, the adhesion of untreated THP-1 cells was increased in a dose-dependent manner with 200 ng/mL treatment group having twice as many of adhered THP-1 cells than the 50 ng/mL treatment group (Figure 4.7C, D). These results suggested that blocking IL-8 signaling through the CXCRs prevented the adhesion of shear-activated THP-1 cells, while amplifying the IL-8 signaling promoted the adhesion of naïve THP-1 cells.

4.4.2 Silencing IL-8 expression in endothelial cells reduced the adhesion of sheared monocytes.

IL-8 can be released by both monocytes and endothelial cells. Identifying the source of IL-8 in the co-culture can help determine the cell type to target when formulating a treatment. To do that, I silenced the IL-8 expression in the HNDMVECs using siRNA. HNDMVECs were incubated with the lipid-siRNA complex for 2 days and then stimulated with 10 ng/mL TNF-α

for 1 hour. As a result, the IL-8 expression in response to TNF-α was significantly reduced in the group treated with siRNA (Figure 4.9A). In the group treated with negative control siRNA and without RNA treatment, the IL-8 expressions were dramatically increased (Figure 4.9A). These results suggest that IL-8 silencing was achieved by using siRNA. The HNDMVECs were then treated with sheared THP-1 cells and adhered cells were quantified after 1 hour of co-culture. The treatment of endothelial cells with IL-8 siRNA significantly reduced the adhesion of THP-1 cells while groups treated with negative control siRNA or no treatment did not change THP-1 adhesion (Figure 4.9B). These results indicate that IL-8 secreted by endothelial cells largely contributes to the increased adhesion of sheared THP-1 in the co-culture.

4.4.3 IL-8 treatment led to increased endothelial membrane permeability

The permeability of endothelial monolayer is measured by TEER. A drop in the TEER reading occurred at 0.5 hour after the IL-8 treatment, suggesting compromised membrane integrity, although it is not statistically significant (Figure 4.11). The TEER reading stayed at a low level throughout the 8-hour testing period (Figure 4.11). No dose-dependent TEER change was observed.

4.4.4 IL-8 upregulated adhesion molecules on the endothelial cells

To further investigate the mechanism that drives mononuclear cell adherence to endothelial cells, I examined the expression of adherence molecules in the endothelial cells. qPCR was performed to measure the expression of adhesion molecules in HNDMVECs, including E-selectin, VCAM-1, and ICAM-1. HNDMVECs treated with TNF-α were used as a positive control to stimulate the endothelial cells. Indeed, all three adhesion molecules were upregulated in the positive control group (Figure 4.12). In the group treated with IL-8, there was

a 5-fold increase in both the expressions of ICAM-1 and VCAM-1 compared to the group without treatment, while the expression of E-selectin remained unchanged (Figure 4.12). These results indicate that IL-8 signaling pathway likely mediated the sheared monocyte adhesion through upregulated ICAM-1 and VCAM-1 expression on the endothelial cells.

4.5 DISCUSSION

In this chapter, I showed that CPB-activated monocyte adhesion to endothelial cells is IL-8 dependent. Inhibiting the activation of the IL-8 receptors, CXCR1/2 on the endothelial cells resulted in the reduction of sheared monocyte adhesion. Treating the endothelial cells with IL-8 increased the adhesion of naïve monocytes in a dose-dependent manner. The adhesion of monocytes is likely mediated by the adhesion molecule on the endothelial cells, upregulated by the IL-8 derived from endothelial cells in the co-culture. These results suggest that IL-8 may promote the adhesion of the monocytes by upregulating a subset of adhesion molecules on the endothelial cells.

The monocyte-endothelial cell interaction was regulated by IL-8 in the *in vitro* CPB model. Accordingly, previous study showed that both IL-8 expression and release in the monocytes is directly upregulated by CPB-induced shear stress (65). In this study, I found elevated IL-8 levels in the co-culture media of THP-1 cells activated by CPB shear and microvascular endothelial cells. Altogether, these results revealed that IL-8 is a main cytokine mediating the interaction between monocytes and endothelial cells in the CPB setting. To identify the cellular contribution of the IL-8 in the co-culture system, siRNA silencing was used. I showed that adhesion of sheared monocytes is reduced by silencing the IL-8 expression in endothelial cells, indicating that the IL-8 in the co-culture is released from endothelial cells.

Based on these results, a proposed mechanism of monocyte adhesion is that THP-1 cells activated by the CPB shear stimulate the IL-8 release from endothelial cells and leads to the activation of adhesion molecules on the endothelial cells, which mediate the adhesion of the THP-1 cells (Figure 4.13). The autocrine signaling of IL-8 in endothelial cells is important in promoting capillary tube formation and neovascularization without external IL-8 stimulation (127-133). However, current study design does not rule out the contribution of IL-8 from monocytes knowing that monocytes produce IL-8 with different types of stimulation. siRNA transfection has been tested to silence the IL-8 expression in the THP-1 cells, but I did not manage to generate viable THP-1 cells with silenced IL-8 expression. Therefore, the last puzzle to this proposed mechanism is to investigate the contribution of monocyte-derived IL-8 in the co-culture system. It is possible that THP-1 cells continue to produce IL-8 when they are removed from the CPB environment, promoting the IL-8 signaling, and encouraging their own adhesion.

IL-8 is known to regulate neutrophil activities including chemotaxis, lysosomal enzyme release, intracellular calcium, and oxidative burst (96-100). Much less is known about its function in monocyte regulation. It has been shown that IL-8 stimulates monocyte adhesion to endothelial cells expressing E-selectin under flow condition (134). IL-8 stimulation in monocytes also leads to production of IL-6 and IL-1β, as well as shifting the polarization towards a pro-inflammatory phenotype (135,136). Interestingly, IL-6 and IL-1β were not detected in the co-culture media in the previous chapter. In addition, endothelial cells express the two IL-8 receptors, including CXCR1 and CXCR2. The activation of these receptors triggers downstream events such as cell proliferation, survival, tube morphogenesis, and MMP production (137). The IL-8-induced cytoskeletal reorganization is mediated by Rho and Rac signaling pathway, which is also correlated to the clustering of adhesion molecules on the endothelial cells (138,139). In

this study, I further demonstrated that the adhesion molecules of endothelial cells were upregulated with IL-8 treatment. Plus, IL-8 treatment increases the permeability of the endothelium, which facilitates the transmigration of monocytes. Altogether, these explain the drop in TEER, increasing gap formation, cytoskeletal rearrangement, and dose-dependent cell adhesion in my model.

In conclusion, the study in this chapter revealed the important role of IL-8 in regulating the CPB-activated monocyte adhesion to the endothelial cells. This is the first study to show that monocytes affected by shear stress can subsequently damage the endothelial integrity through adhesion and transmigration in a IL-8 dependent manner. This correlates to clinical data, where elevated IL-8 level is associated with high incidence of acute kidney injury, brain injury, and longer intensive care stay. Together with my study, blunting the IL-8 signaling may provide benefits to reduce endothelial injury and organ damage in pediatric CPB.

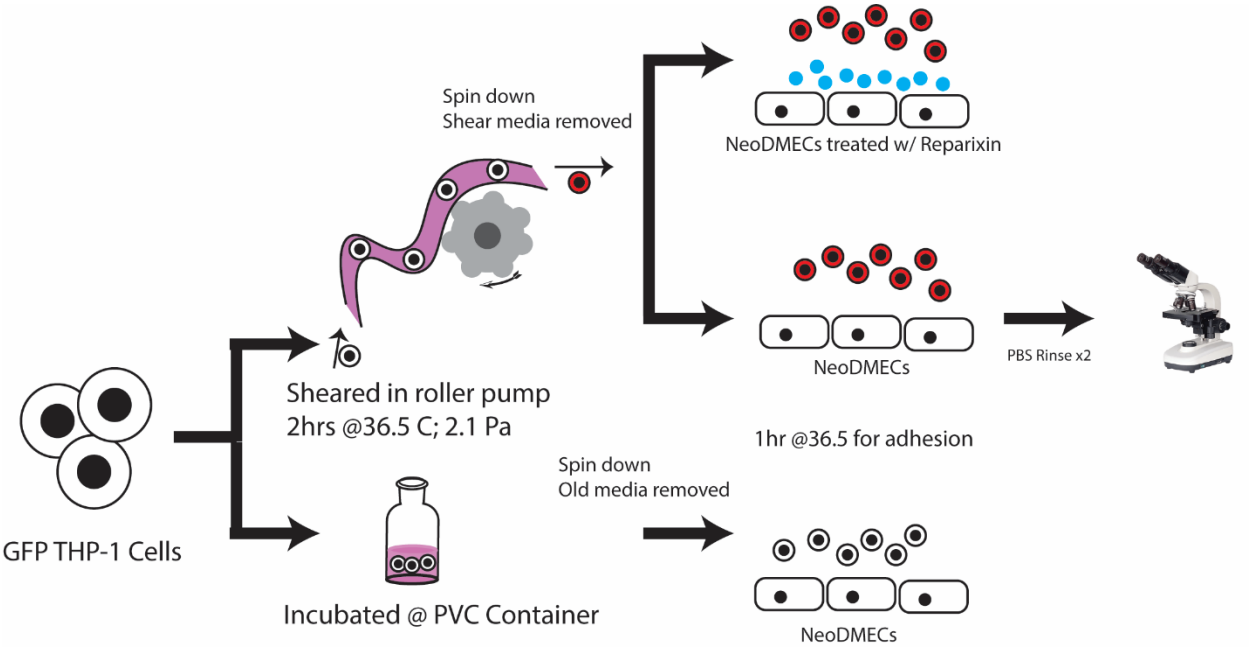

Figure 4.1. Schematic of loss of function cell adhesion assay. Blue dots represent reparixin treatment.

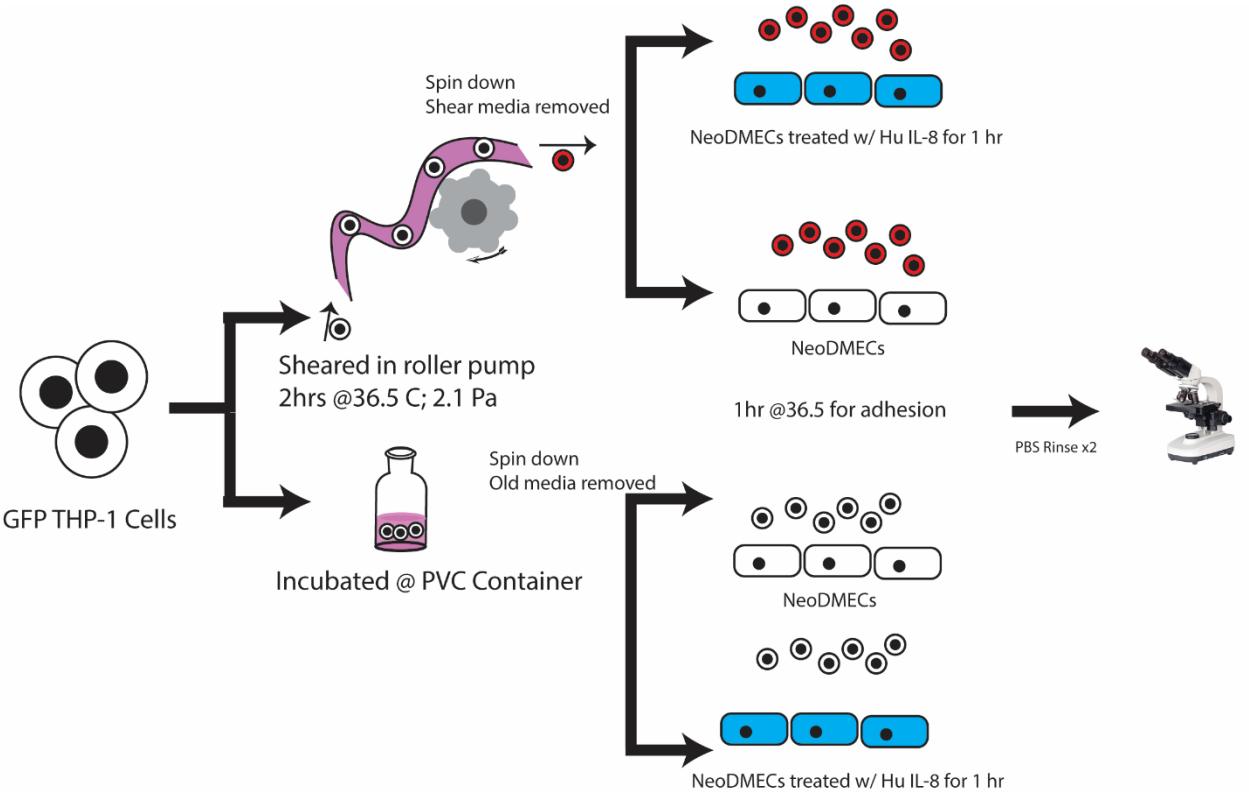

Figure 4.2. Schematic of gain of function cell adhesion assay. Blue endothelial cells were treated with IL-8.

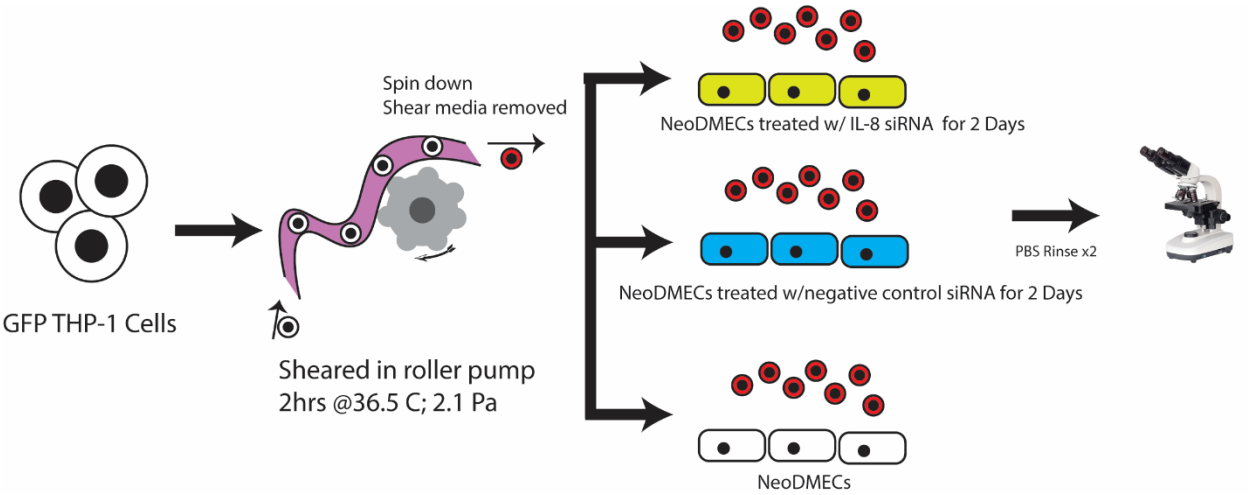

Figure 4.3. Schematic of adhesion assay with IL-8-silenced HNDMVECs. Yellow endothelial cells were treated with IL-8 siRNA. Blue endothelial cells were treated with negative control siRNA.

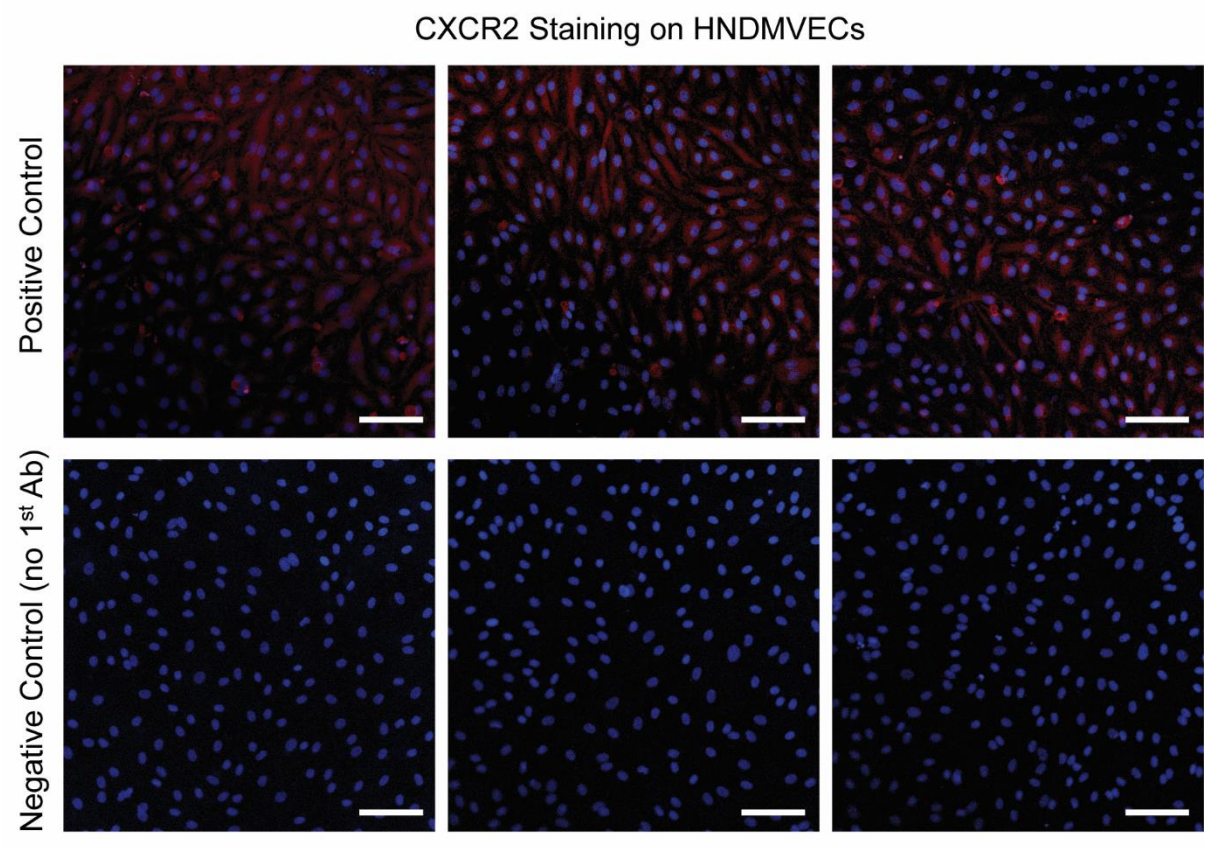

Figure 4.4. CXCR2 staining on HNDMVECs. Scale bar = 100 μm.

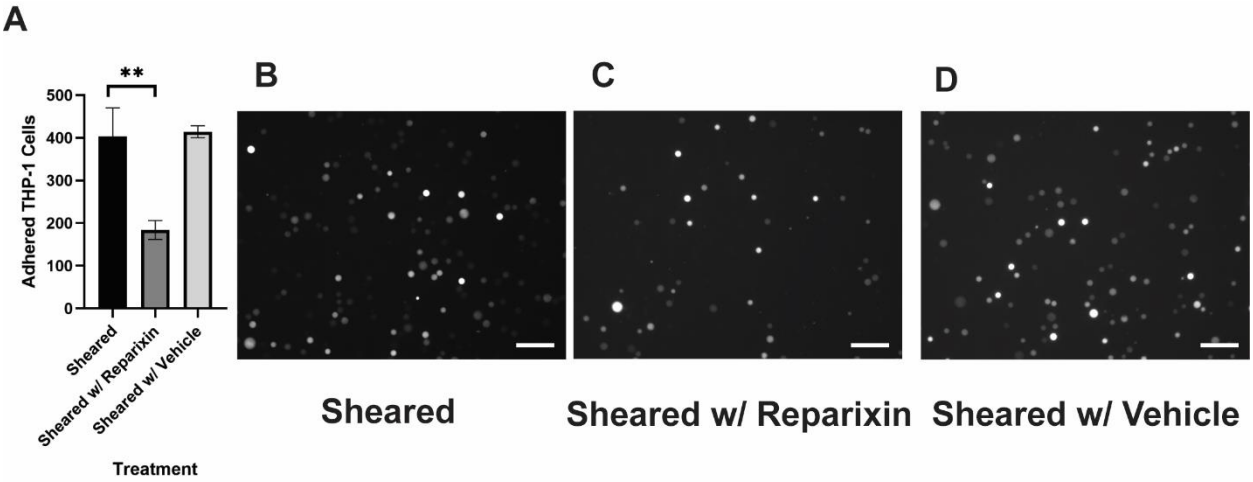

Figure 4.5. A) Quantitative analysis of sheared G-THP-1 cells adhering to B) untreated HNDMVECs, C) HNDMVECs pretreated with 5nM reparixin for 30 minutes, and D) HNDMVECs pretreated with PBS. Scale bar = 100 μm. Additional images see Figure 4.6. Statistical significance is denoted by '*'. P values less than 0.05 are indicated by one star symbol and P values less than 0.01 are indicated by double star symbol.

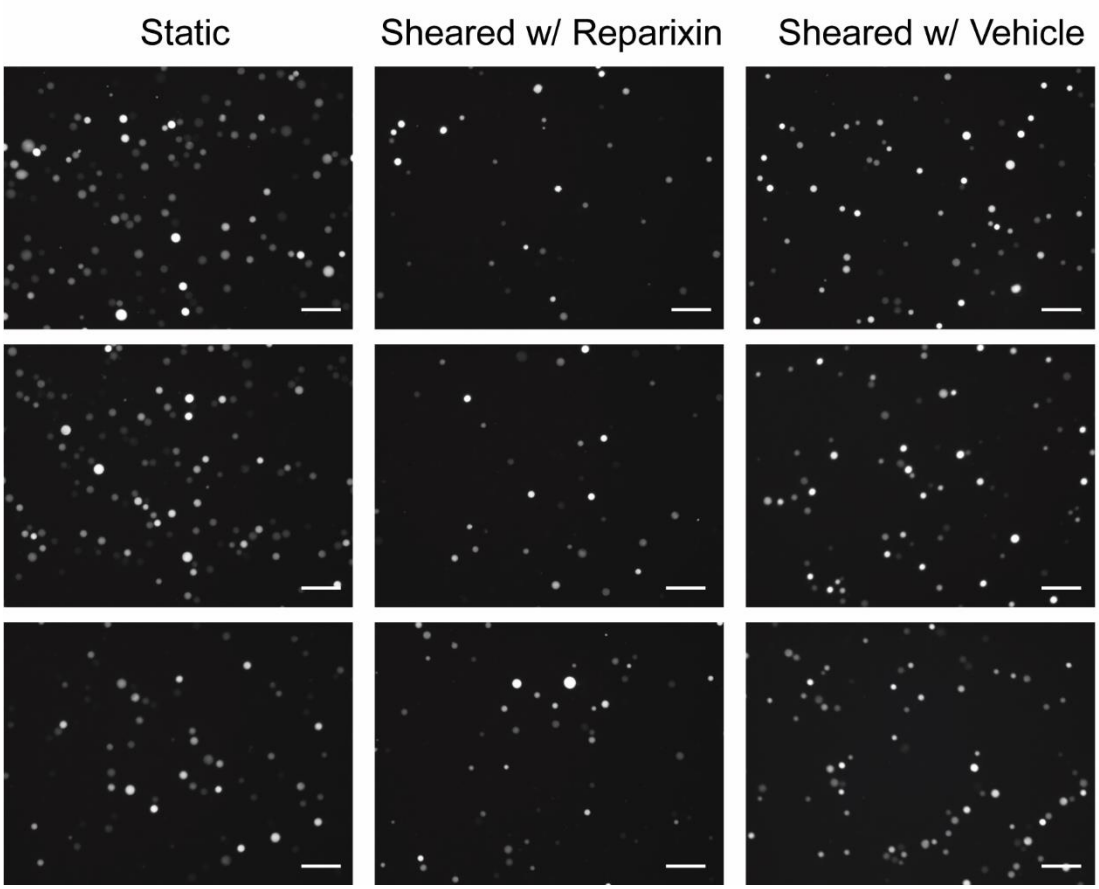

Figure 4.6. Additional images of THP-1 cell adhesion on HNDMVECs treated with or without reparixin. Scale bar = 100 μm.

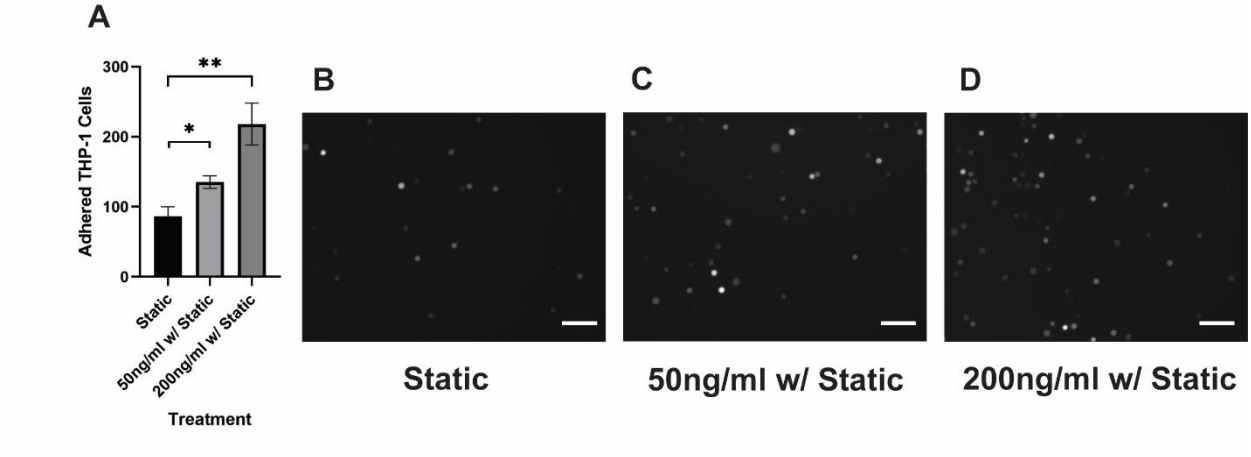

Figure 4.7. A) Quantitative analysis of statically incubated G-THP-1 cells adhering to B) untreated HNDMVECs, C) HNDMVECs pretreated with 50 ng/mL IL-8 for 1 hour, and D) HNDMVECs pretreated with 200 ng/mL IL-8 for 1 hour. Additional images see Figure 4.8. Scale bar = 100 μm. Statistical significance is denoted by '*'. P values less than 0.05 are indicated by one star symbol and P values less than 0.01 are indicated by double star symbol.

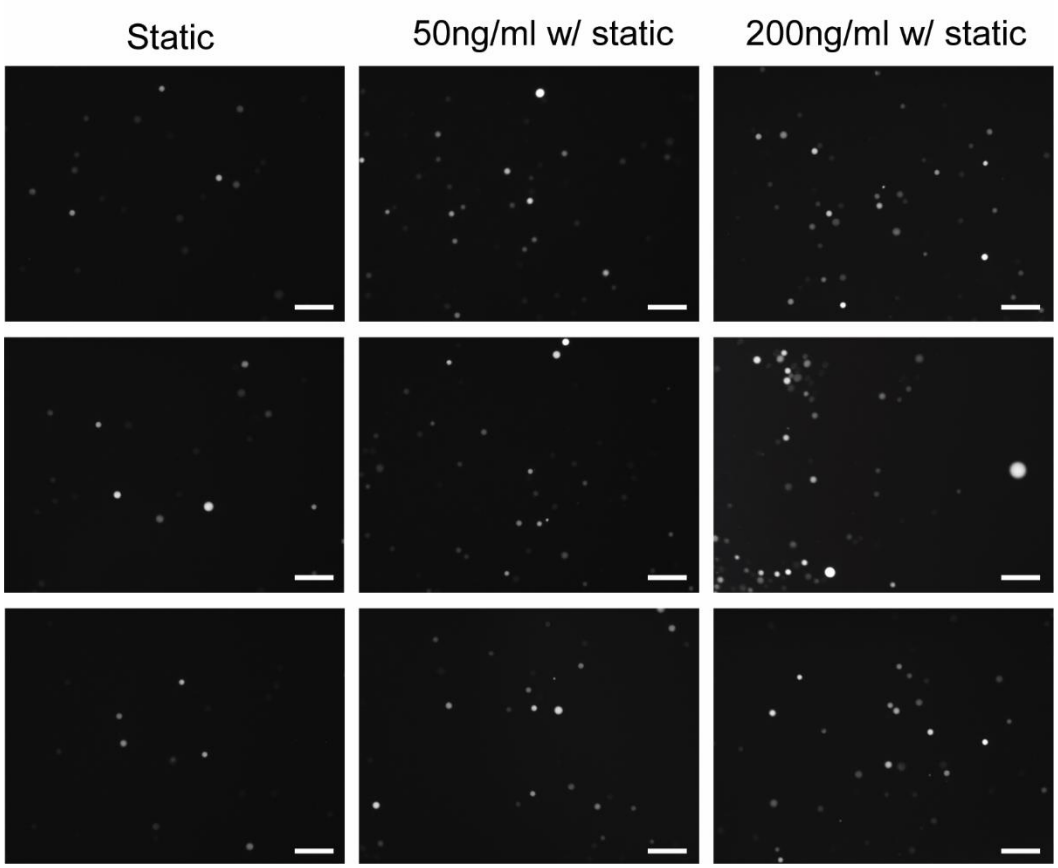

Figure 4.8. Additional images of THP-1 cell adhesion on HNDMVECs treated with or without human recombinant IL-8. Scale bar = 100 μm.

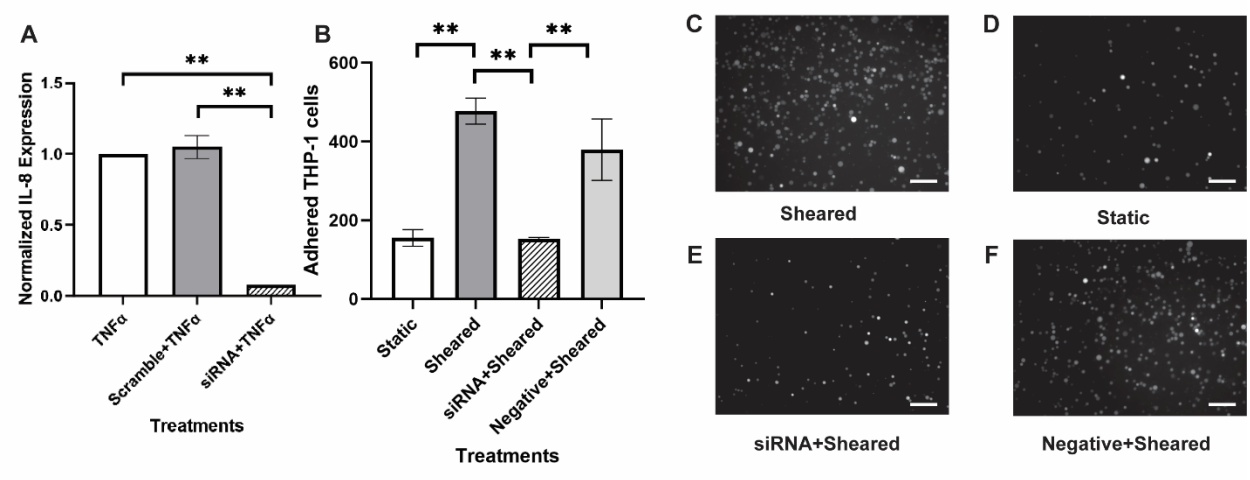

Figure 4.9. A) Expression of IL-8 in HNDMVECs stimulated by TNF-α. B) Quantitative analysis of C) statically incubated G-THP-1 cells adhering to HNDMVECs, and sheared G-THP-1 cells adhering to D) HNDMVECs, E) HNDMVECs treated with IL-8 siRNA, and (F) HNDMVECs treated with negative control siRNA. Additional images see Figure 4.10. Scale bar = 100 μm. Statistical significance is denoted by '*'. P values less than 0.05 are indicated by one star symbol and P values less than 0.01 are indicated by double star symbol.

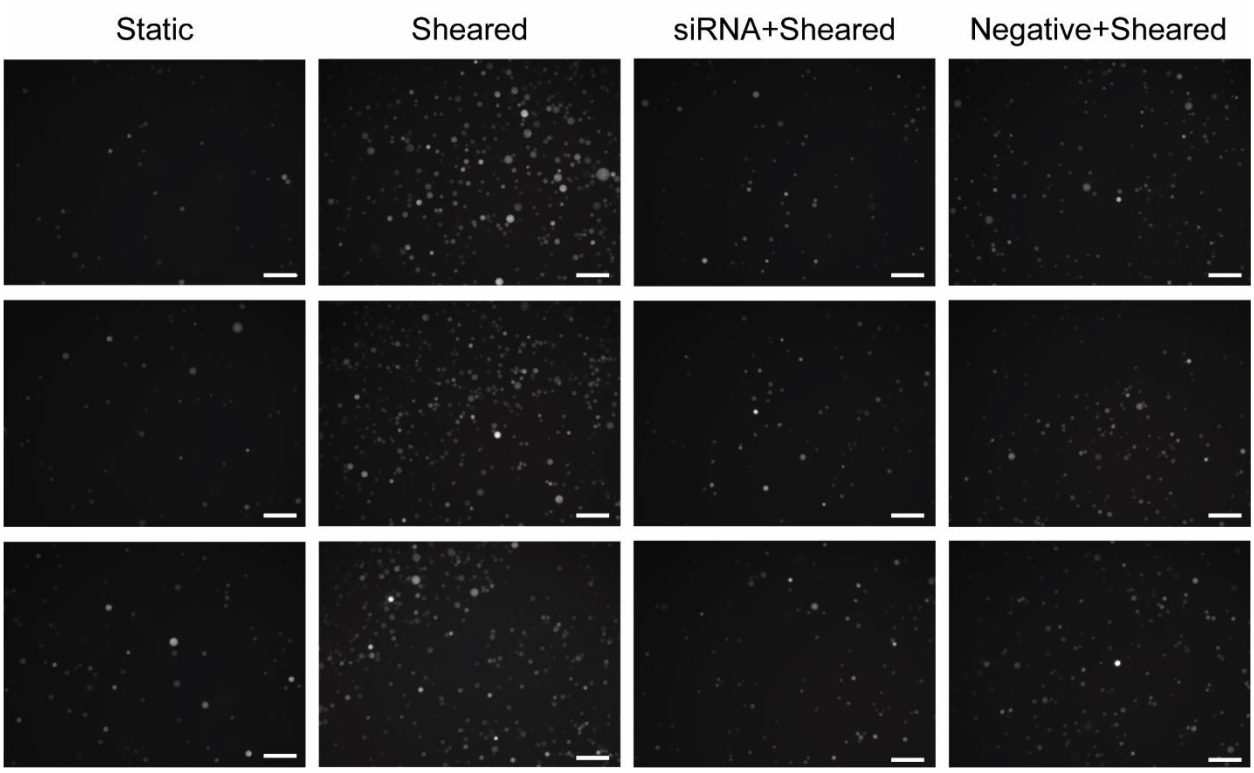

Figure 4.10. Additional images of THP-1 cell adhesion on HNDMVECs treated with siRNA and negative control RNA.

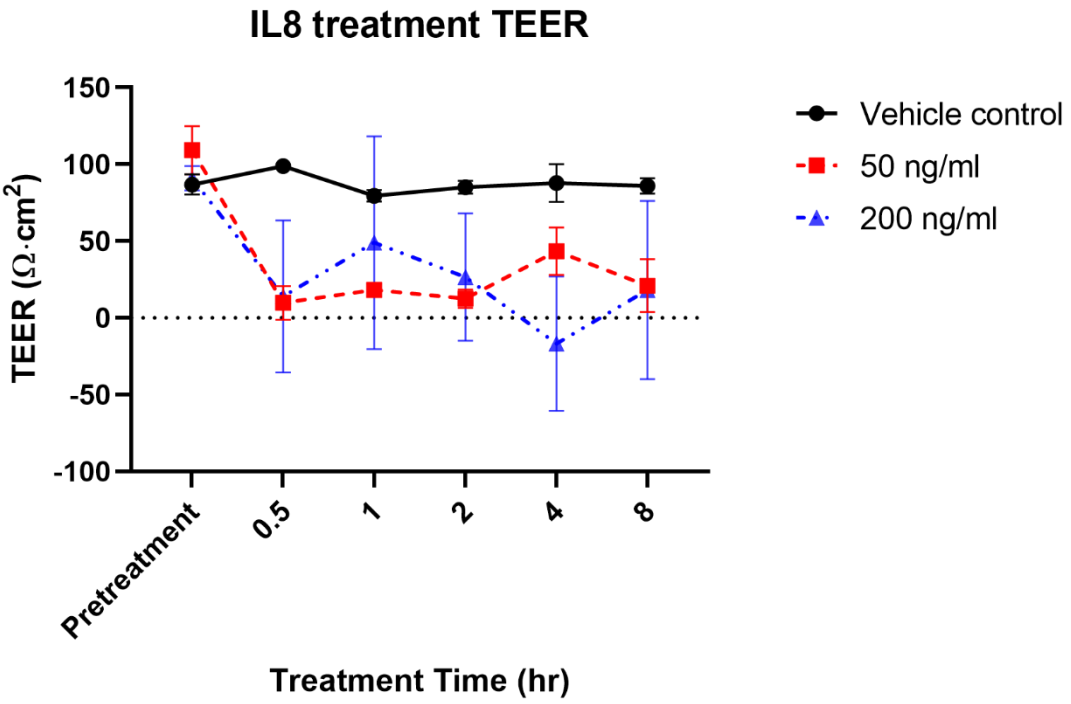

Figure 4.11. TEER of HNDMVECs treated with vehicle control, 50 ng/mL and 200 ng/mL recombinant human IL-8

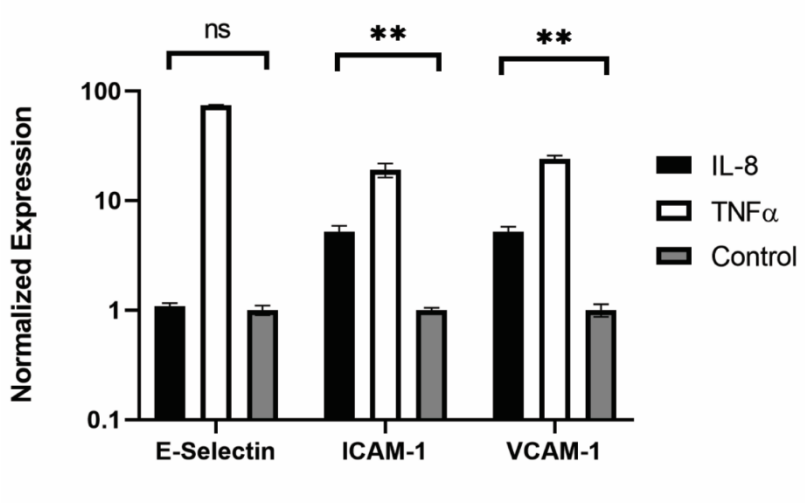

Figure 4.12. Expression of E-selectin, ICAM-1, and VCAM-1 in HNDMVECs treated with IL-8, TNF-α, and control measured by RT-qPCR. Statistical significance is denoted by '*'. P values less than 0.05 are indicated by one star symbol and P values less than 0.01 are indicated by double star symbol.

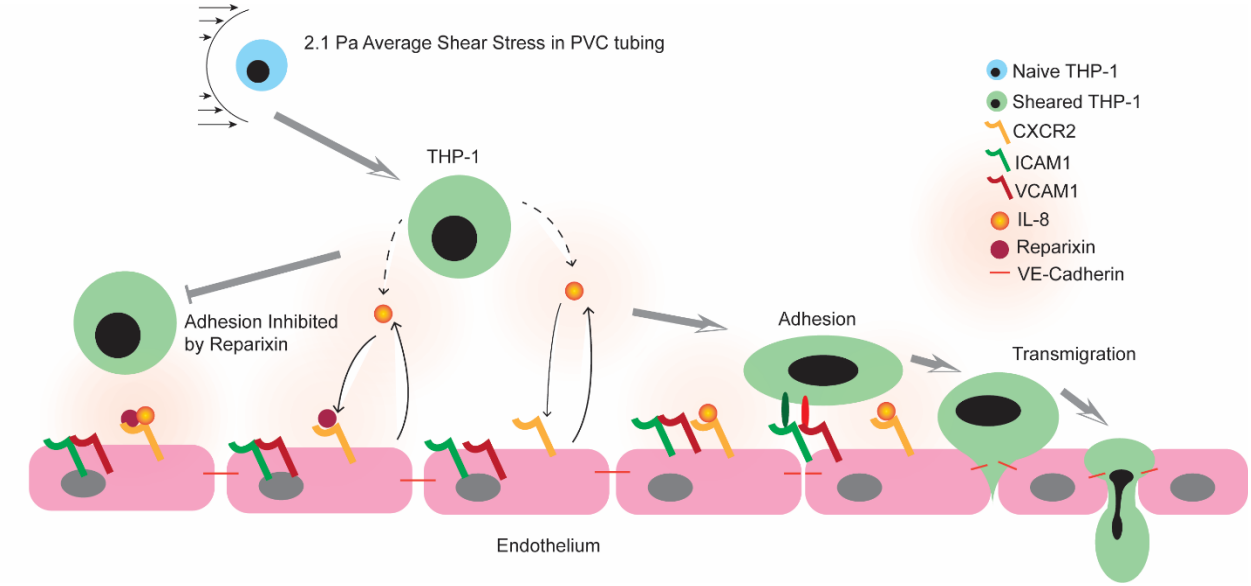

Figure 4.13. Proposed mechanism of CPB-induced monocyte adhesion to endothelium.

Chapter 5. INVESTIGATING THE EFFECT OF ANTI-INFLAMMATORY DRUGS ON THE SOLUBLE FACTOR COMPOSITION OF MEDIA CONDITIONED BY SHEARED MONOCYTES

5.1 ABSTRACT

Corticosteroids have limited benefit in treating CPB-related inflammation despite its promising anti-inflammatory effects. In this chapter, the effect of corticosteroid on the soluble factor composition of sheared THP-1 cells was studied. THP-1 cells were sheared in the *in vitro* CPB circuit with or without dexamethasone and the conditioned media after shearing was collected for ELISA and Luminex multiplex assays. ELISA results showed the dexamethasone treatment reduced the levels of IL-8 and TNF-α in sheared monocyte media. However, dexamethasone's ability to reduce inflammatory cytokine levels is not as effective as the treatment of a calcineurin inhibitor, FK506, suggesting CPB-induced inflammatory response of monocytes is mainly calcium signaling dependent. Luminex multiplex assay revealed that FK506 can increase anti-inflammatory protein levels such as IL-1ra and reduce chemoattractant levels such as macrophage inflammatory protein (MIP)-1b. Dexamethasone treatment led to increasing vascular endothelial growth factor (VEGF) levels in sheared monocyte media, which may contribute to its ability to protect patients from renal injury after CPB.

5.2 INTRODUCTION

Inflammatory response has been effectively treated with corticosteroids, but not in the cases of pediatric CPB patients. Corticosteroids, such as dexamethasone, work by binding to the glucocorticoid receptor in the cytoplasm to form a complex (140). This triggers a translocation of

the complex to the nucleus of cells and further binding of the complex to the DNA orchestrated by glucocorticoid response elements. This leads to the transcriptional activation, including increasing expression of anti-inflammatory proteins and suppression of pro-inflammatory protein expression (140). Dexamethasone has a strong anti-inflammatory effect on monocytes. It can suppress the release of TNF-α, IL-8, CCL5 (RANTES), monocytes chemoattractant protein 1 (MCP-1), and iNOS while promoting the release of anti-inflammatory mediators such as annexin-1, IL-10, and CD163 (141-149). Despite having such promising anti-inflammatory properties, the use of corticosteroids has provided limited benefits to pediatric CPB patients. Clinical trials have shown contradictory or inconclusive results (150-153). While these clinical trials suffered from limited sample size, a recent randomized trial included 1263 infants who either received methylprednisolone or placebo during CPB failed to show clinical benefits in terms of mortality rate, heart transplantation and 13 other post-operative outcomes (154). The failed role of corticosteroids suggests other mechanisms might contribute to the post-CPB complications.

Monocytes are known to release a wide range of soluble factors including cytokine, chemokine and growth factors (155). Some of these soluble factors are also reported to be elevated by CPB such as VEGF, granulocyte-macrophage colony-stimulating factor (GM-CSF), and MIP-1 (156-160). Establishing a soluble factor profile from CPB-activated monocytes will help us gain more insight into the potential mechanism that drives monocyte-related inflammation, while not being covered by the anti-inflammatory benefits of corticosteroids in pediatric CPB patients. In this chapter, I will use ELISA and Luminex-based multiplex assay to determine the soluble factor profile of shear-activated monocytes.

5.3 MATERIALS AND METHODS

5.3.1 Cell Lines and Culture Methods

The human acute leukemia monocytic cell line THP-1 (Cat # TIB-202) was purchased from ATCC and cultured in RPMI 1640 medium (ATCC Modification) (Gibco, Waltham, MA, Cat # A1049101) with 10% FBS. The medium was changed every other day.

5.3.2 Collection of Conditioned Media

THP-1 cells at a density of 2 million cells/mL were sheared in a 10 foot-long Masterflex Tygon E-3603 L/S13 pump tubing (Cole-Parmer, Vernon Hills, IL, Cat # MK-06509-13), using a Masterflex miniflex pump model 115/230 VAC 07525-20 (Cole-Parmer, Vernon Hills, IL, Cat # MK-07525-20) at 10 mL/min for 2 hours. The long side tubing was submerged in a water bath with temperature control at 37°C. During the shear, THP-1 cells were suspended in media with 1μM or 2μM dexamethasone, or 5μM FK506. At the end of the shear, the THP-1 cells were statically incubated in the media that they are sheared in for 1 hour in a 50 mL Falcon tube. At the end of the incubation, the media supernatant was collected and kept frozen at -20°C and used as sheared conditioned media.

5.3.3 Quantitative Real-time PCR

Immediately after the shear or static culture, THP-1 cells were lysed, and total RNA was extracted using the RNeasy Mini Kit (Qiagen, Hilden, Germany, Cat # 74104) and RNase-Free DNAse Set (Qiagen, Hilden, Germany, Cat # 79254). A total RNA of 150 ng was used for producing cDNA with the Omniscript RT Kit (Qiagen, Hilden, Germany, Cat # 205113). Quantitative real-time PCR was performed with Taqman Universal PCR Master Mix

(Thermofisher, Waltham, MA, Cat # 4304437) on a QuantStudio 6 Pro real-time PCR system (Thermofisher, Waltham, MA, Cat # A43180) according to the manufacturer instructions. Both biological and technical triplicates were run. Taqman primers of TNF-α (Mm00443258_m1, Cat # 4331182), and IL-8 (Hs00174103_m1, Cat # 4331182) were purchased from Thermofisher.

5.3.4 Luminex Multiplex Assay

Luminex immunoanalysis of a panel of cytokines was read by a MAGPIX multiplexing system at the Genomics, Bioinformatics and Biostatistics Microphysiological System Facility Core of the Department of Environmental and Occupational Health Science at University of Washington, Seattle. Thirty pre-specified human inflammatory cytokines were analyzed using the Human Cytokine Magnetic 30-Plex Panel kit, including granulocyte colony-stimulating factor (G-CSF), GM-CSF, interferon (IFN)-α, IFN-γ, IL-1β, IL-1 receptor antagonist (ra), IL-2, IL-2R, IL-4, IL-5, IL-6, IL-7, IL-8, IL-10, IL-12 (p40/p70), IL-13, IL-15, IL-17, TNF-α, Eotaxin, interferon gamma-induced protein 10 (IP-10), MCP-1, monokine induced by gamma interferon (MIG), MIP-1α, MIP-1β, RANTES, epidermal growth factor (EGF), fibroblast growth factor (FGF)-basic, hepatocyte growth factor (HGF) and VEGF. The assays were performed according to the manufacturer's instructions.

5.3.5 Statistical Analysis

All experiments were run in triplicates. All quantitative data were expressed as mean ± standard deviation within groups. Pairwise comparisons between groups were conducted using ANOVA test and Tukey's post-hoc test. Statistical significance is denoted by '*'. P values less than 0.05 are indicated by one star symbol and P values less than 0.01 are indicated by double star symbol.

5.4 RESULTS

i. qPCR

To investigate the cytokine profile of shear-activated monocytes under the influence of anti-inflammatory drugs, I sheared THP-1 cells with 1μM dexamethasone in the CPB circuit for 2 hours, rested them for 1 hour, extracted the RNA for qPCR, and collected the conditioned media for ELISA. THP-1 cells sheared with 5μM FK506 were used as a positive control. Two cytokines, IL-8 and TNF-α, were first investigated. CPB shear caused the upregulation of both IL-8 and TNF-α mRNA expression in the monocytes. Shearing THP-1 cells with FK506 reduced the mRNA levels of the two cytokines. Shearing THP-1 cells with 1 μM dexamethasone led to reduction of IL-8 mRNA but not TNF-α mRNA.

ii. ELISA

For the ELISA of the conditioned media, THP-1 cells were treated with a range of drug concentrations including dexamethasone at 0.5, 1, 2 μM, and FK506 at 1, 2.5, 5 μM. At all concentrations of FK506 treatment, the TNF-α and IL-8 levels in sheared THP-1 cell conditioned media were reduced to a half and a quarter of those without treatment, respectively. Dexamethasone treatment led to a twofold decrease in the IL-8 level, which is a less reduction compared to FK506. Interestingly, dexamethasone did not affect the TNF-α level until I increased the concentration to 2 μM. These results suggest that dexamethasone is not as effective in reducing the expression and production of IL-8 and TNF-α by shear-activated THP-1 cells as FK506.

iii. Luminex Multiplex Assay

To further address the mechanism that leads to a lesser performance of corticosteroids in treating shear-activated inflammatory response, I collected the conditioned media and ran the Luminex multiplex assays. 30 human inflammatory cytokines were assayed, and 9 cytokines were released by the monocytes including G-CSF, RANTES, MIP-1a, MIP-1b, HGF, VEGF, IL-1ra, TNF-α, and IL-8 (Figure 5.3). In the group treated with FK506, levels of G-CSF, RANTES, and IL-1ra were elevated and levels of MIP-1b and VEGF was suppressed compared to the dexamethasone-treated groups, suggesting a different anti-inflammatory pathway that damps the inflammatory response of shear-activated monocytes.

5.5 DISCUSSION

In this chapter, I showed that CPB-induced cytokine expression can be modified by both dexamethasone and FK506. Specifically, dexamethasone can reduce the IL-8 and TNF-α mRNA in sheared monocytes, but it is not as effective as FK506. I also probed the cytokine release profile from sheared monocytes using Luminex multiplex assay. I found increasing levels of MIP-1a and MIP-1b in media conditioned by the sheared monocytes. FK506 treatment during CPB shear led to increasing G-CSF, IL-1ra, RANTES in sheared monocyte conditioned media. Dexamethasone treatment during CPB shear resulted in increasing VEGF levels in sheared monocytes conditioned media. Each cytokine will be discussed in this section.

IL-8 and TNF-α are CPB-specific cytokines produced by monocytes. Previous study using the *in vitro* CPB model has demonstrated that monocytes respond to CPB shear by increasing the production of IL-8 and TNF-α. As previously shown, FK506 is a strong inhibitor of the IL-8 and TNF-α production in sheared monocytes since it targets the calcium-dependent pathways (65). In this study, dexamethasone also reduced the production of IL-8 and TNF-α by

the shear monocytes, but to a lesser extent compared to FK506. These results suggest that CPB-induced IL-8 and TNF-α release are mainly regulated by calcium-dependent pathways. Dexamethasone-mediated anti-inflammatory effects are pathway dependent. For example, dexamethasone selectively inhibits the IL-8 production by monocytes stimulated by lipopolysaccharide (LPS) but not phorbol myristate acetate (PMA) (161). This may explain why in cases such as CPB, dexamethasone is not effective at reducing the inflammatory response.

G-CSF is a glycoprotein hormone produced by endothelium and macrophages to stimulate the production of white blood cells by bone marrow. It plays an anti-inflammatory role by reducing the production of inflammatory cytokines such as TNF-α, GM-CSF, while upregulating soluble TNF-α receptor and IL-1ra (162,163). Elevated G-CSF level has been observed in serum of patients after extracorporeal circulation (164). However, in this study, the G-CSF level in the sheared group is not different from the static group, suggesting monocytes are not a contributor to the G-CSF release in response to CPB shear. Monocytes do respond to outside stimulation such as PMA by producing G-CSF, which is an important event to counteract bacterial and fungal infection (165). Study has shown that dexamethasone can augment the G-CSF production by monocytes with PMA stimulation. Hereby, I did not observe a positive effect of dexamethasone on the G-CSF level, but G-CSF release increased with sheared monocytes with FK506 treatment. How FK506 can modify the G-CSF production by the monocytes is not clear, however it is reasonable to speculate that one of the anti-inflammatory mechanisms of FK506 is the upregulation of G-CSF release by the monocytes after exposure to CPB shear.

IL-1ra is a protein that serves as the natural inhibitor of IL-1β through competitive binding. A study has shown that monocytes produce IL-1ra in response to LPS, as well as other cytokine stimulation such as IL-3, GM-CSF (166). TNF-α, however, is not an IL-1ra inducer.

This means that the elevated IL-1ra levels resulted from the FK506 treatment. One of the immunosuppressant effects of FK506 is to downregulate IL-1β production in PBMCs (167). This study also shows that FK506 increases the IL-1ra production, which further protects the cell from IL-1β-induced inflammatory response. Interestingly, CPB shear did not increase the IL-1β level in the monocytes. Dexamethasone at all concentrations did not affect the IL-1ra levels in the conditioned media. This can be explained by the suppressing effect of dexamethasone on the production of IL-1ra by monocytes (168).

MIP-1a/1b are chemokines produced by macrophages and monocytes. Both perform several biological functions including the recruitment of inflammatory cells and maintaining immune response of the effector cells (169). A study has shown that the plasma levels of MIP-1a and MIP-1b were upregulated in CPB patients (170). MIP-1a was indicated as one of the predictors for CPB-induced organ dysfunction (171). In this study, MIP-1 secreted by the monocytes was specifically promoted by CPB shear suggesting a correlation between CPB shear and MIP-1 production by the monocytes. Of all the treatments, only FK506 was able to reduce the MIP-1b release from the monocytes. This calcineurin-dependent mechanism to regulate MIP-1b production has been reported in activated T cells (172). Further investigation will be needed to confirm the mechanism of FK506 dependent MIP-1b production by monocytes. Additionally, Berkman et al. has reported that dexamethasone reduced the MIP-1a production by stimulated monocytes (173). Such an effect of dexamethasone was not observed in this study. Altogether, my results suggest that dexamethasone does not affect the MIP-1 production by sheared monocytes, while FK506 has additional anti-inflammatory effect which selectively reduces the MIP-1b production.

RANTES is a chemokine expressed by T cells, monocytes, epithelial cells, fibroblasts, and thrombocytes. Its function is to recruit leukocytes to the inflammation site. In CPB, plasma RANTES concentration decreases mainly due to the depletion of platelets and lymphocytes (174). In this study, the RANTES concentration derived from sheared monocytes did not change compared to the static control. This indicates that RANTES production is not related to monocytes in the CPB. Moreover, RANTES concentration in the sheared monocytes increased when treated with FK506. This outcome is contradictory to the anti-inflammatory property of FK506 as it has been shown to reduce the RANTES production in other cell types including T cells and keratinocytes (175,176). Further investigation will be needed to understand the mechanism of FK506-induced RANTES production in monocytes.

VEGF is a signaling protein that stimulates the formation of blood vessels. While the effect of CPB on the systemic VEGF level is unknown, one study has shown that VEGF can prevent acute kidney injury caused by CPB (177). In this study, CPB shear did not affect the VEGF production by the monocytes. However, elevated VEGF levels are observed in sheared monocytes treated with dexamethasone. This result may explain the mechanism that leads to the protective effect dexamethasone has on the renal function of CPB patients (178,179).

The monocytes responded differently to the drugs possibly due to their distinct anti-inflammatory mechanisms. Dexamethasone binds to the glucocorticoid receptor in the cytoplasm and translocates into the nucleus. The receptor complex further changes the activation state of transcriptional factors such as NF-κB and AP-1 and regulates downstream gene expression (180). The receptor complex also destabilizes the gene-specific mRNA of inflammatory cytokines, and therefore reduces the production of inflammatory cytokines such as IL-1β, IL-6, IL-12, TNF-α, GM-CSF, IL-8, RANTES, and MCP-1 (181,182). In contrast, FK506 binds macrophilin in cells

and specifically suppresses the activity of calcineurin. This further inhibits transcription factor nuclear factor of activated T-cells (NF-AT) entering the nucleus and regulates the downstream gene expression such as TNF-α, IL-6, IL-12 and MIP-1 (183-185). In this study, 5μM FK506 showed superior anti-inflammatory capability compared to 1μM and 2μM dexamethasone. One reason is that CPB-induced monocyte activation is mediated through calcium-dependent signaling pathways which are specifically inhibited by FK506 (65). Another possibility is that the concentration of FK506 used in this study is well above the therapeutic range. It is not known if the anti-inflammatory effect of FK506 is dependent on dosage. An optimal dosage will need to be determined to reduce the potential cytotoxicity.

The IL-8 and TNF-α levels measured by Luminex multiplex assay were inconsistent with the ones measured by ELISA. Specifically, the sheared groups, sheared with dexamethasone groups, and sheared with vehicle groups had high standard deviations. The inconsistency may stem from the way long side tubing was arranged, the heat generated at the pump head, and tubing wear after several shears. The standard deviation in the sheared with FK506 groups is lower, possibly due to the strong inhibitory effect of FK506 on calcineurin-mediated TNF-α and IL-8 production. Future experiments may improve the *in vitro* model with tubing of set arrangements so that the monocytes are sheared more uniformly.

In conclusion, the study in this chapter showed that dexamethasone has limited anti-inflammatory effect on CPB-induced monocytic response. FK506 is more effective in reducing the IL-8 and TNF-α production by shear-activated monocytes. However, dexamethasone may provide additional protection against renal injury due to its ability to increase VEGF-A production by sheared monocytes.

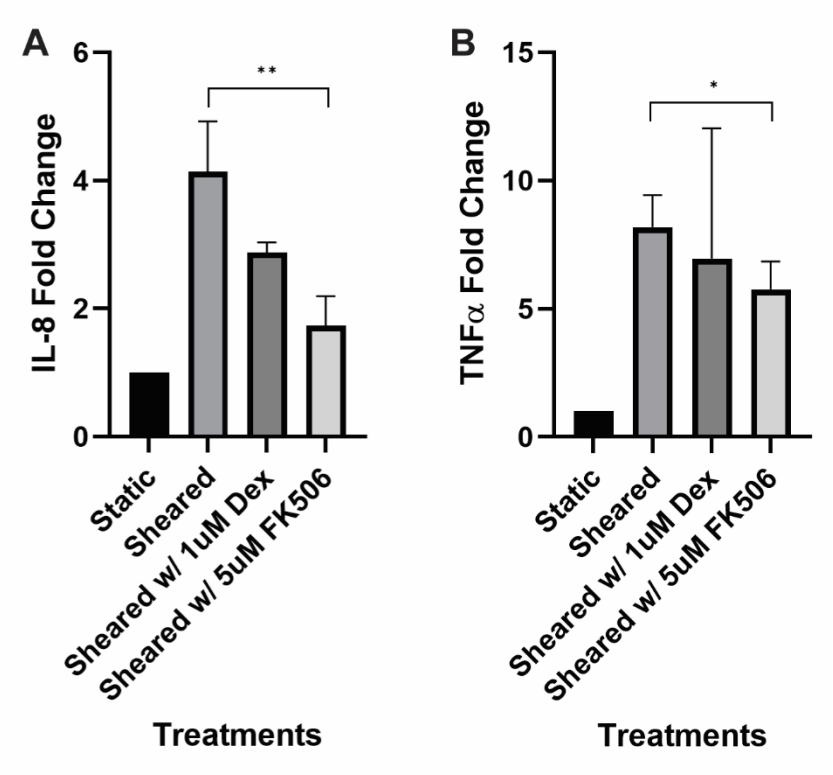

Figure 5.1. qPCR results of A) IL-8 and B) TNF-α expressions of THP-1 cells sheared with or without dexamethasone and FK506. Statistical significance is denoted by '*'. P values less than 0.05 are indicated by one star symbol and P values less than 0.01 are indicated by double star symbol.

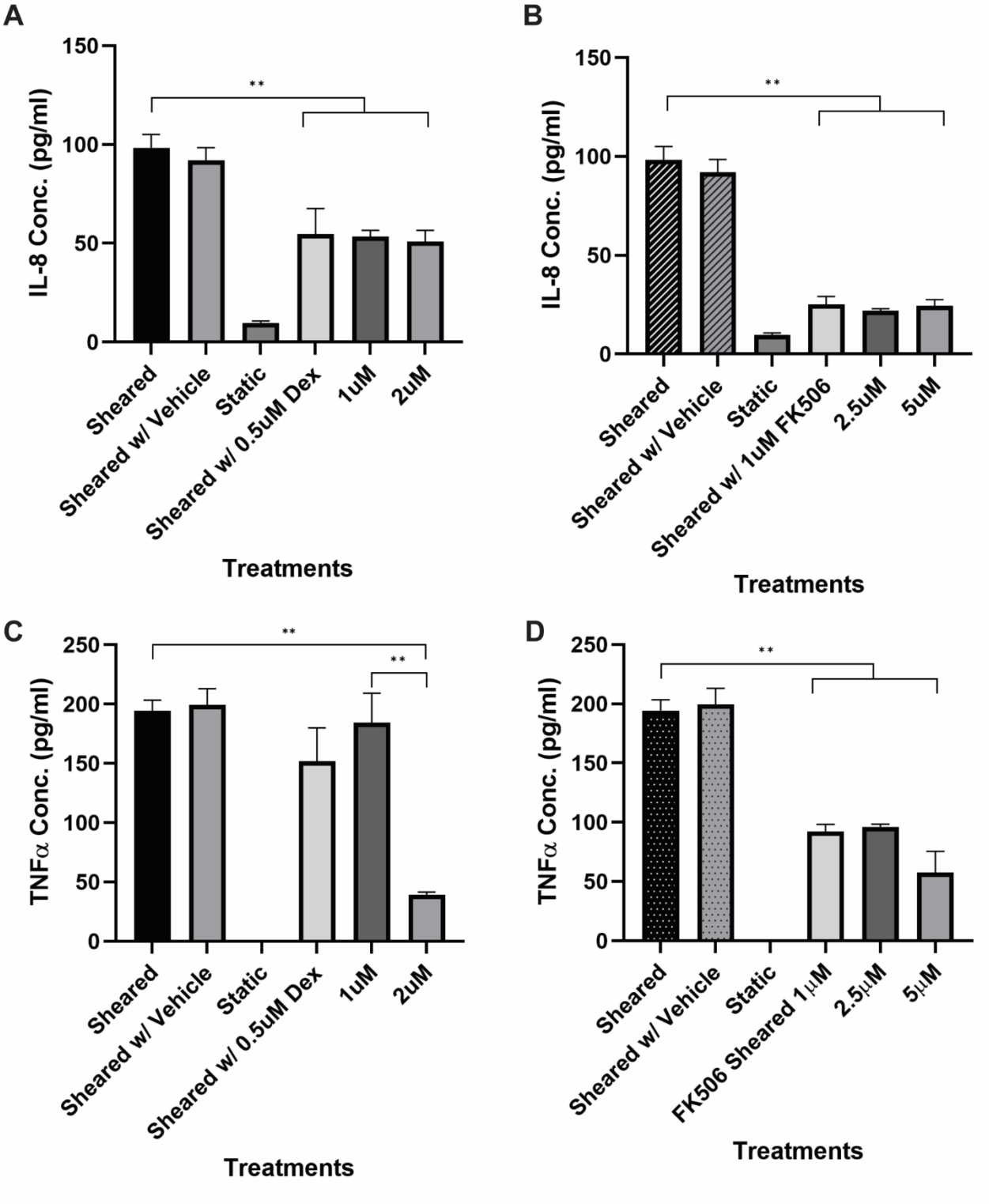

Figure 5.2. Levels of A), B) IL-8 and C), D) TNF-α in the conditioned media of THP-1 cells sheared with or without dexamethasone and FK506 measured by ELISA. Statistical significance

is denoted by '*'. P values less than 0.05 are indicated by one star symbol and P values less than 0.01 are indicated by double star symbol.

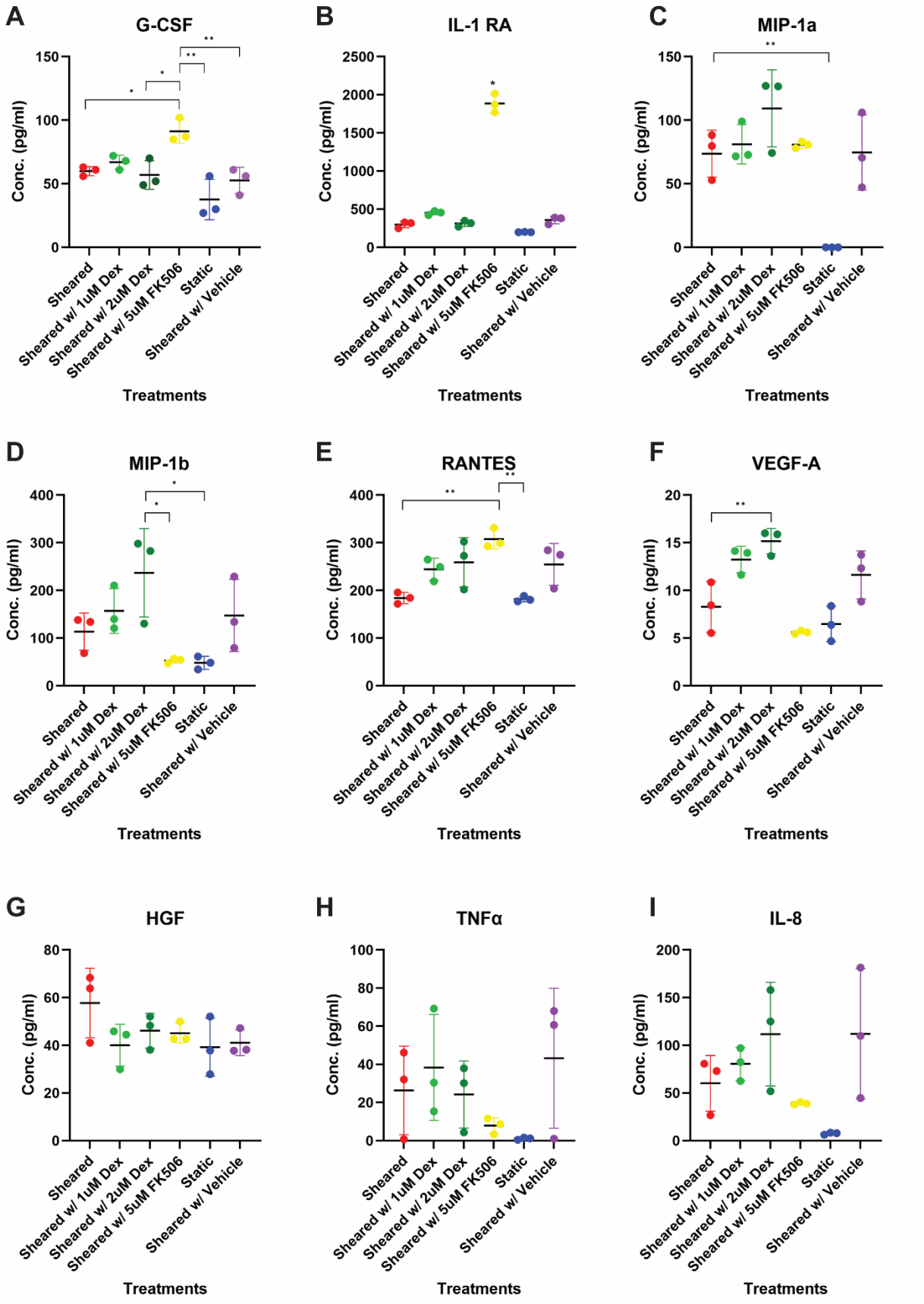
A
G-CSF
Conc. (pg/ml)
150
100
50
0
*
*
**
**
Sheared
Sheared w/ 1uM Dex
Sheared w/ 2uM Dex
Sheared w/ 5uM FK506
Static
Sheared w/ Vehicle
Treatments
B
IL-1 RA
Conc. (pg/ml)
2500
2000
1500
1000
500
0
*
Treatments
C
MIP-1a
Conc. (pg/ml)
150
100
50
0
**
Treatments
D
MIP-1b
Conc. (pg/ml)
400
300
200
100
0
*
*
Treatments
E
RANTES
Conc. (pg/ml)
400
300
200
100
0
**
**
Treatments
F
VEGF-A
Conc. (pg/ml)
20
15
10
5
0
**
Treatments
G
HGF
Conc. (pg/ml)
80
60
40
20
0
Treatments
H
TNFα
Conc. (pg/ml)
100
80
60
40
20
0
Treatments
I
IL-8
Conc. (pg/ml)
200
150
100
50
0
Treatments

Figure 5.3. Levels of A) G-CSF, B) IL-1ra, C) MIP-1a, D) MIP-1b, E) RANTES, F) VEGF-A, G) HGF, H) TNF-α, and I) IL-8 in the conditioned media of THP-1 cells sheared with or without dexamethasone and FK506 measured by Luminex multiplex assay. Statistical significance is denoted by '*'. P values less than 0.05 are indicated by one star symbol and P values less than 0.01 are indicated by double star symbol.

Chapter 6. INVESTIGATING THE EFFECT OF SHEAR CONDITIONED MEDIA ON ENDOTHELIAL CELLS

6.1 ABSTRACT

Endothelial cells play an important role in mediating the inflammatory response in CPB-induced complications. Apart from the monocyte-endothelial interaction, which I investigated in chapter 3 and 4, endothelial cells also respond to the inflammatory cytokines derived from blood cells sheared in the CPB circuit. Particularly, the cytokine profile of sheared monocytes was studied. In this chapter, the effect of shear conditioned media on endothelial cells was examined. Immunofluorescent staining and F-actin staining showed that treatment of conditioned media from sheared THP-1 cells disrupted the VE-cadherin of endothelial cells as well as promoting the formation of intercellular gaps. Treatment of conditioned media from shear THP-1 cells also lead to lower endothelial cell viability, increasing adhesion molecule expression, and increasing monocyte adhesion. The inflammatory response of endothelial cells was attenuated by treatment of conditioned media from THP-1 cells sheared with 2 μM dexamethasone and 5 μM FK506. FK506 showed superior anti-inflammatory effect on the endothelial cells compared to dexamethasone.

6.2 INTRODUCTION

In the last chapter, I investigated the cytokines derived from monocytes sheared in a CPB circuit. These cytokines play in synergy and eventually affect the endothelium to elicit inflammatory response. To understand the effect of these cytokines in the shear conditioned media on the endothelial cells, I treated the endothelial cells with the shear conditioned media and characterized the response of the endothelial cells. I hypothesize that conditioned media

derived from sheared monocytes can stimulate the endothelial cells by disrupting the barrier function of the endothelial monolayer, upregulating the adhesion molecules and promoting monocyte adhesion. In addition, dexamethasone and FK506 treatments showed anti-inflammatory effects by regulating the cytokine release profile of sheared monocytes. To investigate the downstream effects on endothelial cells, I also treated the endothelial cells with the conditioned media derived from sheared monocytes with drug treatment. I hypothesized that the conditioned media from sheared monocytes treated with both dexamethasone and FK506 can reduce the inflammatory response of the endothelial cells, with the FK506 being more effect at preserving the endothelial membrane integrity, reducing the adhesion molecule activation, reducing the monocyte adhesion.

6.3 MATERIALS AND METHODS

6.3.1 Cell Lines and Culture Methods

Primary human neonatal dermal microvascular cells (HNDMVECs, Cat # CC-2516) were purchased from Lonza (Walkersville, MD) and cultured in endothelial cell growth medium MV2 (PromoCell, Heidelberg, Germany, Cat # C-22121) with 100U/mL penicillin-streptomycin (Gibco, Waltham, MA, Cat # 15140122). The medium was changed every other day, and the cells were harvested by trypsinization. The human acute leukemia monocytic cell line THP-1 (Cat # TIB-202) was purchased from ATCC and cultured in RPMI 1640 medium (ATCC Modification) (Gibco, Waltham, MA, Cat # A1049101) with 10% FBS. The medium was changed every other day.

6.3.2 Collection of Conditioned Media

THP-1 cells at a density of 2 million cells/mL were sheared in a 10 foot-long Masterflex Tygon E-3603 L/S13 pump tubing (Cole-Parmer, Vernon Hills, IL, Cat # MK-06509-13), using a Masterflex miniflex pump model 115/230 VAC 07525-20 (Cole-Parmer, Vernon Hills, IL, Cat # MK-07525-20) at 10 mL/min for 2 hours. The long side tubing was submerged in a water bath with temperature control at 37°C. During the shear, THP-1 cells were suspended in media with 1μM dexamethasone, 2μM dexamethasone, 5μM FK506, or vehicle DMSO. At the end of the shear, the THP-1 cells were statically incubated in the media that they are sheared in for 1 hour in a 50 mL Falcon tube. At the end of the incubation, the media supernatant was collected and kept frozen at -20°C and used as sheared conditioned media.

6.3.3 Effect of Shear Conditioned Media on HNDMVECs

i. Immunofluorescent Staining

HNDMVECs were seeded on 8-chamber slides (354118, Corning, NY) at 5000 cells/cm^2 and cultured 7 days to form a confluent monolayer. Next, HNDMVECs were treated with shear conditioned media for 6 hours at 37°C with 5% CO_2. The cells were then washed twice with sterile PBS, fixed with formalin. Fixed cells were permeabilized with 0.1% Triton-X-100 for 10 minutes, blocked with 1% BSA for 1 hour, followed by incubation with 1:200 vascular endothelial cadherin (VE-cadherin) monoclonal antibody (16B1), Biotin (Thermofisher, Waltham, MA, Cat # 13-1449-82) for 1 hour, 1:500 streptavidin, Alexa Fluor 594 Conjugate (Thermofisher, Waltham, MA, Cat # S11227) for 45 minutes. Nuclei were stained with DAPI. The slides were then washed, mounted, and imaged using a Leica DMI6000 microscope with Leica SP8X confocal. VE-cadherin staining was quantified by fluorescent intensity using ImageJ.

ii. Phalloidin Staining

HNDMVECs were seeded on 8-chamber slides (354118, Corning, NY) at 5000 cells/cm^2 and cultured 7 days to form a confluent monolayer. Next, HNDMVECs were treated with shear conditioned media for 6 hours at 37°C with 5% CO_2. The cells were then washed twice with sterile PBS, fixed with formalin, permeabilized with 0.1% Triton-X-100, and blocked with 1% BSA. The cells were then incubated with Rhodamine Phalloidin (ThermoFisher, Cat # R415) for 20 minutes at room temperature, stained with DAPI, washed, mounted, and imaged using a Leica DMI6000 microscope with Leica SP8X confocal. Intercellular gap area was quantified using ImageJ on the slides stained by the Rhodamine Phalloidin.

iii. Live/Dead Assays

HNDMVECs were seeded on 8-chamber slides (354118, Corning, NY) at 5000 cells/cm^2 and cultured 7 days to form a confluent monolayer. Next, HNDMVECs were treated with shear conditioned media for 6 hours at 37°C with 5% CO_2. After that, the cells were rinsed with PBS twice. The Live/Dead assays were performed using the LIVE/DEAD Cell Imaging Kit (488/570) (Thermofisher, Waltham, MA, Cat # R37601). Briefly, the Calcein AM live green dye was mixed with the BOBO-3 dead red dye to form a 2x working solution. The mixture was diluted with an equal volume of PBS and applied to live cells for 20 minutes. The stained HNDMVECs were visualized using a Nikon Eclipse TE200 microscope (Tokyo, Japan) and a Photometric CoolSNAP MYO camera (Tucson, AZ) with a Rhodamine and FITC filter.

iv. Quantitative Real Time PCR

HNDMVECs were treated with shear conditioned media for 1 hour, and total RNA was extracted using the RNeasy Mini Kit (Qiagen, Hilden, Germany, Cat # 74104) and RNase-Free

DNAse Set (Qiagen, Hilden, Germany, Cat # 79254). A total RNA of 150 ng was used for producing cDNA with the Omniscript RT Kit (Qiagen, Hilden, Germany, Cat # 205113). Quantitative real-time PCR was performed with Taqman Universal PCR Master Mix (Thermofisher, Waltham, MA, Cat # 4304437) on a QuantStudio 6 Pro real-time PCR system (Thermofisher, Waltham, MA, Cat # A43180) according to the manufacturer instructions. Both biological and technical triplicates were run. Taqman primers of selectin E (Hs00174057_m1, Cat # 4331182), intercellular adhesion molecule 1 (ICAM-1) (Hs00164932_m1, Cat # 4331182) and vascular cell adhesion molecule 1 (VCAM-1) (Hs01003372_m1, Cat # 4331182) were purchased from Thermofisher.

v. Monocyte Adhesion Assay

HNDMVECs were seeded on 24-well plates at 5000 cells/cm^2 and cultured 7 days to form a confluent monolayer. HNDMVECs were then incubated with shear conditioned media for 1 hour and then rinsed with PBS. Statically incubated G-THP-1 cells were then added to a monolayer of HNDMVECs ($1x10^6$ cells per well), followed by incubation for 1 hour. The co-cultures were gently rinsed twice with sterile PBS to remove non-adherent G-THP-1 cells. The adhered G-THP-1 were visualized using a Nikon Eclipse TE200 microscope (Tokyo, Japan) and a Photometric CoolSNAP MYO camera (Tucson, AZ) with a GFP filter. The adhered hPBMCs were visualized with the same microscope and camera with brightfield imaging. The experiments were run in triplicates. The number of adherent G-THP-1 cells or hPBMCs were counted in five randomly selected visible fields and quantified using ImageJ.

6.3.4 Statistical Analysis

All experiments were run in triplicates. All quantitative data were expressed as mean ± standard deviation within groups. Pairwise comparisons between groups were conducted using ANOVA test and Tukey's post-hoc test. Statistical significance is denoted by '*'. P values less than 0.05 are indicated by single star symbol and P values less than 0.01 are indicated by double star symbol.

6.4 RESULTS

6.4.1 Shear conditioned media treatment leads to disruption of VE-cadherin and intercellular gap formation

To characterize the barrier function of the endothelial cells, HNDMVECs were treated with shear conditioned media and the VE cadherin and F actin filaments were examined using immunofluorescent staining and rhodamine phalloidin staining. Treating the HNDMVECs with conditioned media of sheared THP-1 cells resulted in disruption of the VE cadherin (Figure 6.1B). Treating the HNDMVECs with conditioned media of THP-1 cells sheared with 2μM dexamethasone and 5μM FK506 retained the VE cadherin (Figure 6.1D, E). In HNDMVECs treated with conditioned media of static THP-1 cells, robust VE cadherin was maintained (Figure 6.1F).

Similar protective effect of dexamethasone and FK506 was observed in the F actin staining. Quantification of intercellular gap area showed increasing gap area formation in the HNDMVECs treated with the conditioned media of shear THP-1 cells (Figure 6.3B). Conditioned media of THP-1 cells sheared with 2μM dexamethasone and 5μM FK506 significantly reduced the intercellular gap area in the HNDMVECs (Figure 6.3D, E).

6.4.2 Shear conditioned media reduced the viability of HNDMVECs

Inflammatory mediators can induce endothelial cell apoptosis during and after CPB. In the previous chapter, I showed that CPB shear can induce release of proinflammatory cytokines, which can be attenuated by treatment of dexamethasone and FK506. To further assess the effect of inflammatory mediators in shear conditioned media on the viability of HNDMVECs, I performed the live and dead assays. Treating the HNDMVECs with conditioned media of sheared THP-1 cells resulted in increasing cellular death (Figure 6.5B). In other groups, the treatment did not affect the viability of the endothelial cells.

6.4.3 Shear conditioned media selectively alters the expression of adhesion molecule in HNDMVECs

Exposure to an environment of inflammatory mediators can change the expression of adhesion molecules in endothelial cells, which further facilitates the adhesion of blood cells. To examine the effect of conditioned media on the adhesion molecules of HNDMVECs, qPCR was performed to measure the E-selectin, ICAM-1, VCAM-1 expressions in the HNDMVECs treated with conditioned media. Treating the HNDMVECs with conditioned media of sheared THP-1 cells significantly upregulated the expression E-selectin and ICAM-1 (Figure 6.6A, B), while the VCAM-1 expression remained unchanged (Figure 6.6C). Treatment of conditioned media of THP-1 cells sheared with FK506 and dexamethasone both lead to decrease in E-selectin and ICAM-1 expression, but only the decrease in E-selectin resulted from FK506 conditioned media treatment was statistically significant (Figure 6.6A).

6.4.4 Shear conditioned media treatment promoted the adhesion of static THP-1 cells on HNDMVECs

After characterizing the adhesion molecules of endothelial cells treated with the conditioned media, I performed the adhesion assay by examining the capability of conditioned media to induce monocyte adhesion. Statically incubated the THP-1 cells were co-cultured with HNDMVECs stimulated with conditioned media and adhered cells were quantified. Treating the HNDMVECs with conditioned media of sheared THP-1 cells led to increasing monocyte adhesion (Figure 6.8B). Treating the HNDMVECs with conditioned media of THP-1 cells sheared with FK506 reduced the monocyte adhesion by half (Figure 6.6E). While conditioned media of THP-1 cells sheared with 2μM dexamethasone also reduced the monocyte adhesion (Figure 6.6D), it is not as effective as the FK506 conditioned media.

6.5 DISCUSSION

In this study, the effect of conditioned media derived from sheared monocytes on endothelial cells was examined. Treatment of conditioned media from sheared monocytes led to disruption of VE-cadherin, increasing intercellular gap area, upregulation of adhesion molecules, and decreasing cell viability. The conditioned media from monocytes sheared with dexamethasone and FK506 attenuated the inflammatory response of the endothelial cells. These results indicate that cytokines derived from sheared monocytes elicit inflammatory response of endothelial cells and both dexamethasone and FK506 can provide protection against the insult of CPB-induced cytokines.

The inflammatory response of endothelial cells to the shear conditioned media may be a synergetic effect of the mediators released by the sheared monocytes. The effects of TNF-α and

IL-8 on endothelial cells have been well studied. TNF-α downregulates the VE-cadherin expression (186-188), causes rearrangement of cytoskeleton, and upregulates the adhesion molecules. IL-8 downregulates the tight junction of endothelial cells to increase the endothelial permeability (189). In Chapter 4 of this dissertation, I also showed that IL-8 is an inducer of ICAM-1 and VCAM-1 expression in the endothelial cells, which mediated monocyte adhesion. In cases of CPB, these two cytokines act in synergy to stimulate an inflammatory response. The synergetic effect of TNF-α and IL-8 on endothelial cells is less known. Plus, the Luminex study showed that CPB shear may subject the endothelial cells to a more complex biochemical environment created just by shearing monocytes. Further study will be needed to characterize the response of endothelial cells to the combined effect of the cytokines derived from CPB shear.

Treatment of conditioned media from monocytes sheared with anti-inflammatory drugs ameliorated the inflammatory response of the endothelial cells. This can be caused by two mechanisms. The first mechanism has been demonstrated in Chapter 5 where the pro-inflammatory mediators released by sheared monocytes were reduced by both drugs. In the second mechanism, the endothelial inflammatory response was attenuated by the residual drugs in the conditioned media. The anti-inflammatory effect of dexamethasone includes retaining the barrier function of the endothelium by upregulating the junction protein and preventing cell adhesion by downregulating the adhesion molecules (190-194). My results showed that dexamethasone can protect the endothelial cells from the inflammatory mediators derived from sheared monocytes. Reports of the effect of FK506 on the endothelial cells are mixed. Edda et al. and Virginia et al. showed that FK506 rescues endothelial dysfunction, while Ryoji et al. reported the opposite (195-197). In this study, the conditioned media with FK506 treatment contains reduced inflammatory mediators and residual FK506. Therefore, the exact effect of FK506 on

the inflammatory response of endothelial cells cannot be determined. Further investigation will be needed to decouple the effect of reduced cytokines presented in the conditioned media.

Treatment of conditioned media from sheared monocytes led to increasing endothelial cell death. Hermann et al. has described the increasing apoptosis of human umbilical endothelial cells when treated with serum of CPB patients (198). In CPB, endothelial apoptosis can be attributed to multiple factors such as the pro-inflammatory mediators, temperature change, osmolality, and shear stress. In my model, shear stress is the main variable that alters the content of the conditioned media derived from the monocytes. This shows that the pro-inflammatory mediators derived from sheared monocytes are responsible for the endothelial deaths and the dysfunction of endothelium.

Both treatments of conditioned media from monocytes sheared with dexamethasone and FK506 prevented the endothelial death. This can also be the result of residual drugs from the conditioned media. Dexamethasone-meidated changes in endothelial cell viability are both dose-dependent (199). One study has shown that dexamethasone at 1μM is more likely to induce apoptosis. The anti-apoptosis effect significantly increases with lower concentration. At concentration higher than 1μM, the anti-apoptosis effect increases with less intensity. In this study, the viability of endothelial cells treated with conditioned media from monocytes sheared with 1μM and 2μM is comparable to the endothelial cells treated with static conditioned media. It is possible that the dexamethasone concentration dropped below 1μM in conditioned media due to degradation during CPB shear, which allows the dexamethasone shear conditioned media to amplify its anti-apoptotic effect. Interestingly, the anti-apoptotic effect of dexamethasone on the endothelial cells is also dependent on the stimulant on the endothelial cells. For example, 1μM dexamethasone inhibits endothelial apoptosis induced by the treatment of statin (200).

Therefore, the exact protective mechanism of dexamethasone in this model may be more complicated. Treatment of conditioned media from monocytes sheared with FK506 reduced endothelial cell death. Contrary to my finding, FK506 has been shown to disturb the function of endothelial cells. The therapeutic concentration of FK506 ranging from 10ng/mL to 20ng/mL can significantly induce endothelial cell death (199). The cytotoxicity of FK506 is not dependent on the calcineurin inhibition effect but mediated by the Akt and ERK1/2 pathways (199). In this study, the FK506 concentration is several magnitudes greater than the therapeutic concentration range. The preserved endothelial cell viability may be caused by the degradation of FK506 or other molecular mechanisms that protected endothelial cells from apoptosis.

In conclusion, conditioned media from sheared monocytes causes the inflammatory response of endothelial cells, which is attenuated by the conditioned media from monocytes sheared with dexamethasone and FK506. The protection provided by dexamethasone may be due to its ability to reduce the inflammatory mediators in the conditioned media as well as its anti-inflammatory effect on endothelial cells. For FK506, its effect on the endothelial cells is unclear. Therefore, the protective effect may mainly be the result of its superior mechanism to reduce the inflammatory mediators and induce anti-inflammatory cytokine production.

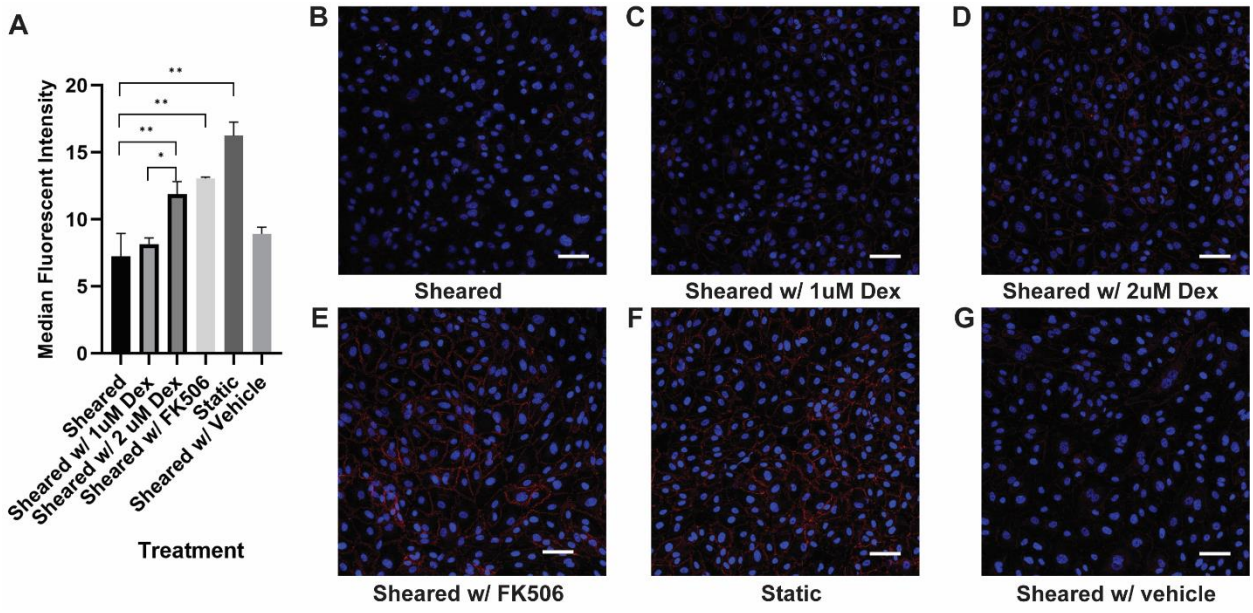

Figure 6.1. A) Quantification of VE cadherin staining. VE-cadherin of HNDMVECs treated with B) condition media of sheared THP-1 cells, C) condition media of THP-1 cells sheared with 1μM dexamethasone, D) condition media of THP-1 cells sheared with 2μM dexamethasone, E) condition media of THP-1 cells sheared with 5μM FK506, F) condition media of statically incubated THP-1 cells, and G) condition media of THP-1 cells sheared with vehicle DMSO. visualized by immunofluorescent staining. Additional images see Figure 6.2. Red = VE-Cadherin, Blue = DAPI. Scale bar = 100 μm. Statistical significance is denoted by '*'. P values less than 0.05 are indicated by one star symbol and P values less than 0.01 are indicated by double star symbol.

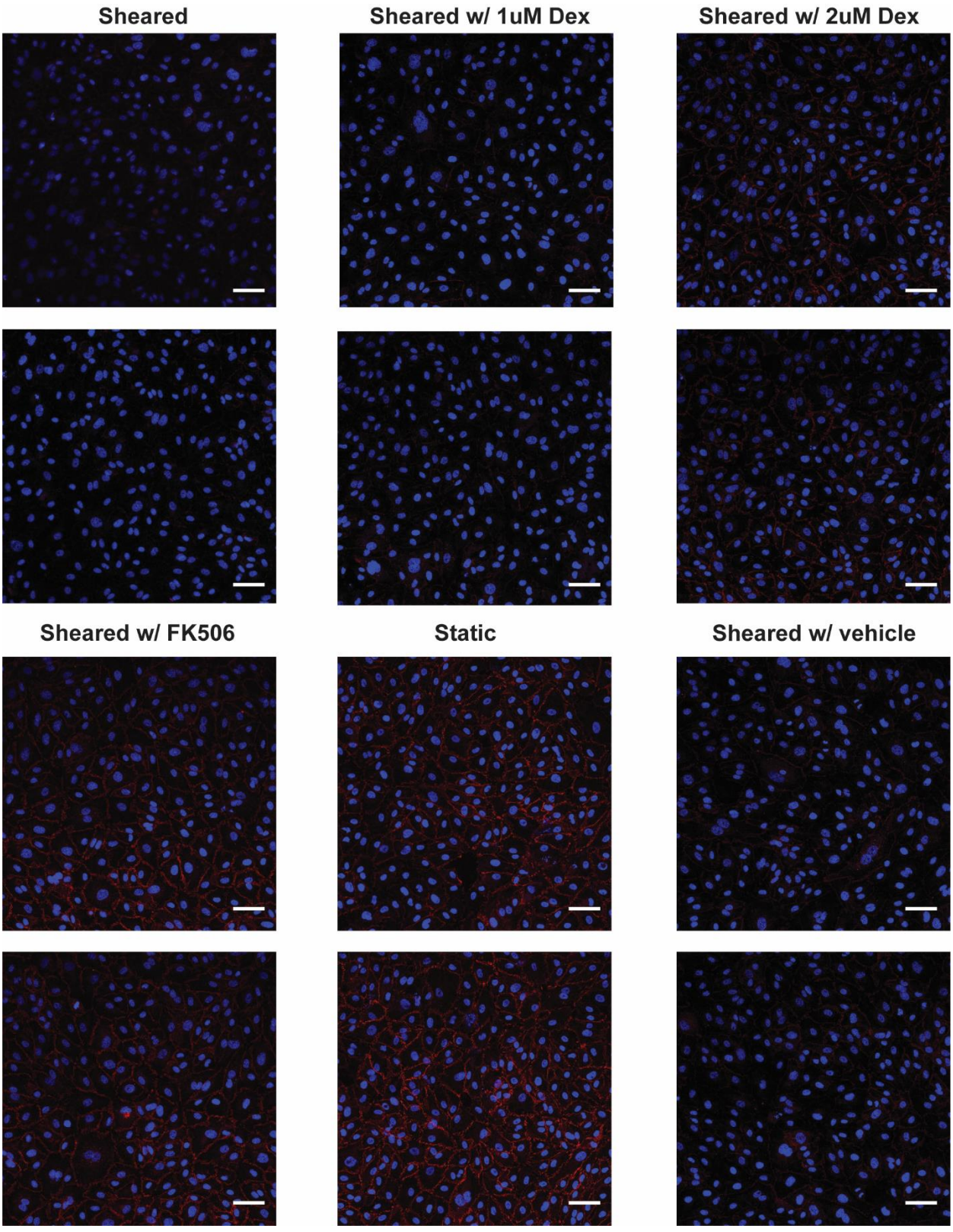

Figure 6.2. Additional images of VE-cadherin staining. Scale bar = 100 μm.

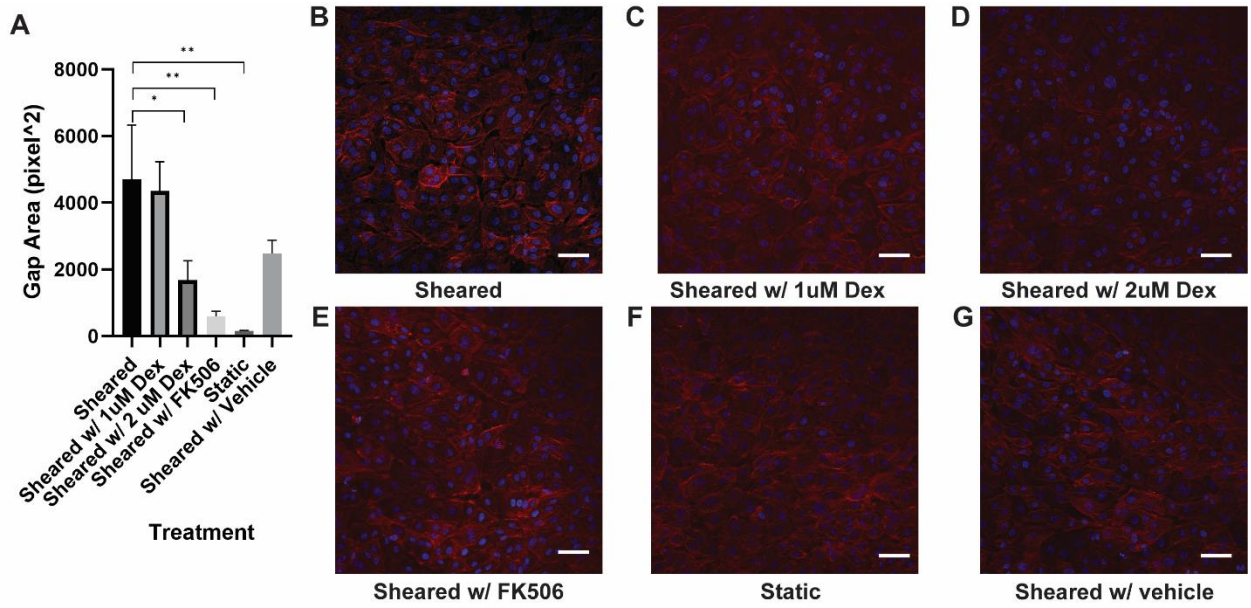

Figure 6.3. A) Quantification of intercellular gap area. F-actin of HNDMVECs treated with B) condition media of sheared THP-1 cells, C) condition media of THP-1 cells sheared with 1μM dexamethasone, D) condition media of THP-1 cells sheared with 2μM dexamethasone, E) condition media of THP-1 cells sheared with 5μM FK506, F) condition media of statically incubated THP-1 cells, and G) condition media of THP-1 cells sheared with vehicle DMSO. visualized by rhodamine phalloidin staining. Additional images see Figure 6.4. Red = VE-Cadherin, Blue = DAPI. Scale bar = 100 μm. Statistical significance is denoted by '*'. P values less than 0.05 are indicated by one star symbol and P values less than 0.01 are indicated by double star symbol.

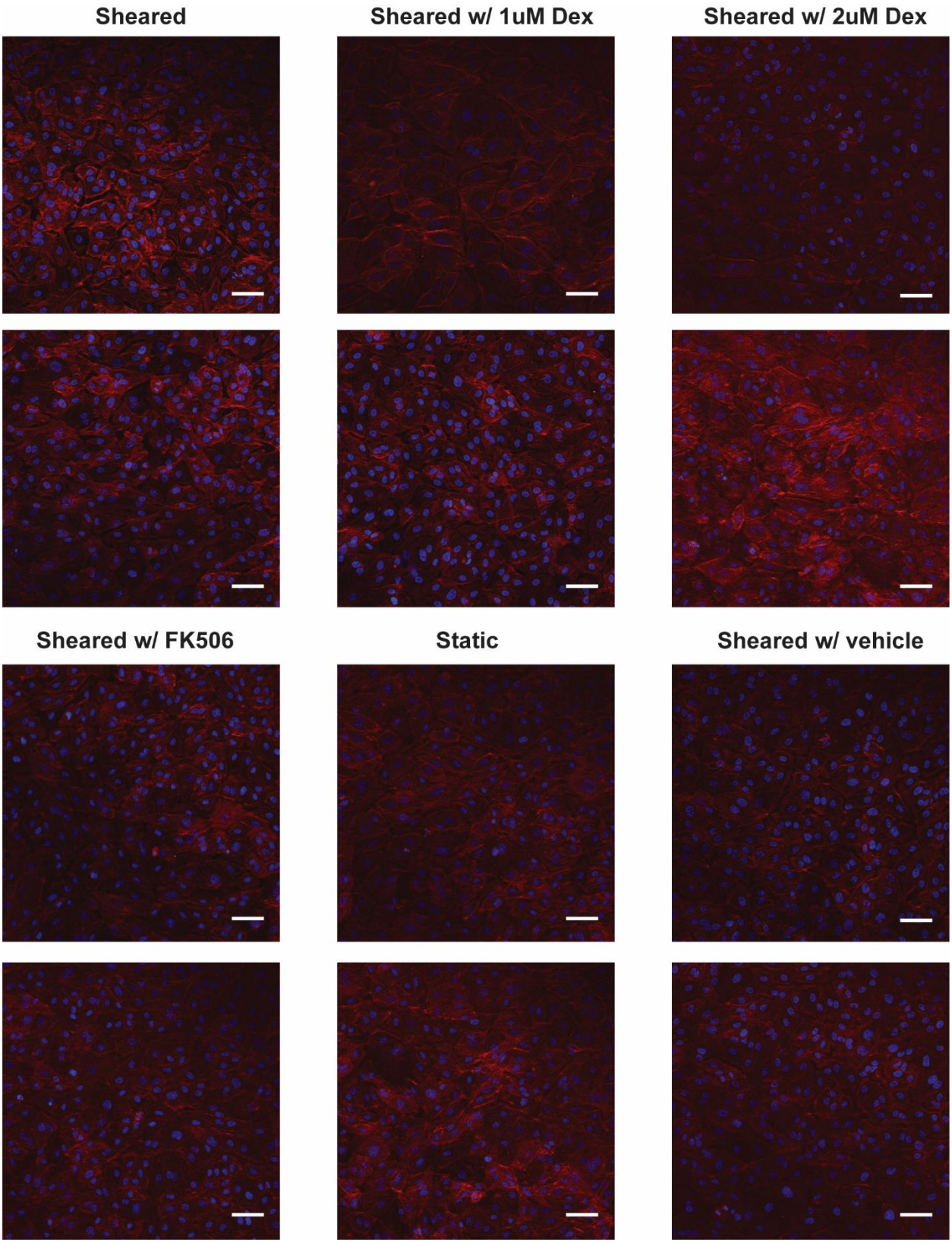

Figure 6.4. Additional images of F-actin staining. Scale bar = 100 μm.

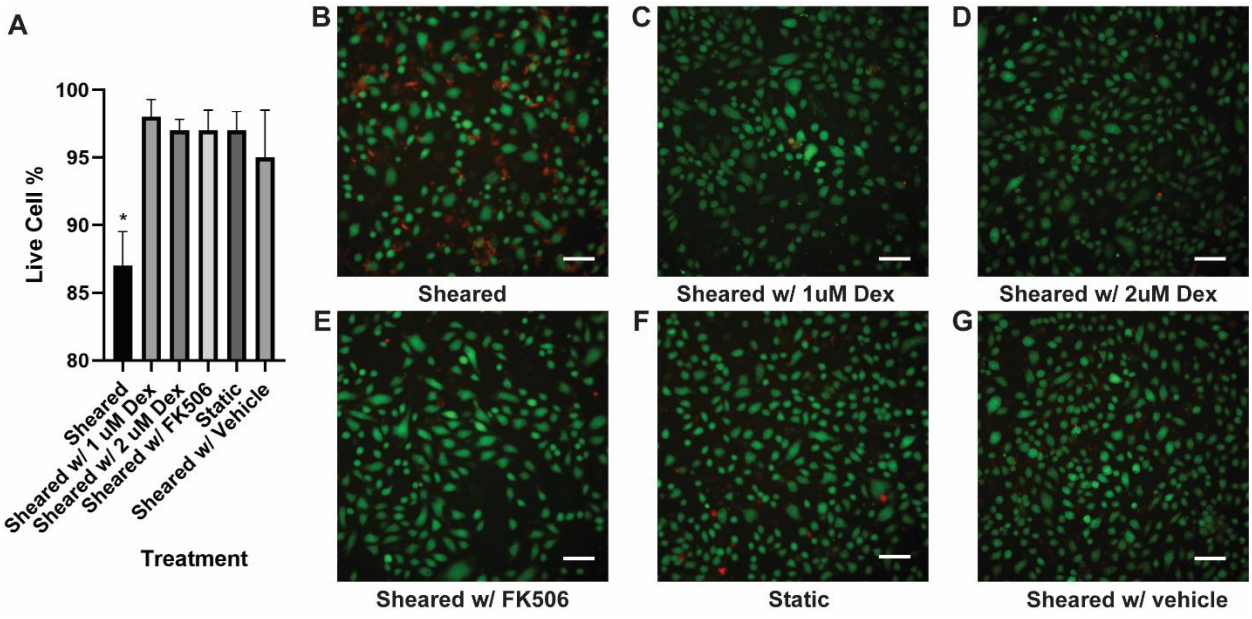

Figure 6.5. A) HNDMVEC cell viability after conditioned media treatment. Live and dead assays of HNDMVECs treated with B) condition media of sheared THP-1 cells, C) condition media of THP-1 cells sheared with 1μM dexamethasone, D) condition media of THP-1 cells sheared with 2μM dexamethasone, E) condition media of THP-1 cells sheared with 5μM FK506, F) condition media of statically incubated THP-1 cells, and G) condition media of THP-1 cells sheared with vehicle DMSO. visualized by calcein AM (green) and BOBO3 (red) staining. Scale bar = 100 μm.

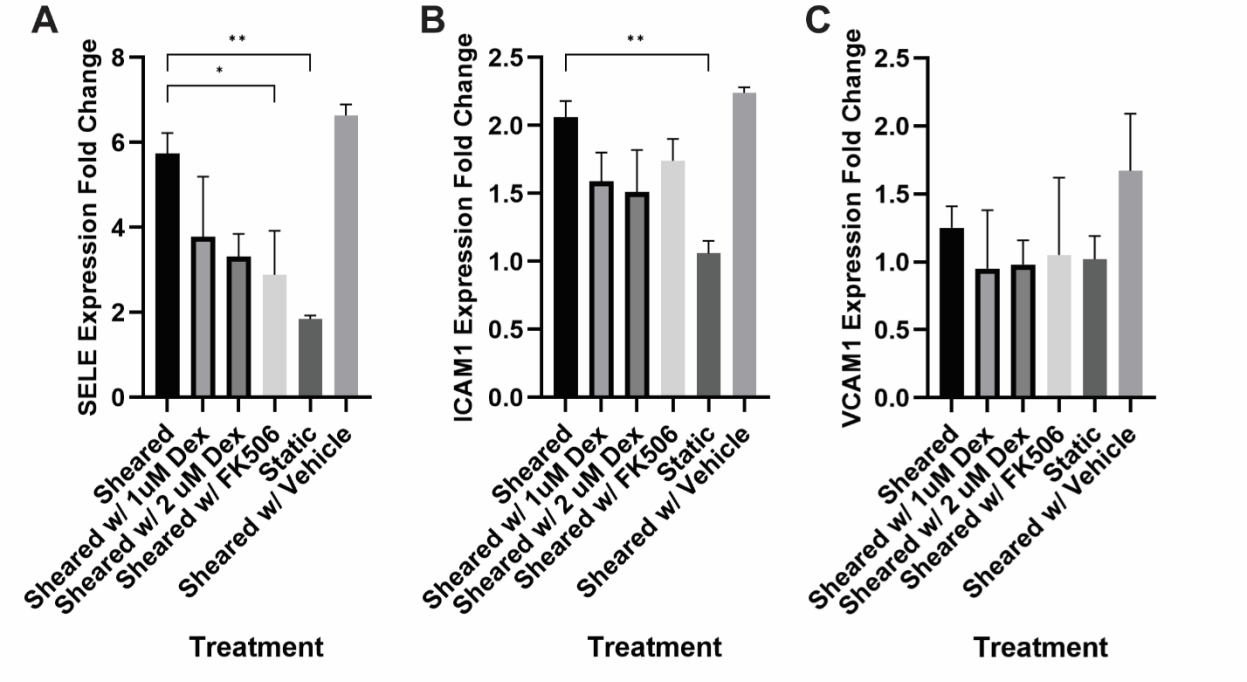

Figure 6.6. Expression of A) E-selectin, B) ICAM-1, and C) VCAM-1 in HNDMVECs treated with conditioned media measured by RT-qPCR. Statistical significance is denoted by '*'. P values less than 0.05 are indicated by one star symbol and P values less than 0.01 are indicated by double star symbol.

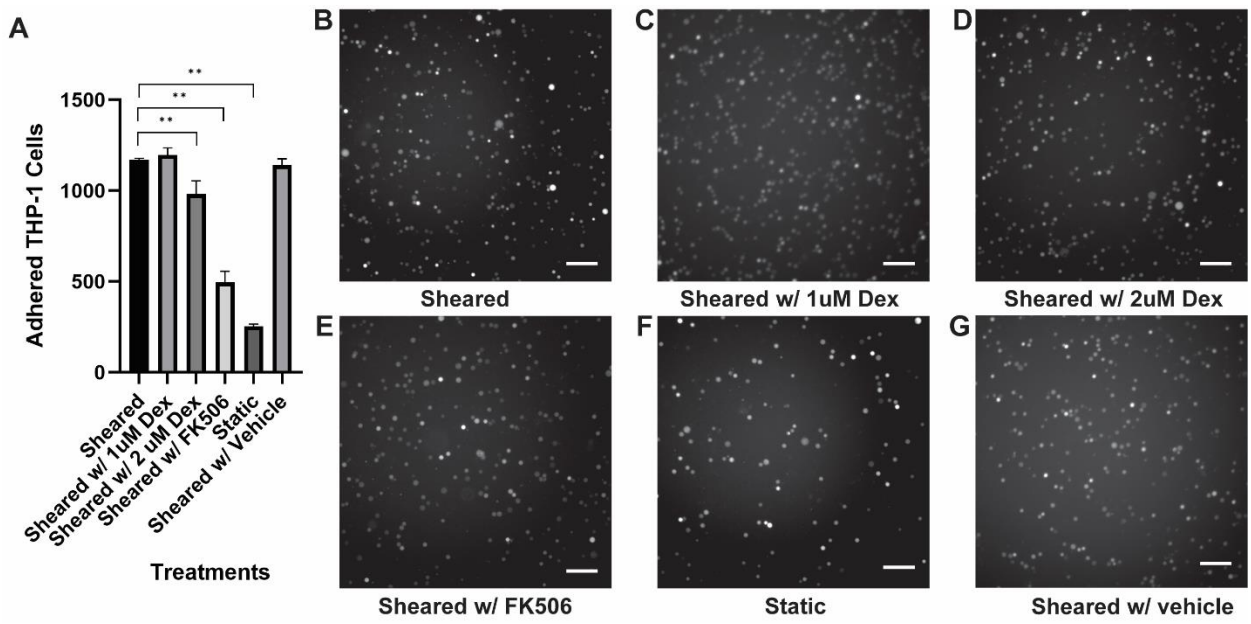

Figure 6.7. A) Quantitative analysis of adhered G-THP-1 cells on the endothelial cell monolayer. Adhesion of static THP-1 cells to HNDMVECs treated with B) condition media of sheared THP-1 cells, C) condition media of THP-1 cells sheared with 1μM dexamethasone, D) condition media of THP-1 cells sheared with 2μM dexamethasone, E) condition media of THP-1 cells sheared with 5μM FK506, F) condition media of statically incubated THP-1 cells, and G) condition media of THP-1 cells sheared with vehicle DMSO. Scale bar = 100 μm. Additional images see Figure 6.8. Statistical significance is denoted by '*'. P values less than 0.05 are indicated by one star symbol and P values less than 0.01 are indicated by double star symbol.

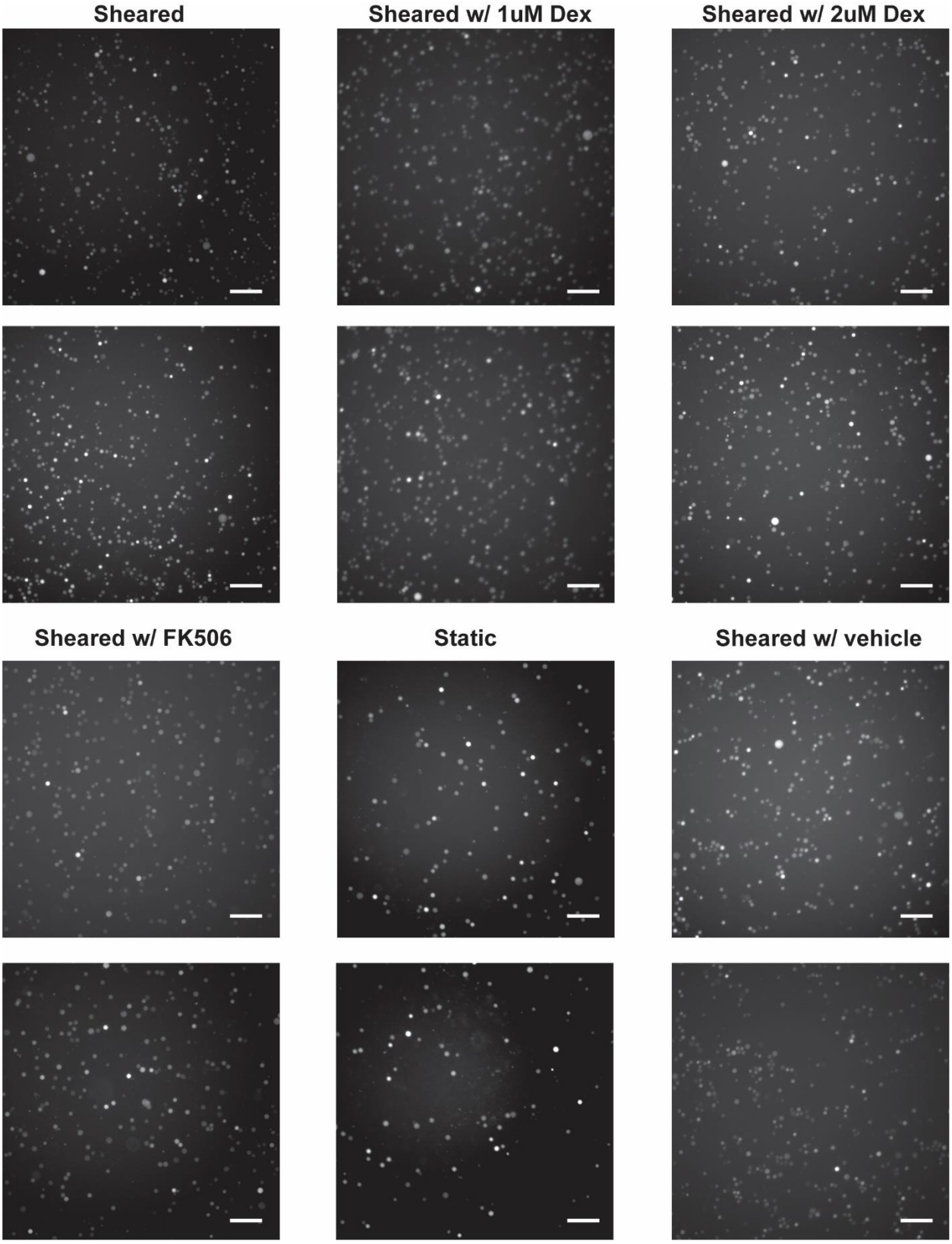
Sheared
Sheared w/ 1uM Dex
Sheared w/ 2uM Dex
Sheared w/ FK506
Static
Sheared w/ vehicle

Figure 6.8. Additional images of adhered THP-1 cells were used for quantitative analysis. Scale bar = 100 μm.

Chapter 7. CONCLUSION AND FUTURE STUDY

7.1 CONCLUSION

CBP-induced inflammatory response and postoperative complications affect the quality of life of pediatric patients. The failure of conventional interventions to counteract the complications prompt us to seek therapeutic strategies that target CPB-specific pathways. In this dissertation, I used an *in vitro* CPB model to study the inflammatory response of endothelial cells while interacting with shear-activated monocytes and the conditioned media derived from sheared monocytes. I showed that endothelial cell derived IL-8 played a positive role in mediating the adhesion of shear-activated monocytes. A possible mechanism is that IL-8 cause upregulation of ICAM-1 and VCAM-1 in the endothelial cells. Disrupting the IL-8 signaling pathway showed promising effect in preventing the monocyte adhesion. Therefore, a potential therapy may be developed targeting the IL-8 signaling pathway. CPB shear altered the cytokine profile of the monocytes. Both FK506 and dexamethasone had some anti-inflammatory effect either by reducing pro-inflammatory cytokines or upregulating the release of anti-inflammatory cytokines. However, dexamethasone was less effective at downregulating the key inflammatory cytokines, IL-8 and TNF-α, compared to FK506. Conditioned media treatment further showed the cytokines derived from sheared monocytes elicits inflammatory response of endothelial cell, which is attenuated by the treatment of conditioned media with FK506 and dexamethasone. To conclude, the results of this study provided insight into the mechanism that leads to the inflammatory response of monocytes and endothelial cells in pediatric CPB. Targeted therapy can be developed based on the findings of this study.

7.2 FUTURE DIRECTIONS OF THE STUDY

In this study, an *in vitro* CPB model was used to study the CPB-induced inflammatory response including the interaction between monocytes and endothelial cells and the effect of CPB-induced cytokines derived from monocytes on the endothelial cells. The inflammatory response, however, begins when the blood components are exposed to the CPB circuit. Therefore, a model that mimics the CPB scenario will include the interaction between monocytes and endothelial cells during the time of CPB. This inspires the design of a dynamic CPB model (Figure 8.1). In this model a flow chamber loaded with endothelial cells is included in the short tubing side of the CPB circuit. Monocytes will interact with the endothelial cells in the flow chamber while being sheared. The inclusion of the flow chamber allows endothelial cells to function under a flow condition, which resembles the native blood vessel environment. The presence of laminar flow is important to induce quiescence state in the endothelial cells, which is less likely to be stimulated (201). However, fluid shear stress below 8 dynes/cm^2 can induce increasing ICAM-1 expression, which mediates leukocyte adhesion (202,203). These studies show that endothelial cells behave differently under flow conditions. Therefore, the response of endothelial cells will be characterized more accurately using this dynamic model. So far, I have tested growing HNDMVECs on the ibidi channel slides. The main challenge is to maintain the HNDMVECs on these slides since the channel does not hold enough media for the growth of the endothelial cells. Using the current seeding density for culture vessel resulted in robust attachment but inferior cell proliferation and rapid cell death, presumably due to limited volume of culture media and gas exchange. An optimal seeding density will need to be determined so that the endothelial cells reach confluence in a shorter period and are ready to be incorporated in

the CPB circuit. Based on how this dynamic model can recapitulate the CPB condition, I recommend that future experiments are designed based on this dynamic CPB model.

The endothelial cells used in this study are derived from dermal tissue which does not have organ specificity. The insult induced by CPB, however, involves injuries to the endothelium of different organs including brain, kidney, and lung (204-206). The endothelial cells from different organs are heterogeneous due to distinct tissue environment (207,208). Therefore, it is reasonable to speculate that endothelial cells from different organs respond differently towards CPB shear and shear-activated blood cells. For example, it has been shown that aortic endothelial cells are prone to TNF-α-mediated monocyte adhesion compared to pulmonary microvascular endothelial cells and renal glomerular endothelial cells (209). Knowing the organ-specific response to CPB can help develop targeted therapy to treat endothelial dysfunction in different organs. Therefore, I recommend testing the *in vitro* CPB model with endothelial cells derived from different organs.

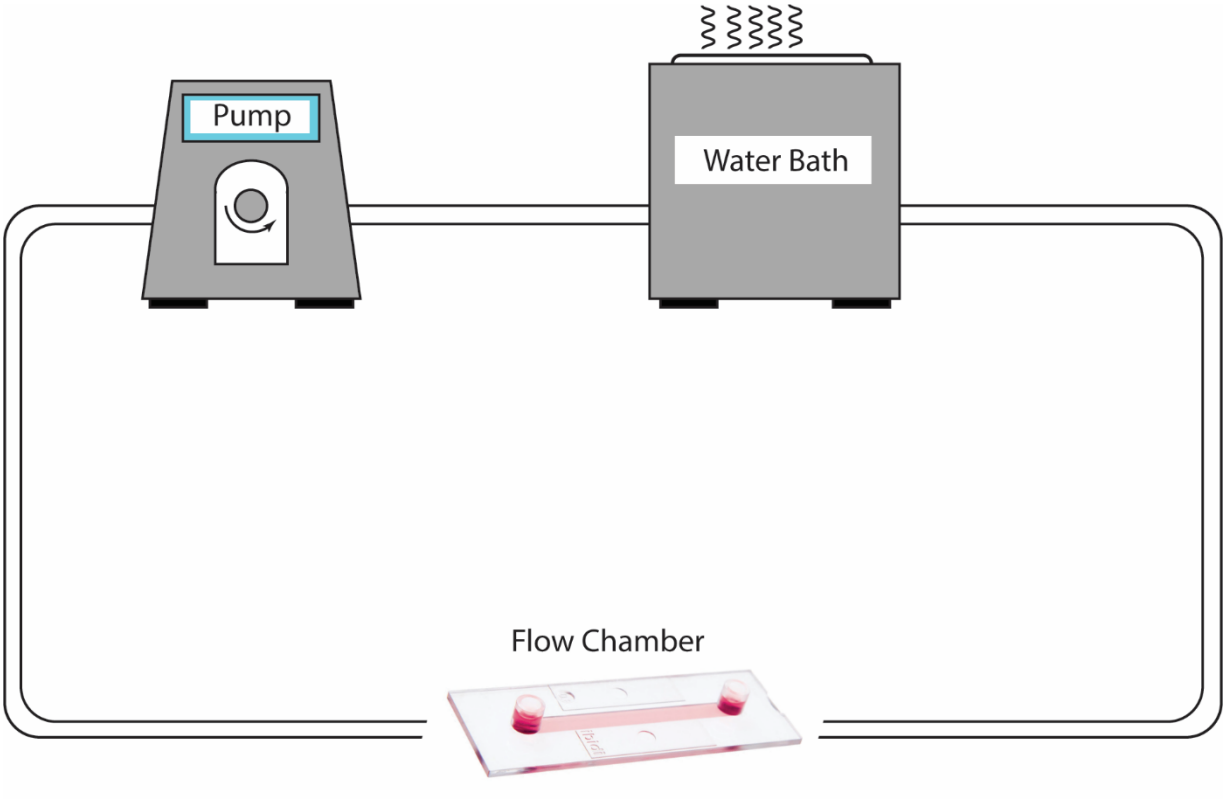

Figure 8.1. Design of a dynamic *in vitro* CPB model. A flow chamber seeded with endothelial cells is integrated into the bypass circuit.

REFERENCE

1. Sarkar M, Prabhu V. Basics of cardiopulmonary bypass. Indian J Anaesth. 2017 Sep;61(9):760–7.
2. Ismail A, Semien G, Miskolczi SY. Cardiopulmonary Bypass. In: StatPearls [Internet]. Treasure Island (FL): StatPearls Publishing; 2024 [cited 2024 Jul 12]. Available from: http://www.ncbi.nlm.nih.gov/books/NBK482190/
3. Cooley DA. Development of the Roller Pump for Use in the Cardiopulmonary Bypass Circuit. Tex Heart Inst J. 1987 Jun;14(2):112–8.
4. Saczkowski R, Maklin M, Mesana T, Boodhwani M, Ruel M. Centrifugal Pump and Roller Pump in Adult Cardiac Surgery: A Meta-Analysis of Randomized Controlled Trials. Artificial Organs. 2012;36(8):668–76.
5. Melchior RW, Sutton SW, Harris W, Dalton HJ. Evolution of membrane oxygenator technology for utilization during pediatric cardiopulmonary bypass. Pediatric Health Med Ther. 2016 Jun 28;7:45–56.
6. Ni YM, Leskosek B, Shi LP, Chen YL, Qian LF, Li RY, et al. Optimization of venous return tubing diameter for cardiopulmonary bypass. Eur J Cardiothorac Surg. 2001 Sep;20(3):614–20.
7. Bednarski Spiwak AJ, Horbal A, Leatherbury R, Hansford DJ. Extracorporeal Tubing in the Roller Pump Raceway: Physical Changes and Particulate Generation. J Extra Corpor Technol. 2008 Sep;40(3):188–92.
8. Somer FD. Evidence-Based Used, Yet Still Controversial: The Arterial Filter. J Extra Corpor Technol. 2012 Mar;44(1):P27–30.
9. Searles B. Ultrafiltration Techniques and CPB: What We Know and What We Think We Know. J Extra Corpor Technol. 2006 Mar;38(1):64–5.
10. Kandil OA, Motawea KR, Darling E, Riley JB, Shah J, Elashhat MAM, et al. Ultrafiltration and cardiopulmonary bypass associated acute kidney injury: A systematic review and meta-analysis. Clin Cardiol. 2021 Nov 27;44(12):1700–8.
11. Carvajal C, Goyal A, Tadi P. Cardioplegia. In: StatPearls [Internet]. Treasure Island (FL): StatPearls Publishing; 2024 [cited 2024 Jul 12]. Available from: http://www.ncbi.nlm.nih.gov/books/NBK554463/
12. Ali JM, Miles LF, Abu-Omar Y, Galhardo C, Falter F. Global Cardioplegia Practices: Results from the Global Cardiopulmonary Bypass Survey. J Extra Corpor Technol. 2018 Jun;50(2):83–93.
13. Mauney MC, Kron IL. The physiologic basis of warm cardioplegia. The Annals of Thoracic Surgery. 1995 Sep;60(3):819–23.
14. Hayashida N, Ikonomidis JS, Weisel RD, Shirai T, Ivanov J, Carson SM, et al. The optimal cardioplegic temperature. Ann Thorac Surg. 1994 Oct;58(4):961–71.
15. Kot TKM, Chan JSK, Froghi S, Lau DHH, Morgan K, Magni F, et al. Warm versus cold cardioplegia in cardiac surgery: A meta-analysis with trial sequential analysis. JTCVS Open. 2021 Mar 31;6:161–90.
16. Auer J, Weber T, Berent R, Ng CK, Lamm G, Eber B. Risk factors of postoperative atrial fibrillation after cardiac surgery. J Card Surg. 2005;20(5):425–31.
17. Gunaydin S, Ayrancioglu K, Dikmen E, Mccusker K, Vijay V, Sari T, et al. Clinical effects of leukofiltration and surface modification on post-cardiopulmonary bypass atrial fibrillation in different risk cohorts. Perfusion. 2007 Jul;22(4):279–88.

18. Creswell LL, Alexander JC, Ferguson TB, Lisbon A, Fleisher LA. Intraoperative Interventions: American College of Chest Physicians Guidelines for the Prevention and Management of Postoperative Atrial Fibrillation After Cardiac Surgery. Chest. 2005 Aug 1;128(2, Supplement):28S-35S.
19. Schlensak C, Beyersdorf F. Lung injury during CPB: pathomechanisms and clinical relevance. Interactive CardioVascular and Thoracic Surgery. 2005 Oct 1;4(5):381–2.
20. Ng CSH, Wan S, Yim APC, Arifi AA. Pulmonary Dysfunction After Cardiac Surgery. CHEST. 2002 Apr 1;121(4):1269–77.
21. Milot J, Perron J, Lacasse Y, Létourneau L, Cartier PC, Maltais F. Incidence and Predictors of ARDS After Cardiac Surgery. CHEST. 2001 Mar 1;119(3):884–8.
22. Rosner MH, Okusa MD. Acute kidney injury associated with cardiac surgery. Clin J Am Soc Nephrol. 2006 Jan;1(1):19–32.
23. Ascione R, Lloyd CT, Underwood MJ, Gomes WJ, Angelini GD. On-pump versus off-pump coronary revascularization: evaluation of renal function. Ann Thorac Surg. 1999 Aug;68(2):493–8.
24. Ramakrishna MN, Hegde VD, Kumarswamy GN, Gupta R, Moola NS, Suresh KP. Impact of preoperative mild renal dysfunction on short term outcome in isolated Coronary Artery Bypass (CABG) patients. Indian J Crit Care Med. 2008;12(4):158–62.
25. Massoudy P, Wagner S, Thielmann M, Herold U, Kottenberg-Assenmacher E, Marggraf G, et al. Coronary artery bypass surgery and acute kidney injury--impact of the off-pump technique. Nephrol Dial Transplant. 2008 Sep;23(9):2853–60.
26. Sear JW. Kidney dysfunction in the postoperative period. British Journal of Anaesthesia. 2005 Jul 1;95(1):20–32.
27. van Dijk D, Spoor M, Hijman R, Nathoe HM, Borst C, Jansen EWL, et al. Cognitive and Cardiac Outcomes 5 Years After Off-Pump vs On-Pump Coronary Artery Bypass Graft Surgery. JAMA. 2007 Feb 21;297(7):701–8.
28. Hogue CWJ, Palin CA, Arrowsmith JE. Cardiopulmonary Bypass Management and Neurologic Outcomes: An Evidence-Based Appraisal of Current Practices. Anesthesia & Analgesia. 2006 Jul;103(1):21.
29. Carrascal Y, Guerrero AL, Maroto LC, Cortina JM, Rodríguez JE, Renes E, et al. Neurological complications after cardiopulmonary bypass: An update. Eur Neurol. 1999;41(3):128–34.
30. Paparella D, Yau TM, Young E. Cardiopulmonary bypass induced inflammation: pathophysiology and treatment. An update. European Journal of Cardio-Thoracic Surgery. 2002 Feb 1;21(2):232–44.
31. Warltier DC, Laffey JG, Boylan JF, Cheng DCH. The Systemic Inflammatory Response to Cardiac Surgery: Implications for the Anesthesiologist. Anesthesiology. 2002 Jul 1;97(1):215–52.
32. Kirklin JK, Westaby S, Blackstone EH, Kirklin JW, Chenoweth DE, Pacifico AD. Complement and the damaging effects of cardiopulmonary bypass. J Thorac Cardiovasc Surg. 1983 Dec;86(6):845–57.
33. Ranucci M, Mazzucco A, Pessotto R, Grillone G, Casati V, Porreca L, et al. Heparin-coated circuits for high-risk patients: a multicenter, prospective, randomized trial. The Annals of Thoracic Surgery. 1999 Apr 1;67(4):994–1000.
34. Fitch JCK, Rollins S, Matis L, Alford B, Aranki S, Collard CD, et al. Pharmacology and Biological Efficacy of a Recombinant, Humanized, Single-Chain Antibody C5

Complement Inhibitor in Patients Undergoing Coronary Artery Bypass Graft Surgery With Cardiopulmonary Bypass. Circulation. 1999 Dec 21;100(25):2499–506.
35. Ulus AT, Aksoyek A, Ozkan M, Katircioglu SF, Basu S. Cardiopulmonary bypass as a cause of free radical-induced oxidative stress and enhanced blood-borne isoprostanes in humans. Free Radical Biology and Medicine. 2003 Apr 1;34(7):911–7.
36. Sablotzki A, Mann V, Simm A, Czeslick E. [Changes in the cytokine network through escalating SIRS after heart surgery]. Anasthesiol Intensivmed Notfallmed Schmerzther. 2001 Sep;36(9):552–9.
37. Kawamura T, Wakusawa R, Okada K, Inadat S. Elevation of cytokines during open heart surgery with cardiopulmonary bypass: participation of interleukin 8 and 6 in reperfusion injury. Can J Anaesth. 1993 Nov 1;40(11):1016–21.
38. Yu X, Ge L, Niu L, Lian X, Ma H, Pang L. The Dual Role of Inducible Nitric Oxide Synthase in Myocardial Ischemia/Reperfusion Injury: Friend or Foe? Oxid Med Cell Longev. 2018 Oct 28;2018:8364848.
39. Maeda K, Ruel M. Prevention of ischemia-reperfusion injury in cardiac surgery: Therapeutic strategies targeting signaling pathways. The Journal of Thoracic and Cardiovascular Surgery. 2015 Mar 1;149(3):910–1.
40. Verrier ED, Morgan EN. Endothelial response to cardiopulmonary bypass surgery. The Annals of Thoracic Surgery. 1998 Nov 1;66(5):S17–9.
41. Aljure OD, Fabbro M. Cardiopulmonary Bypass and Inflammation: The Hidden Enemy. Journal of Cardiothoracic and Vascular Anesthesia. 2019 Feb 1;33(2):346–7.
42. Giacinto O, Satriano U, Nenna A, Spadaccio C, Lusini M, Mastroianni C, et al. Inflammatory Response and Endothelial Dysfunction Following Cardiopulmonary Bypass: Pathophysiology and Pharmacological Targets. http://www.eurekaselect.com [Internet]. [cited 2024 Jul 12]; Available from: https://www.eurekaselect.com/article/99913
43. Cohn LH. Fifty Years of Open-Heart Surgery. Circulation. 2003 May 6;107(17):2168–70.
44. Kozik DJ, Tweddell JS. Characterizing the Inflammatory Response to Cardiopulmonary Bypass in Children. The Annals of Thoracic Surgery. 2006 Jun 1;81(6):S2347–54.
45. Saleem Y, Darbari A, Sharma R, Vashisth A, Gupta A. Recent advancements in pediatric cardiopulmonary bypass technology for better outcomes of pediatric cardiac surgery. The Cardiothoracic Surgeon. 2022 Aug 15;30(1):23.
46. Hendrix BB, Reagor JA, Tweddell JS. Neonatal Cardiopulmonary Bypass Circuit Blood Prime Quality Analysis. J Extra Corpor Technol. 2021 Jun;53(2):140–5.
47. Whiting D, Yuki K, DiNardo JA. Cardiopulmonary bypass in the pediatric population. Best Practice & Research Clinical Anaesthesiology. 2015 Jun 1;29(2):241–56.
48. Kipps AK, Wypij D, Thiagarajan RR, Bacha EA, Newburger JW. BLOOD TRANSFUSION IS ASSOCIATED WITH PROLONGED DURATION OF MECHANICAL VENTILATION IN INFANTS UNDERGOING REPARATIVE CARDIAC SURGERY. Pediatr Crit Care Med. 2011 Jan;12(1):52–6.
49. Kneyber MCJ, Grotenhuis F, Berger RFM, Ebels TW, Burgerhof JGM, Albers MJIJ. Transfusion of leukocyte-depleted RBCs is independently associated with increased morbidity after pediatric cardiac surgery. Pediatr Crit Care Med. 2013 Mar;14(3):298–305.

50. Onorati F, Santini F, Raffin F, Menon T, Graziani MS, Chiominto B, et al. Clinical evaluation of new generation oxygenators with integrated arterial line filters for cardiopulmonary bypass. Artif Organs. 2012 Oct;36(10):875–85.
51. Miyaji K, Miyamoto T, Kohira S, Nakashima K, Inoue N, Sato H, et al. Miniaturized cardiopulmonary bypass system in neonates and small infants. Interactive CardioVascular and Thoracic Surgery. 2008 Feb 1;7(1):75–9.
52. Boettcher W, Sinzobahamvya N, Miera O, Redlin M, Dehmel F, Cho MY, et al. Routine Application of Bloodless Priming in Neonatal Cardiopulmonary Bypass: A 3-Year Experience. Pediatr Cardiol. 2017 Apr 1;38(4):807–12.
53. Redlin M, Huebler M, Boettcher W, Kukucka M, Schoenfeld H, Hetzer R, et al. Minimizing intraoperative hemodilution by use of a very low priming volume cardiopulmonary bypass in neonates with transposition of the great arteries. J Thorac Cardiovasc Surg. 2011 Oct;142(4):875–81.
54. Ando M, Takahashi Y, Suzuki N. Open heart surgery for small children without homologous blood transfusion by using remote pump head system. Ann Thorac Surg. 2004 Nov;78(5):1717–22.
55. Xiong Y, Sun Y, Ji B, Liu J, Wang G, Zheng Z. Systematic Review and Meta-Analysis of benefits and risks between normothermia and hypothermia during cardiopulmonary bypass in pediatric cardiac surgery. Pediatric Anesthesia. 2015;25(2):135–42.
56. Gravlee GP. Cardiopulmonary Bypass: Principles and Practice. Lippincott Williams & Wilkins; 2008. 814 p.
57. Sturmer D, Beaty C, Clingan S, Jenkins E, Peters W, Si MS. Recent innovations in perfusion and cardiopulmonary bypass for neonatal and infant cardiac surgery. Transl Pediatr. 2018 Apr;7(2):139–50.
58. Haider A, Khwaja IA, Qureshi AB, Khan I, Majeed KA, Yousaf MS, et al. Effectiveness of Mild to Moderate Hypothermic Cardiopulmonary Bypass on Early Clinical Outcomes. J Cardiovasc Dev Dis. 2022 May 9;9(5):151.
59. Saad H, Aladawy M. Temperature management in cardiac surgery. Glob Cardiol Sci Pract. 2013 Nov 1;2013(1):44–62.
60. Ramakrishnan K, Kumar TS, Boston US, Allen J, Knott-Craig CJ. Cardiopulmonary bypass in neonates and infants: advantages of high flow high hematocrit bypass strategy—clinical practice review. Transl Pediatr. 2023 Jul 31;12(7):1431–8.
61. Reagor JA, Clingan S, Gao Z, Morales DLS, Tweddell JS, Bryant R, et al. Higher Flow on Cardiopulmonary Bypass in Pediatrics Is Associated With a Lower Incidence of Acute Kidney Injury. Semin Thorac Cardiovasc Surg. 2020 Winter;32(4):1015–20.
62. Kirshbom PM, Skaryak LA, DiBernardo LR, Kern FH, Greeley WJ, Gaynor JW, et al. Effects of Aortopulmonary Collaterals on Cerebral Cooling and Cerebral Metabolic Recovery After Circulatory Arrest. Circulation. 1995 Nov;92(9):490–4.
63. Topper JN, Cai J, Falb D, Gimbrone MA. Identification of vascular endothelial genes differentially responsive to fluid mechanical stimuli: cyclooxygenase-2, manganese superoxide dismutase, and endothelial cell nitric oxide synthase are selectively up-regulated by steady laminar shear stress. Proc Natl Acad Sci U S A. 1996 Sep 17;93(19):10417–22.
64. Mulholland JW, Shelton JC, Luo XY. Blood flow and damage by the roller pumps during cardiopulmonary bypass. Journal of Fluids and Structures. 2005 Jan 1;20(1):129–40.

65. Tu LN, Hsieh L, Kajimoto M, Charette K, Kibiryeva N, Forero A, et al. Shear stress associated with cardiopulmonary bypass induces expression of inflammatory cytokines and necroptosis in monocytes. JCI Insight. 6(1):e141341.
66. Vercaemst L. Hemolysis in Cardiac Surgery Patients Undergoing Cardiopulmonary Bypass: A Review in Search of a Treatment Algorithm. J Extra Corpor Technol. 2008 Dec;40(4):257–67.
67. Ricci Z. Hemolysis during pediatric cardiac surgery: an old issue with renewed concerns. Journal of Laboratory and Precision Medicine [Internet]. 2018 Feb 5 [cited 2024 Jul 12];3(2). Available from: https://jlpm.amegroups.org/article/view/3994
68. Hoffman JIE, Kaplan S. The incidence of congenital heart disease. J Am Coll Cardiol. 2002 Jun 19;39(12):1890–900.
69. Oster ME, Lee KA, Honein MA, Riehle-Colarusso T, Shin M, Correa A. Temporal Trends in Survival Among Infants With Critical Congenital Heart Defects. Pediatrics. 2013 May;131(5):e1502–8.
70. Stoney WS. Evolution of Cardiopulmonary Bypass. Circulation. 2009 Jun 2;119(21):2844–53.
71. Kansy A, Tobota Z, Maruszewski P, Maruszewski B. Analysis of 14,843 neonatal congenital heart surgical procedures in the European Association for Cardiothoracic Surgery Congenital Database. Ann Thorac Surg. 2010 Apr;89(4):1255–9.
72. Gu Y j., Boonstra P w., Graaff R, Rijnsburger A a., Mungroop H, van Oeveren W. Pressure Drop, Shear Stress, and Activation of Leukocytes During Cardiopulmonary Bypass: A Comparison Between Hollow Fiber and Flat Sheet Membrane Oxygenators. Artificial Organs. 2000;24(1):43–8.
73. He G, Gao Y, Feng L, He G, Wu Q, Gao W, et al. Correlation Between Wall Shear Stress and Acute Degradation of the Endothelial Glycocalyx During Cardiopulmonary Bypass. J of Cardiovasc Trans Res. 2020 Dec 1;13(6):1024–32.
74. Bhirowo YP, Raksawardana YK, Setianto BY, Sudadi S, Tandean TN, Zaharo AF, et al. Hemolysis and cardiopulmonary bypass: meta-analysis and systematic review of contributing factors. Journal of Cardiothoracic Surgery. 2023 Oct 13;18(1):291.
75. Butler J, Rocker GM, O'Brien JR, Etherington M, Pillai R, Westaby S. Platelet responses to cardiopulmonary bypass. Assessment by a shear stress activation technique. J Cardiovasc Surg (Torino). 1992 Jan 1;33(1):33–7.
76. Rossaint J, Berger C, Van Aken H, Scheld HH, Zahn PK, Rukosujew A, et al. Cardiopulmonary Bypass during Cardiac Surgery Modulates Systemic Inflammation by Affecting Different Steps of the Leukocyte Recruitment Cascade. PLoS One. 2012 Sep 19;7(9):e45738.
77. Graham EM, Atz AM, McHugh KE, Butts RJ, Baker NL, Stroud RE, et al. Preoperative Steroid Treatment Does Not Improve Markers of Inflammation Following Cardiac Surgery in Neonates: Results from a Randomized Trial. J Thorac Cardiovasc Surg. 2014 Mar;147(3):902–8.
78. Horton SB, Butt WW, Mullaly RJ, Thuys CA, O'Connor EB, Byron K, et al. IL-6 and IL-8 levels after cardiopulmonary bypass are not affected by surface coating. The Annals of Thoracic Surgery. 1999 Nov 1;68(5):1751–5.
79. Chew MS, Brix-Christensen V, Ravn HB, Brandslund I, Ditlevsen E, Pedersen J, et al. Effect of modified ultrafiltration on the inflammatory response in paediatric open-heart surgery: a prospective, randomized study. Perfusion. 2002 Sep 1;17(5):327–33.

80. Effects of cardiopulmonary bypass on neonatal and paediatric inflammatory profiles. European Journal of Cardio-Thoracic Surgery. 1997 Dec 1;12(6):862–8.
81. Alcaraz AJ, Manzano L, Sancho L, Vigil MD, Esquivel F, Maroto E, et al. Different Proinflammatory Cytokine Serum Pattern in Neonate Patients Undergoing Open Heart Surgery. Relevance of IL-8. J Clin Immunol. 2005 May 1;25(3):238–45.
82. Mahle WT, Matthews E, Kanter KR, Kogon BE, Hamrick SEG, Strickland MJ. Inflammatory Response After Neonatal Cardiac Surgery and Its Relationship to Clinical Outcomes. The Annals of Thoracic Surgery. 2014 Mar 1;97(3):950–6.
83. Liu KD, Altmann C, Smits G, Krawczeski CD, Edelstein CL, Devarajan P, et al. Serum Interleukin-6 and interleukin-8 are early biomarkers of acute kidney injury and predict prolonged mechanical ventilation in children undergoing cardiac surgery: a case-control study. Critical Care. 2009 Jul 1;13(4):R104.
84. Finn A, Naik S, Klein N, Levinsky RJ, Strobel S, Elliott M. Interleukin-8 release and neutrophil degranulation after pediatric cardiopulmonary bypass. The Journal of Thoracic and Cardiovascular Surgery. 1993 Feb 1;105(2):234–41.
85. Madhok AB, Ojamaa K, Haridas V, Parnell VA, Pahwa S, Chowdhury D. Cytokine Response in Children Undergoing Surgery for Congenital Heart Disease. Pediatr Cardiol. 2006 Aug 1;27(4):408–13.
86. McBride WT, Armstrong MA, Gilliland H, McMurray TJ. THE BALANCE OF PRO AND ANTI-INFLAMMATORY CYTOKINES IN PLASMA AND BRONCHOALVEOLAR LAVAGE (BAL) AT PAEDIATRIC CARDIAC SURGERY. Cytokine. 1996 Sep 1;8(9):724–9.
87. Serum TNF--α levels in children with congenital heart disease undergoing cardiopulmonary bypass: A cohort study in China and a meta-analysis of the published literature. [cited 2024 Jul 12]; Available from: https://onlinelibrary.wiley.com/doi/10.1002/jcla.22112
88. Park kum S, Do SH, Chung IY, Kim HS, Kim CS. Change of Tumor Necrosis Factor-alpha Concentration after Pediatric Cardiopulmonary Bypass and Its Relationship with Postoperative Course. Korean Journal of Anesthesiology. 2002;56–63.
89. Hammer S, Fuchs AT, Rinker C, Daebritz S, Kozlik-Feldmann R, Netz H. Interleukin-6 and procalcitonin in serum of children undergoing cardiac surgery with cardiopulmonary bypass. Acta Cardiol. 2004 Dec;59(6):624–9.
90. Robich M, Ryzhov S, Kacer D, Palmeri M, Peterson SM, Quinn RD, et al. Prolonged cardiopulmonary bypass is associated with endothelial glycocalyx degradation. J Surg Res. 2020 Jul;251:287–95.
91. Burns SA, DeGuzman BJ, Newburger JW, Mayer JE, Neufeld EJ, Briscoe DM. P-selectin expression in myocardium of children undergoing cardiopulmonary bypass. The Journal of Thoracic and Cardiovascular Surgery. 1995 Oct 1;110(4, Part 1):924–33.
92. Galea J, Rebuck N, Finn A, Manché A, Moat N. Expression of soluble endothelial adhesion molecules in clinical cardiopulmonary bypass. Perfusion. 1998 Sep;13(5):314–21.
93. Tsang GM, Allen S, Pagano D, Wong C, Graham TR, Bonser RS. von Willebrand factor and urinary albumin excretion are possible indicators of endothelial dysfunction in cardiopulmonary bypass. Eur J Cardiothorac Surg. 1998 Apr;13(4):385–91.

94. Giuliano JS, Lahni PM, Bigham MT, Manning PB, Nelson DP, Wong HR, et al. Plasma Angiopoietin-2 Levels Increase in Children Following Cardiopulmonary Bypass. Intensive Care Med. 2008 Oct;34(10):1851–7.
95. Dekker NAM, van Leeuwen ALI, van Strien WWJ, Majolée J, Szulcek R, Vonk ABA, et al. Microcirculatory perfusion disturbances following cardiac surgery with cardiopulmonary bypass are associated with *in vitro* endothelial hyperpermeability and increased angiopoietin-2 levels. Crit Care. 2019 Apr 11;23:117.
96. Harada A, Sekido N, Akahoshi T, Wada T, Mukaida N, Matsushima K. Essential involvement of interleukin-8 (IL-8) in acute inflammation. J Leukoc Biol. 1994 Nov;56(5):559–64.
97. Huber AR, Kunkel SL, Todd RF, Weiss SJ. Regulation of Rransendothelial Neutrophil Migration by Endogenous Interleukin-8. Science. 1991 Oct 4;254(5028):99–102.
98. Detmers PA, Lo SK, Olsen-Egbert E, Walz A, Baggiolini M, Cohn ZA. Neutrophil-activating protein 1/interleukin 8 stimulates the binding activity of the leukocyte adhesion receptor CD11b/CD18 on human neutrophils. J Exp Med. 1990 Apr 1;171(4):1155–62.
99. Bréchard S, Bueb JL, Tschirhart EJ. Interleukin-8 primes oxidative burst in neutrophil-like HL-60 through changes in cytosolic calcium. Cell Calcium. 2005 Jun;37(6):531–40.
100. Henkels KM, Frondorf K, Gonzalez-Mejia ME, Doseff AL, Gomez-Cambronero J. IL-8-induced neutrophil chemotaxis is mediated by Janus kinase 3 (JAK3). FEBS Letters. 2011;585(1):159–66.
101. Wang P, Fu C, Bai G, Cuan L, Tang X, Jin C, et al. Risk factors of postoperative low cardiac output syndrome in children with congenital heart disease: A systematic review and meta-analysis. Front Pediatr. 2023 Jan 10;10:954427.
102. Blatchford JW, Barragry TP, Lillehei TJ, Ring WS. Effects of cardioplegic arrest on left ventricular systolic and diastolic function of the intact neonatal heart. The Journal of Thoracic and Cardiovascular Surgery. 1994 Feb;107(2):527–35.
103. Chandler HK, Kirsch R. Management of the Low Cardiac Output Syndrome Following Surgery for Congenital Heart Disease. Curr Cardiol Rev. 2016 May;12(2):107–11.
104. Liu H, Zhang Y, Wu Z, Zhang L. Identification of IL-6 as a potential mediator of the myocardial fibrosis that occurs in response to surgery with cardiopulmonary bypass in children with Tetralogy of Fallot. Cardiology in the Young. 2022 Feb;32(2):223–9.
105. Tanner TG, Colvin MO. Pulmonary Complications of Cardiac Surgery. Lung. 2020;198(6):889–96.
106. Vu T, Smith JA. An Update on Postoperative Cognitive Dysfunction Following Cardiac Surgery. Front Psychiatry. 2022 Jun 15;13:884907.
107. Dhari Z, Leonetti C, Lin S, Prince A, Howick J, Zurakowski D, et al. Impact of Cardiopulmonary Bypass on Neurogenesis and Cortical Maturation. Ann Neurol. 2021 Dec;90(6):913–26.
108. Schindelin J, Arganda-Carreras I, Frise E, Kaynig V, Longair M, Pietzsch T, et al. Fiji: an open-source platform for biological-image analysis. Nat Methods. 2012 Jul;9(7):676–82.
109. Urschel K, Wörner A, Daniel WG, Garlichs CD, Cicha I. Role of shear stress patterns in the TNF-α-induced atherogenic protein expression and monocytic cell adhesion to endothelium. Clin Hemorheol Microcirc. 2010;46(2–3):203–10.

110. Baratchi S, Khoshmanesh K, Woodman OL, Potocnik S, Peter K, McIntyre P. Molecular Sensors of Blood Flow in Endothelial Cells. Trends Mol Med. 2017 Sep;23(9):850–68.
111. Evani SJ, Murthy AK, Mareedu N, Montgomery RK, Arulanandam BP, Ramasubramanian AK. Hydrodynamic Regulation of Monocyte Inflammatory Response to an Intracellular Pathogen. PLoS One. 2011 Jan 7;6(1):e14492.
112. Son H, Choi HS, Baek SE, Kim YH, Hur J, Han JH, et al. Shear stress induces monocyte/macrophage-mediated inflammation by upregulating cell-surface expression of heat shock proteins. Biomed Pharmacother. 2023 May;161:114566.
113. Fahy N, Menzel U, Alini M, Stoddart MJ. Shear and Dynamic Compression Modulates the Inflammatory Phenotype of Human Monocytes *in vitro*. Front Immunol [Internet]. 2019 Mar 5 [cited 2024 Jul 12];10. Available from: https://www.frontiersin.org/journals/immunology/articles/10.3389/fimmu.2019.00383/full
114. Bosshart H, Heinzelmann M. THP-1 cells as a model for human monocytes. Ann Transl Med. 2016 Nov;4(21):438.
115. Beaubien-Souligny W, Neagoe PE, Gagnon D, Denault AY, Sirois MG. Increased Circulating Levels of Neutrophil Extracellular Traps During Cardiopulmonary Bypass. CJC Open. 2019 Dec 16;2(2):39–48.
116. Abdel-Rahman U, Margraf S, Aybek T, Lögters T, Bitu-Moreno J, Francischetti I, et al. Inhibition of neutrophil activity improves cardiac function after cardiopulmonary bypass. Journal of Inflammation. 2007 Oct 10;4(1):21.
117. Mitchell MJ, Lin KS, King MR. Fluid Shear Stress Increases Neutrophil Activation via Platelet-Activating Factor. Biophys J. 2014 May 20;106(10):2243–53.
118. Ide H, Kakiuchi T, Furuta N, Matsumoto H, Sudo K, Furuse A, et al. The effect of cardiopulmonary bypass on T cells and their subpopulations. Ann Thorac Surg. 1987 Sep;44(3):277–82.
119. Jiménez-Aguilar R, Sánchez-Zauco N, Tiburcio-Felix R, López JZ, Solano-Gutiérrez A, Riera C, et al. Effects of cardiopulmonary bypass on the development of lymphopenia and sepsis after cardiac surgery in children with congenital cardiopathy. Exp Ther Med. 2020 Jan;19(1):435–42.
120. Hosoki K, Ying S, Corrigan C, Qi H, Kurosky A, Jennings K, et al. Data from: Analysis of a panel of 48 cytokines in BAL fluids specifically identifies IL-8 levels as the only cytokine that distinguishes controlled asthma from uncontrolled asthma, and correlates inversely with FEV1 [Internet]. Dryad; 2015 [cited 2024 Jul 12]. p. 50529 bytes. Available from: https://datadryad.org/stash/dataset/doi:10.5061/dryad.r1mb0
121. Apostolakis S, Vogiatzi K, Amanatidou V, Spandidos DA. Interleukin 8 and cardiovascular disease. Cardiovascular Research. 2009 Dec 1;84(3):353–60.
122. Miller EJ, Cohen AB, Nagao S, Griffith D, Maunder RJ, Martin TR, et al. Elevated levels of NAP-1/interleukin-8 are present in the airspaces of patients with the adult respiratory distress syndrome and are associated with increased mortality. Am Rev Respir Dis. 1992 Aug;146(2):427–32.
123. Petreaca ML, Yao M, Liu Y, Defea K, Martins-Green M. Transactivation of vascular endothelial growth factor receptor-2 by interleukin-8 (IL-8/CXCL8) is required for IL-8/CXCL8-induced endothelial permeability. Mol Biol Cell. 2007 Dec;18(12):5014–23.

124. Gessler P, Pfenninger J, Pfammatter JP, Carrel T, Baenziger O, Dahinden C. Plasma levels of interleukin-8 and expression of interleukin-8 receptors on circulating neutrophils and monocytes after cardiopulmonary bypass in children. J Thorac Cardiovasc Surg. 2003 Sep;126(3):718–25.
125. Liangos O, Kolyada A, Tighiouart H, Perianayagam MC, Wald R, Jaber BL. Interleukin-8 and acute kidney injury following cardiopulmonary bypass: a prospective cohort study. Nephron Clin Pract. 2009;113(3):c148-154.
126. Kalfin RE, Engelman RM, Rousou JA, Flack JE, Deaton DW, Kreutzer DL, et al. Induction of interleukin-8 expression during cardiopulmonary bypass. Circulation. 1993 Nov;88(5 Pt 2):II401-406.
127. Li A, Varney ML, Valasek J, Godfrey M, Dave BJ, Singh RK. Autocrine role of interleukin-8 in induction of endothelial cell proliferation, survival, migration and MMP-2 production and angiogenesis. Angiogenesis. 2005;8(1):63–71.
128. Bosch I, Xhaja K, Estevez L, Raines G, Melichar H, Warke RV, et al. Increased production of interleukin-8 in primary human monocytes and in human epithelial and endothelial cell lines after dengue virus challenge. J Virol. 2002 Jun;76(11):5588–97.
129. Oude Nijhuis CSM, Vellenga E, Daenen SMGJ, Kamps WA, De Bont ESJM. Endothelial cells are main producers of interleukin 8 through Toll-like receptor 2 and 4 signaling during bacterial infection in leukopenic cancer patients. Clin Diagn Lab Immunol. 2003 Jul;10(4):558–63.
130. Kaplanski G, Teysseire N, Farnarier C, Kaplanski S, Lissitzky JC, Durand JM, et al. IL-6 and IL-8 production from cultured human endothelial cells stimulated by infection with Rickettsia conorii via a cell-associated IL-1 alpha-dependent pathway. J Clin Invest. 1995 Dec;96(6):2839–44.
131. Hastings NE, Feaver RE, Lee MY, Wamhoff BR, Blackman BR. Human IL-8 Regulates Smooth Muscle Cell VCAM-1 Expression in Response to Endothelial Cells Exposed to Atheroprone Flow. Arteriosclerosis, Thrombosis, and Vascular Biology. 2009 May;29(5):725–31.
132. Qazi BS, Tang K, Qazi A. Recent Advances in Underlying Pathologies Provide Insight into Interleukin-8 Expression-Mediated Inflammation and Angiogenesis. Int J Inflam. 2011;2011:908468.
133. Nilsen EM, Johansen FE, Jahnsen FL, Lundin KE, Scholz T, Brandtzaeg P, et al. Cytokine profiles of cultured microvascular endothelial cells from the human intestine. Gut. 1998 May;42(5):635–42.
134. Meniailo ME, Malashchenko VV, Shmarov VA, Gazatova ND, Melashchenko OB, Goncharov AG, et al. Interleukin-8 favors pro-inflammatory activity of human monocytes/macrophages. International Immunopharmacology. 2018 Mar 1;56:217–21.
135. Gerszten RE, Garcia-Zepeda EA, Lim YC, Yoshida M, Ding HA, Gimbrone MA, et al. MCP-1 and IL-8 trigger firm adhesion of monocytes to vascular endothelium under flow conditions. Nature. 1999 Apr;398(6729):718–23.
136. Arndt H, Bolanowski MA, Granger DN. Role of interleukin 8 on leucocyte-endothelial cell adhesion in intestinal inflammation. Gut. 1996 Jun;38(6):911–5.
137. Li A, Dubey S, Varney ML, Dave BJ, Singh RK. IL-8 Directly Enhanced Endothelial Cell Survival, Proliferation, and Matrix Metalloproteinases Production and Regulated Angiogenesis1. The Journal of Immunology. 2003 Mar 15;170(6):3369–76.

138. Schraufstatter IU, Chung J, Burger M. IL-8 activates endothelial cell CXCR1 and CXCR2 through Rho and Rac signaling pathways. Am J Physiol Lung Cell Mol Physiol. 2001 Jun;280(6):L1094-1103.
139. Wójciak-Stothard B, Williams L, Ridley AJ. Monocyte Adhesion and Spreading on Human Endothelial Cells Is Dependent on Rho-regulated Receptor Clustering. J Cell Biol. 1999 Jun 14;145(6):1293–307.
140. Beck I, Berghe W, Vermeulen L, Yamamoto K, Haegeman G, Bosscher K. Crosstalk in Inflammation: The Interplay of Glucocorticoid Receptor-Based Mechanisms and Kinases and Phosphatases. Endocrine reviews. 2009 Nov 1;30:830–82.
141. Joyce DA, Kloda A, Steer JH. Dexamethasone suppresses release of soluble TNF- receptors by human monocytes concurrently with TNF-alpha suppression. Immunol Cell Biol. 1997 Aug;75(4):345–50.
142. Franchimont D, Martens H, Hagelstein MT, Louis E, Dewe W, Chrousos GP, et al. Tumor necrosis factor alpha decreases, and interleukin-10 increases, the sensitivity of human monocytes to dexamethasone: potential regulation of the glucocorticoid receptor. J Clin Endocrinol Metab. 1999 Aug;84(8):2834–9.
143. Cain DW, Cidlowski JA. Immune regulation by glucocorticoids. Nat Rev Immunol. 2017 Apr;17(4):233–47.
144. Larsson S, Linden M. Effects of a corticosteroid, budesonide, on production of bioactive IL-12 by human monocytes. Cytokine. 1998 Oct;10(10):786–9.
145. Ma W, Gee K, Lim W, Chambers K, Angel JB, Kozlowski M, et al. Dexamethasone Inhibits IL-12p40 Production in Lipopolysaccharide-Stimulated Human Monocytic Cells by Down-Regulating the Activity of c-Jun N-Terminal Kinase, the Activation Protein-1, and NF-κB Transcription Factors1. The Journal of Immunology. 2004 Jan 1;172(1):318–30.
146. Visser J, van Boxel-Dezaire A, Methorst D, Brunt T, de Kloet ER, Nagelkerken L. Differential regulation of interleukin-10 (IL-10) and IL-12 by glucocorticoids *in vitro*. Blood. 1998 Jun 1;91(11):4255–64.
147. Di Rosa M, Radomski M, Carnuccio R, Moncada S. Glucocorticoids inhibit the induction of nitric oxide synthase in macrophages. Biochem Biophys Res Commun. 1990 Nov 15;172(3):1246–52.
148. Mozo L, Suárez A, Gutiérrez C. Glucocorticoids up-regulate constitutive interleukin-10 production by human monocytes. Clin Exp Allergy. 2004 Mar;34(3):406–12.
149. Svendsen P, Graversen JH, Etzerodt A, Hager H, Røge R, Grønbæk H, et al. Antibody-Directed Glucocorticoid Targeting to CD163 in M2-type Macrophages Attenuates Fructose-Induced Liver Inflammatory Changes. Mol Ther Methods Clin Dev. 2017 Mar 17;4:50–61.
150. Gibbison B, Villalobos Lizardi JC, Avilés Martínez KI, Fudulu DP, Medina Andrade MA, Pérez-Gaxiola G, et al. Prophylactic corticosteroids for paediatric heart surgery with cardiopulmonary bypass. Cochrane Database Syst Rev. 2020 Oct 12;2020(10):CD013101.
151. Pasquali SK, Hall M, Li JS, Peterson ED, Jaggers J, Lodge AJ, et al. Corticosteroids and Outcome in Children Undergoing Congenital Heart Surgery. Circulation. 2010 Nov 23;122(21):2123–30.

152. Bronicki RA, Backer CL, Baden HP, Mavroudis C, Crawford SE, Green TP. Dexamethasone reduces the inflammatory response to cardiopulmonary bypass in children. Ann Thorac Surg. 2000 May;69(5):1490–5.
153. Chen D, Du Y. Analysis of perioperative corticosteroid therapy in children undergoing cardiac surgery: A systematic review and meta-analysis. Clinical Cardiology. 2023;46(6):607–14.
154. Hill KD, Kannankeril PJ, Jacobs JP, Baldwin HS, Jacobs ML, O'Brien SM, et al. Methylprednisolone for Heart Surgery in Infants — A Randomized, Controlled Trial. New England Journal of Medicine. 2022 Dec 7;387(23):2138–49.
155. Schutte RJ, Parisi-Amon A, Reichert WM. Cytokine profiling using monocytes/macrophages cultured on common biomaterials with a range of surface chemistries. J Biomed Mater Res A. 2009 Jan;88(1):128–39.
156. Natanov R, Gueler F, Falk CS, Kühn C, Maus U, Boyle EC, et al. Blood cytokine expression correlates with early multi-organ damage in a mouse model of moderate hypothermia with circulatory arrest using cardiopulmonary bypass. PLoS One. 2018 Oct 11;13(10):e0205437.
157. Kusumanto YH, Tio RA, Loef BG, Sluiter WJ, Mulder NH, Hospers GAP. Systemic VEGF levels after coronary artery bypass graft surgery reflects the extent of inflammatory response. Acute Card Care. 2006;8(1):41–5.
158. Tofukuji M, Metais C, Li J, Franklin A, Simons M, Sellke FW. Myocardial VEGF expression after cardiopulmonary bypass and cardioplegia. Circulation. 1998 Nov 10;98(19 Suppl):II242-246; discussion II247-248.
159. Rosenthal LM, Tong G, Wowro S, Walker C, Pfitzer C, Boettcher W, et al. A Prospective Clinical Trial Measuring the Effects of Cardiopulmonary Bypass Under Mild Hypothermia on the Inflammatory Response and Regulation of Cold-Shock Protein RNA-Binding Motif 3. Therapeutic Hypothermia and Temperature Management. 2019 Apr 11;10.
160. Drennan SE, Burge KY, Szyld EG, Eckert JV, Mir AM, Gormley AK, et al. Clinical and Laboratory Predictors for the Development of Low Cardiac Output Syndrome in Infants Undergoing Cardiopulmonary Bypass: A Pilot Study. J Clin Med. 2021 Feb 11;10(4):712.
161. ANTTILA HSI, REITAMO S, CESKA M, HURME M. Signal transduction pathways leading to the production of IL-8 by human monocytes are differentially regulated by dexamethasone. Clinical and Experimental Immunology. 1992 Sep 1;89(3):509–12.
162. Hartung T, Döcke WD, Gantner F, Krieger G, Sauer A, Stevens P, et al. Effect of Granulocyte Colony-Stimulating Factor Treatment on Ex Vivo Blood Cytokine Response in Human Volunteers. Blood. 1995 May 1;85(9):2482–9.
163. Hartung T, Volk HD, Wendel A. G-CSF - an anti-inflammatory cytokine. Journal of Endotoxin Research. 1995 Jun 1;2(3):195–201.
164. Denizot Y, Karoutsos S, Nathan N. Differential alterations in plasma colony-stimulating factor concentrations after coronary artery bypass graft surgery with extracorporeal circulation. Cytokine. 2001 Mar 7;13(5):314–6.
165. Witek-Janusek L, Mathews HL. Differential Effects of Glucocorticoids on Colony Stimulating Factors Produced By Neonatal Mononuclear Cells. Pediatr Res. 1999 Feb;45(2):224–9.

166. Jenkins JK, Arend WP. Interleukin 1 receptor antagonist production in human monocytes is induced by IL-1α, IL-3, IL-4 and GM-CSF. Cytokine. 1993 Sep 1;5(5):407–15.
167. Sakuma S, Kato Y, Nishigaki F, Sasakawa T, Magari K, Miyata S, et al. FK506 potently inhibits T cell activation induced TNF-alpha and IL-1beta production *in vitro* by human peripheral blood mononuclear cells. Br J Pharmacol. 2000 Aug;130(7):1655–63.
168. Joyce DA, Steer JH, Kloda A. Dexamethasone antagonizes IL-4 and IL-10-induced release of IL-1RA by monocytes but augments IL-4-, IL-10-, and TGF-beta-induced suppression of TNF-alpha release. J Interferon Cytokine Res. 1996 Jul;16(7):511–7.
169. Bhavsar I, Miller CS, Al-Sabbagh M. Macrophage Inflammatory Protein-1 Alpha (MIP-1 alpha)/CCL3: As a Biomarker. General Methods in Biomarker Research and their Applications. 2015 Jun 1;223–49.
170. Liangos O, Domhan S, Schwager C, Zeier M, Huber PE, Addabbo F, et al. Whole Blood Transcriptomics in Cardiac Surgery Identifies a Gene Regulatory Network Connecting Ischemia Reperfusion with Systemic Inflammation. PLoS One. 2010 Oct 27;5(10):e13658.
171. Benscoter AL, Alten JA, Atreya MR, Cooper DS, Byrnes JW, Nelson DP, et al. Biomarker-based risk model to predict persistent multiple organ dysfunctions after congenital heart surgery – A prospective observational cohort study. Res Sq. 2023 Jan 27;rs.3.rs-2488327.
172. Staruch MJ, Camacho R, Dumont FJ. Distinctive calcineurin-dependent (FK506-sensitive) mechanisms regulate the production of the CC chemokines macrophage inflammatory protein (MIP)-1alpha, MIP-1beta, and RANTES vs IL-2 and TNF-alpha by activated human T cells. Cell Immunol. 1998 Dec 15;190(2):121–31.
173. Berkman N, Jose PJ, Williams TJ, Schall TJ, Barnes PJ, Chung KF. Corticosteroid inhibition of macrophage inflammatory protein-1 alpha in human monocytes and alveolar macrophages. American Journal of Physiology-Lung Cellular and Molecular Physiology. 1995 Oct;269(4):L443–52.
174. Lin TC, Li CY, Wong CS, Ho ST. Plasma rantes concentrations during on-pump or off-pump coronary artery bypass grafting surgery. Can J Anesth. 2005 Jun 1;52(1):A84–A84.
175. Wakugawa M, Nakamura K, Akatsuka M, Nakagawa H, Tamaki K. Interferon-gamma-induced RANTES production by human keratinocytes is enhanced by IL-1beta, TNF-alpha, IL-4 and IL-13 and is inhibited by dexamethasone and tacrolimus. Dermatology. 2001;202(3):239–45.
176. Staruch MJ, Camacho R, Dumont FJ. Distinctive Calcineurin-Dependent (FK506-Sensitive) Mechanisms Regulate the Production of the CC Chemokines Macrophage Inflammatory Protein (MIP)-1α, MIP-1β, and RANTES vs IL-2 and TNF-α by Activated Human T Cells. Cellular Immunology. 1998 Dec 15;190(2):121–31.
177. Bai Y, Zhang Y, Yang S, Wu M, Fang Y, Feng J, et al. Protective effect of vascular endothelial growth factor against cardiopulmonary bypass-associated acute kidney injury in beagles. Exp Ther Med. 2018 Jan;15(1):963–9.

178. Venugopal H, Jacob KA, Dieleman JM, Leaf DE. Dexamethasone for Preventing Major Adverse Kidney Events following Cardiac Surgery: Post-Hoc Analysis to Identify Subgroups. Kidney360. 2020 Apr 30;1(6):530–3.
179. Jacob KA, Leaf DE, Dieleman JM, van Dijk D, Nierich AP, Rosseel PM, et al. Intraoperative High-Dose Dexamethasone and Severe AKI after Cardiac Surgery. J Am Soc Nephrol. 2015 Dec;26(12):2947–51.
180. Kato A, Chustz RT, Ogasawara T, Kulka M, Saito H, Schleimer RP, et al. Dexamethasone and FK506 Inhibit Expression of Distinct Subsets of Chemokines in Human Mast Cells. J Immunol. 2009 Jun 1;182(11):7233–43.
181. Stellato C, Matsukura S, Fal A, White J, Beck LA, Proud D, et al. Differential Regulation of Epithelial-Derived C-C Chemokine Expression by IL-4 and the Glucocorticoid Budesonide. The Journal of Immunology. 1999 Nov 15;163(10):5624–32.
182. Ehrchen JM, Roth J, Barczyk-Kahlert K. More Than Suppression: Glucocorticoid Action on Monocytes and Macrophages. Front Immunol [Internet]. 2019 Aug 27 [cited 2024 Jul 12];10. Available from: https://www.frontiersin.org/journals/immunology/articles/10.3389/fimmu.2019.02028/full
183. Rao A, Luo C, Hogan PG. Transcription factors of the NFAT family: regulation and function. Annu Rev Immunol. 1997;15:707–47.
184. Martínez-Martínez S, Redondo JM. Inhibitors of the calcineurin/NFAT pathway. Curr Med Chem. 2004 Apr;11(8):997–1007.
185. Juchem KW, Gounder AP, Gao JP, Seccareccia E, Yeddula N, Huffmaster NJ, et al. NFAM1 Promotes Pro-Inflammatory Cytokine Production in Mouse and Human Monocytes. Front Immunol [Internet]. 2022 Jan 13 [cited 2024 Jul 12];12. Available from: https://www.frontiersin.org/journals/immunology/articles/10.3389/fimmu.2021.773445/full
186. Adjuto-Saccone M, Soubeyran P, Garcia J, Audebert S, Camoin L, Rubis M, et al. TNF-α induces endothelial–mesenchymal transition promoting stromal development of pancreatic adenocarcinoma. Cell Death Dis. 2021 Jun 25;12(7):1–15.
187. Petrache I, Birukova A, Ramirez SI, Garcia JGN, Verin AD. The Role of the Microtubules in Tumor Necrosis Factor-α–Induced Endothelial Cell Permeability. Am J Respir Cell Mol Biol. 2003 May;28(5):574–81.
188. Sawant DA, Tharakan B, Wilson RL, Stagg HW, Hunter FA, Childs EW. Regulation of TNF-α-Induced Microvascular Endothelial Cell Hyperpermeability by Recombinant Bcl-xL. J Surg Res. 2013 Sep;184(1):628–37.
189. Yu H, Huang X, Ma Y, Gao M, Wang O, Gao T, et al. Interleukin-8 Regulates Endothelial Permeability by Down-regulation of Tight Junction but not Dependent on Integrins Induced Focal Adhesions. Int J Biol Sci. 2013 Sep 23;9(9):966–79.
190. Li AF, Lee SM, Yin PH, Chi CW. Dexamethasone (Dex) Ameliorates Reduced VE-Cadherin Expression by High Glucose in Microvascular Endothelial cells. Investigative Ophthalmology & Visual Science. 2008 May 14;49(13):4901.
191. Salvador E, Shityakov S, Förster C. Glucocorticoids and endothelial cell barrier function. Cell Tissue Res. 2014;355(3):597–605.

192. Dufour A, Corsini E, Gelati M, Ciusani E, Zaffaroni M, Giombini S, et al. Modulation of ICAM-1, VCAM-1 and HLA-DR by cytokines and steroids on HUVECs and human brain endothelial cells. J Neurol Sci. 1998 May 7;157(2):117–21.
193. Gelati M, Corsini E, Dufour A, Massa G, Giombini S, Solero CL, et al. High-dose methylprednisolone reduces cytokine-induced adhesion molecules on human brain endothelium. Can J Neurol Sci. 2000 Aug;27(3):241–4.
194. Brostjan C, Anrather J, Csizmadia V, Natarajan G, Winkler H. Glucocorticoids inhibit E-selectin expression by targeting NF-kappaB and not ATF/c-Jun. The Journal of Immunology. 1997 Apr 15;158(8):3836–44.
195. Spiekerkoetter E, Tian X, Cai J, Hopper RK, Sudheendra D, Li CG, et al. FK506 activates BMPR2, rescues endothelial dysfunction, and reverses pulmonary hypertension. J Clin Invest. 2013 Aug 1;123(8):3600–13.
196. Albiñana V, Sanz-Rodríguez F, Recio-Poveda L, Bernabéu C, Botella LM. Immunosuppressor FK506 Increases Endoglin and Activin Receptor-Like Kinase 1 Expression and Modulates Transforming Growth Factor-β1 Signaling in Endothelial Cells. Mol Pharmacol. 2011 May 1;79(5):833–43.
197. Eguchi R, Kubo S, Ohta T, Kunimasa K, Okada M, Tamaki H, et al. FK506 induces endothelial dysfunction through attenuation of Akt and ERK1/2 independently of calcineurin inhibition and the caspase pathway. Cellular Signalling. 2013 Sep 1;25(9):1731–8.
198. Aebert H, Kirchner S, Keyser A, Birnbaum DE, Holler E, Andreesen R, et al. Endothelial apoptosis is induced by serum of patients after cardiopulmonary bypass☆. European Journal of Cardio-Thoracic Surgery. 2000 Nov 1;18(5):589–93.
199. Pouya F, Kercahian MA. Time- and Dose-Dependent Effect of Dexamethasone on Endothelial Cell Apoptosis. 2021;8(1).
200. Newton C, Ran G, Xie YX, Bilko D, Burgoyne C, Adams I, et al. Statin-induced apoptosis of vascular endothelial cells is blocked by dexamethasone. The Journal of endocrinology. 2002 Aug 1;174:7–16.
201. Tanke NT, Liu Z, Gore MT, Bougaran P, Linares MB, Marvin A, et al. Endothelial Cell Flow–Mediated Quiescence Is Temporally Regulated and Utilizes the Cell Cycle Inhibitor p27. Arteriosclerosis, Thrombosis, and Vascular Biology. 2024 Jun;44(6):1265–82.
202. Morigi M, Zoja C, Figliuzzi M, Foppolo M, Micheletti G, Bontempelli M, et al. Fluid Shear Stress Modulates Surface Expression of Adhesion Molecules by Endothelial Cells. Blood. 1995 Apr 1;85(7):1696–703.
203. Chen Y, Chen H, Liu X, Lei S, Mao Y, Zhang W. [Effect of flow shear stress on the expression of adhesion molecules of endothelial cells]. Sheng Wu Yi Xue Gong Cheng Xue Za Zhi. 2001 Jun;18(2):201–5.
204. Gillinov AM, Davis EA, Curtis WE, Schleien CL, Koehler RC, Gardner TJ, et al. Cardiopulmonary bypass and the blood-brain barrier. The Journal of Thoracic and Cardiovascular Surgery. 1992 Oct;104(4):1110–5.
205. Schuller AM, Windolf J, Blaheta R, Cinatl J, Kreuter J, Wimmer-Greinecker G, et al. Degradation of microvascular brain endothelial cell β-catenin after co-culture with activated neutrophils from patients undergoing cardiac surgery with prolonged cardiopulmonary bypass. Biochemical and Biophysical Research Communications. 2005 Apr 8;329(2):616–23.

206. Chen K, Wang N, Diao Y, Dong W, Sun Y, Liu L, et al. Hydrogen-Rich Saline Attenuates Brain Injury Induced by Cardiopulmonary Bypass and Inhibits Microvascular Endothelial Cell Apoptosis Via the PI3K/Akt/GSK3β Signaling Pathway in Rats. Cellular Physiology and Biochemistry. 2017 Oct 17;43(4):1634–47.
207. Marcu R, Choi YJ, Xue J, Fortin CL, Wang Y, Nagao RJ, et al. Human Organ-Specific Endothelial Cell Heterogeneity. iScience. 2018 Jun 29;4:20–35.
208. Przysinda A, Feng W, Li G. Diversity of Organism-Wide and Organ-Specific Endothelial Cells. Curr Cardiol Rep. 2020 Feb 8;22(4):19.
209. Gunawardana H, Romero T, Yao N, Heidt S, Mulder A, Elashoff DA, et al. Tissue-specific endothelial cell heterogeneity contributes to unequal inflammatory responses. Sci Rep. 2021 Jan 21;11(1):1949.

CURRICULUM VITAE

Hao Zhou

4550 11th Ave NE, Seattle, WA 98105 · 608-886-8359 (mobile) · hz457@uw.edu

EDUCATION

University of Washington-Seattle, WA *September 2019 – Present*
PhD in Bioengineering. Expected graduation in May 2024 (Current GPA: 3.75):

Cornell University, NY *August 2017 - June 2019*
M.S. in Material Science and Engineering (GPA: 3.91/4.0).

University of Wisconsin-Madison, WI *September 2012 - December 2016*
B.S. in Material Science and Engineering; B.S. Chemistry (overall GPA: 3.57/4.0).

RESEARCH AND WORK EXPERIENCE

Graduate Research Assistant *September 2019 – Present*
Department of Bioengineering, Scatena group & Giacheli group, University of Washington, Seattle

- Optimizing shear-stress-induced inflammatory response after cardiopulmonary bypass in pediatric patients using an *in vitro* model.
- Characterizing immune cell-endothelial cell interactions with qRT-PCR, ELISA, flow cytometry, cell-based assays, lentiviral transfection, and immunostaining.

Graduate Researcher *August 2017 - June 2019*
Department of Material Science & Engineering, Estroff group & Department of Biomedical Engineering, Bonassar group, Cornell University

- Contributed to the development of a scaffold containing mineral gradient, targeting the study of tissue engineered soft tissue-bone interface.

Teaching Assistant, Exploration in Engineering *Summer 2018*
College of Engineering, Cornell University

- Arranged activities in lab sessions for high school students seeking engineering experience at college level.

Research & Development Intern *Summer 2016*
Federal Mogul Powertrain, Waupun, WI

- Characterized the mechanical properties and microstructure of powder-pressed alloy using Bruker wear testing and 3D microscope.
- Developed a new method to quantitatively compare the thermal conductivity of metal alloys.

Undergraduate Researcher *September 2015 – May 2016*
Department of Chemistry, Hermans group, University of Wisconsin-Madison

- Synthesized metal oxide catalysts and characterized them using BET, ICP, RAMAN and UV-vis.

PROFESSIONAL SKILLS

Biological Characterization: RT-qPCR, Ingenuity Pathway Analysis (IPA) by QIAGEN, various histological staining, immunohistological study (IHC, IF), ELISA, micro/nano-computed tomography, scanning electronic microscopy, confocal microscopy, RAMAN spectroscopy, primary cell isolation
Visualization: Avizo by Thermo Fisher Scientific, ImageJ by NIH, Adobe Illustrator
Programming: Basic Matlab coding, R studio, ImageJ macro programming for automatic analysis

PUBLICATIONS

H. Zhou, A.J. Boys, J.B. Harrod, L.J. Bonassar, L.A. Estroff, Mineral Distribution Spatially Patterns Bone Marrow Stromal Cell Behavior on Monolithic Bone Scaffolds. *Acta Biomaterialia*, 112 (2020), 274-285.

A.J. Boys, H. Zhou, J.B. Harrod, M.C. Mccorry, L.A. Estroff, L.J. Bonassar, Top-Down Fabrication of Spatially Controlled Mineral-Gradient Scaffolds for Interfacial Tissue Engineering, *ACS Biomater. Sci. Eng.* 5 (2019) 2988–2997.

SCHOLARSHIPS AND AWARDS

- 2015 Fall & 2016 Spring Material Science and Engineering Scholarships.
- 2016 Spring Department of Chemistry Scholarship, Ackerman Award.
- 2022&2023 Bioengineering Cardiovascular Training Grant.

COFERENCE PRESENTATIONS

Zhou, H., Tu, L., Nigam, V., Giachelli, C., Scatena, M. (2024) An In-vitro Model To Study Monocyte-Endothelial Interaction in Pediatric Cardiopulmonary Bypass, BCTP Symposium, Seattle, WA. (Oral Presentation)

Zhou, H., Tu, L., Nigam, V., Giachelli, C., Scatena, M. (2023) Cardiopulmonary Bypass Shearing Resutls in IL-8 Dependent Monocytic Insult on the Endothelium, BMES, Seattle, WA. (Poster Presentation)

Zhou, H., Tu, L., Nigam, V., Giachelli, C., Scatena, M. (2023) CPB Shear Stress Stimulates Monocytes Adhesion to and Transmigration Through Endothelial Cell Through IL-8 Signaling, BCTP Symposium, Seattle, WA. (Oral Presentation)

Zhou, H., Tu, L., Nigam, V., Giachelli, C., Scatena, M. (2023). Cardiopulmonary Bypass in PVC Tubing Results in IL-8 Dependent Monocytic Insult on Endothelium, SFB Annual Meeting, San Diego, CA. (Poster Presentation)

Zhou, H., Nguyen, C., Tu, L., Nigam, V., Giachelli, C., Scatena, M. (2022). *An In-vitro Cardiopulmonary Bypass Model to Study Endothelial Cell Responses to Shear Activated Monocytes*, Vasculata, Durham, NC. (Poster Presentation)

Zhou, H., Nguyen, C., Tu, L., Nigam, V., Giachelli, C., Scatena, M. (2022). *PVC Tubing Results in Monocytic Insult on Neonatal Endothelial Cells: Role of Shear Stress*, Joint Symposium – SFB+JSB, Honolulu, HI. (Poster Presentation)

Zhou, H., Boys, A., Harrod, J., Bonassar, L., Estroff, L. (2019). *The Fabrication of A Mineral Gradient Containing Bone Scaffold and Its Effect on the Behavior of Mesenchymal Stem Cells*, Orthopaedic Research Society Annual Meeting, Austin, TX. (Poster Presentation)

Zhou, H., Boys, A., Harrod, J., Bonassar, L., Estroff, L. (2018). *Fabrication of A Mineral Gradient Containing Bone Matrix Scaffold and Its Biocompatibility towards Mesenchymal Stem Cells*, Biomedical Engineering Society Annual Meeting, Atlanta, GA. (Poster Presentation)